SCIENTIFIC COMMITTEE
FOURTEENTH REGULAR SESSION

Busan, Republic of Korea
8-16 August 2018

Stock assessment of South Pacific albacore tuna

WCPFC-SC14-2018/ SA-WP-05
Rev. 2* (2 August 2018)

Tremblay-Boyer L[1], J. Hampton[1], S. McKechnie[1] and G. Pilling[1]

***Update Fig. 46**

[1] Oceanic Fisheries Programme, The Pacific Community (SPC)

Contents

List of Tables

List of Figures

Revision 1: August 1st 2018

The previous version has incorrectly specified penalties for fitting CPUE for region 2 under the traditional CPUE grid level only, such that penalties were much higher than they should have been for the start of the time-series (which normally should have had the lowest penalty). This impacted reference points for the grid by lowering $SB_{latest}/SB_{F=0}$ by 4 points and $SB_{recent}/SB_{F=0}$ by 6 points. We updated the results to reflect these corrected runs (Figures 43 to 48, Tables 6 to 10). Stepwise steps using misspecified early penalties were also corrected (Figures 14 and 15).

A recommendation that alternative growth models than the von Bertalanffy be explored was added to the discussion.

1 Executive Summary

This paper describes the 2018 stock assessment of albacore tuna (*Thunnus alalunga*) in the southern hemisphere component of the Western and Central Pacific Fisheries Commission (WCPFC) convention area. A further three years data were available since the last stock assessment was conducted in 2015, and the model time period extends to the end of 2016. Further developments to the stock assessment have been undertaken to address the recommendations of the 2015 stock assessment report (Harley et al., 2015), to address the recommendations of the 2018 pre-assessment workshop (PAW; Pilling and Brouwer (2018)), and to explore uncertainties in the assessment model, particularly in response to the inclusion of additional years of data and to improve diagnostic weaknesses in previous assessments. This assessment is supported by the analysis of longline CPUE data, background analyses of other data inputs and definition of the regional and fisheries structures for the updated assessment (Tremblay-Boyer and McKechnie, 2018).

Key changes made in the progression from the 2015 reference case to the 2018 diagnostic case model include:

- Updating all data up to the end of 2016.
- Utilising standardised CPUE indices calculated from the recently collated operational longline CPUE data set, including historical Japanese longline data within the CPUE which were not available in 2015, and treating targeting cluster as a covariate (rather than filtering the data).
- Moving to a simplified regional structure (2018 region structure).
- Moving from the traditional CPUE standardized index to one based upon a geostatistical model.
- Applying the CPUE standardized index to an 'index fishery' in each region.

In addition to the diagnostic case model, we report the results of one-off sensitivity models to explore the relative impacts of key data and model assumptions for the diagnostic case model on the stock assessment results and conclusions. We also undertook a structural uncertainty analysis (model grid) for consideration in developing management advice, where all possible combinations of the most important axes of uncertainty from the one-off models were included. It is recommended that management advice is formulated from the results of the structural uncertainty grid.

Across the range of models run in this assessment, the most important factors when evaluating stock status were the assumed level of natural mortality, and growth. For natural mortality, age invariant M values of 0.3 yr^{-1} (consistent with the 2015 assessment) and 0.4 yr^{-1} were assumed, with the latter resulting in more optimistic assessment outcomes. Age-dependent M settings were also evaluated as one-off sensitivities. Natural mortality remains a key uncertainty in this assessment, and it is appropriate that such uncertainty continue to be reflected in the overall stock assessment results. For growth, the conditional age-at-length data from recent work was incorporated into the diagnostic case model, while an alternative scenario fixed at the parameter values of the sex-combined 'Chen-Wells' growth model used within the 2017 North Pacific albacore reference case model run was also evaluated. Use of the latter resulted in more pessimistic assessment outcomes. There remains an unresolved inconsistency in the growth rates indicated by the VB curve fitted to the age-at-length data (approximately 20 cm per year for albacore 20-70 cm in length) and presumed annual modes with 10 cm spacing that consistently appear in the troll size composition data, and historically in the driftnet size composition data. Additional analysis of otoliths taken from 50-70 cm albacore in the troll fishery is required to identify the reason for this inconsistency. This is work that needs to be undertaken with high priority.

The general conclusions of this assessment are as follows:

- While biomass is estimated to have declined initially, estimates of spawning potential, and biomass vulnerable to the various longline fisheries, have been stable or possibly increasing slightly over the past 20 years. This has been influenced mainly by the estimated recruitment, which has generally been somewhat higher since 2000 than in the two decades previous.
- Most models also estimate an increase in spawning and longline vulnerable biomass since about 2011, driven by some high estimated recruitments, particularly around 2009.
- A steady increase in fishing mortality of adult age-classes is estimated to have occurred over most of the assessment period, accelerating since the 1990s but declining following the decline in longline catch seen since 2010. Juvenile fishing mortality increased until around 1990, and has remained stable at a low level since that time.
- Key stock assessment results across all models in the structural uncertainty grid show a wide range of estimates.
- All models indicate that South Pacific albacore is above the limit reference point (of $0.2SB_{F=0}$), with overall median depletion for 2016 ($SB_{latest}/SB_{F=0}$) estimated at 0.52 (80 percentile range 0.37-0.69).
- Recent average fishing mortality is estimated to be well below F_{MSY} (median $F_{recent}/F_{\mathrm{MSY}} =$ 0.2, 80 percentile range 0.08-0.41).
- A number of key research needs have been identified in undertaking this assessment that should be investigated either internally or through directed research. These include: the analysis of otoliths from individuals within the presumed annual modes seen in the troll data; studies on albacore size-related vulnerability to longline fishing; further development of the geostatistical analysis of operational-level CPUE data; further development of relevant MULTIFAN-CL functionality.

2 Introduction

This paper presents the 2018 stock assessment of South Pacific albacore tuna (*Thunnus alalunga*) covering the southern hemisphere component of the Western and Central Pacific Fisheries Commission (WCPFC) convention area and fisheries for the period 1960 to 2016. Since 1999, the stock has been assessed regularly and the most recent assessments are documented in Hoyle et al. (2008b); Hoyle and Davies (2009); Hoyle (2011); Hoyle et al. (2012); Harley et al. (2015).

The current assessment continues the development of stock assessment models for the species, facilitated by the ongoing development of the statistical stock assessment software, known as MULTIFAN-CL[2] (Fournier et al., 1998; Hampton and Fournier, 2001; Kleiber et al., 2017), that is routinely used by the Pacific Community (SPC). Further developments to the stock assessment have been undertaken to address the recommendations of the 2015 stock assessment report (Harley et al., 2015), to address the recommendations of the 2018 pre-assessment workshop (PAW; Pilling and Brouwer, 2018), to explore uncertainties in the assessment model, particularly in response to the inclusion of additional years of data and to improve diagnostic weaknesses in previous assessments.

The objectives of this assessment are to estimate population parameters, such as time series of recruitment, biomass, biomass depletion and fishing mortality, which indicate the stock status and impacts of fishing. We summarize the stock status in terms of reference points adopted by the WCPFC. The methodology used for the assessment is based on the general approach of integrated modelling (Fournier and Archibald, 1982), which is carried out using MULTIFAN-CL, and implements a size-based, age- and spatially-structured population model. Model parameters are estimated by maximizing an objective function, consisting of both likelihood (data) and prior information components (penalties).

This assessment report should not be seen as a standalone document and should be read in conjunction with several supporting papers, specifically the analyses of longline CPUE data (Tremblay-Boyer and McKechnie, 2018), background analyses of other data inputs (Tremblay-Boyer and McKechnie, 2018), definition of the regional and fisheries structures for the updated assessment (Tremblay-Boyer and McKechnie, 2018), and presentation of recent trends in the South Pacific albacore fishery (Brouwer et al., 2018). Finally, many of these issues were discussed in detail, and recommendations to the assessment approach made, at the PAW held in Noumea over 17–20 April, 2018 (Pilling and Brouwer, 2018).

3 Background

3.1 Biology and ecology

Albacore tuna comprise a discrete stock in the South Pacific (Murray, 1994). Mature albacore, above a minimum fork length (FL) of about 80 cm (M_{50} ~85cm), spawn in tropical and subtropical waters between latitudes 10° S and 30° S during the austral summer (Muhling et al., 2017). Juveniles are caught in surface fisheries in New Zealand's coastal waters, and in the vicinity of the sub-tropical convergence zone (STCZ, at about 40° S) in the central Pacific, at about one year old and at a size of 45–50 cm FL.

[2] www.multifan-cl.org

Albacore appear to gradually disperse north from the southern latitudes as they grow, but adult longline catch data indicates that they appear to migrate seasonally between tropical and sub-tropical waters (Langley, 2004; Nikolic et al., 2017). These data show that albacore in the sourthern hemisphere are most abundant in sub-equatorial waters during December-January and May-July, indicating that albacore migrate south during early summer, and north during winter. This movement tends to correspond with the seasonal shift in the 23–28° C sea surface temperature isotherm. Albacore tuna are more challenging to tag than other species of commercial tuna so there are no long-term large-scale tagging programs that can confirm those movement trends (Williams et al., 2009).

Daily otolith growth increments indicate that initial growth is rapid (Murua et al., 2017), with albacore reaching 45–50 cm (FL) in their first year (Leroy and Lehody, 2004; Williams et al., 2012). Subsequent growth is slower, at approximately 12 cm per year from years 2 to 4, and declining thereafter (Williams et al., 2012). Maximum recorded length is about 120 cm (FL) but sex-combined von Bertalanffy growth models for both the South and North Pacific albacore predict L_∞ around 105 cm (Williams et al., 2012; Xu et al., 2014). Recent analyses of age-at-length from otolith data have identified important patterns in South Pacific albacore growth (Williams et al., 2012; Farley et al., 2013). Males grow to larger sizes than females, and their lengths-at-age start to diverge above about 85 cm when they reach maturity. Lengths-at-age of both sexes also appear to vary with longitude, with both growth rates and maximum sizes increasing toward the east and reaching a maximum at about 160° W. In the New Zealand troll fishery, there are clear 10 cm modes in the length frequency data for juveniles between 50 and 80 cm. These modes should be annual based on maturity ogives for this species combined with indicated annual spawning, peaking in January (Farley et al., 2014).

The instantaneous natural mortality rate is believed to be between 0.2 and 0.5 per year, with significant numbers of fish reaching 10 years or more. The default M of 0.4 used in assessments was updated in 2015 to 0.3 to match that used in other stocks, including the North Pacific. A recent meta-analysis of mortality for the North Pacific stock indicated M should be closer to 0.4, higher for females, and age-specific (Kinney and Teo, 2016).

Currently, the longest period at liberty for a recaptured tagged albacore in the South Pacific is 11 years, but in the North Pacific (the same species, but viewed as a separate biological stock) there has been one recapture of 15 years (ISC Albacore Working Group, 2011). Tag mortality is thought to be high in albacore and as a result there have been limited tagging programs for this species, the main ones being the RTTP in the early 1990s and the EU SCIFISH-funded South Pacific Albacore Tagging Project over 2009-2010.

3.2 Fisheries

Distant-water longline fleets from Japan, Korea, Chinese Taipei, and China, and the domestic longline fleets from a number of Pacific Island countries, catch adult albacore over a large proportion of their geographic range (Figure 1). The Chinese Taipei fleet, in particular, have targeted albacore consistently since the 1960s. Since the mid-1990's, the longline catch has increased considerably with the development (or expansion) of longline fisheries targeting albacore in several Pacific Island EEZs, notably American Samoa, Cook Islands, Fiji, French Polynesia, New Caledonia, Samoa, Solomon Islands, Tonga, and Vanuatu. There has been a decrease in longline catch over the last few years, with a significant rebound in 2017 (Brouwer et al., 2018), but this last year is not included

in the assessment as data for the most recent year is generally subject to updates (see below).

The South Pacific albacore fishery was slow to develop, with catch fluctuating at low levels from the 1960s through to the late 1990s. Post-2000 catch increased to over 60,000 mt, and subsequently to over 80,000 mt (Figure 2, see also Brouwer et al., 2018). The longline fishery harvested most of the catch, about 25,000–30,000 mt per year on average, prior to about 1998. The increase in longline catch to approximately 70,000 mt in 2005 was due to the development of small-scale longline fisheries in Pacific Island Countries and Territories, and a recent increase in the catch also occurs in the Chinese and Chinese Taipei longline fisheries. A troll fishery for juvenile albacore has operated in New Zealand's coastal waters since the 1960s and in the central Pacific (in the region of the STCZ) since the mid-1980s. Catches from the troll fishery are relatively small, generally less than 10,000 mt per year. Driftnet vessels from Japan and Chinese Taipei also targeted albacore in the central Tasman Sea and in the central Pacific near the STCZ for a short period during the 1980s and early 1990s (Figure 1). Driftnet catch reached 22,000 mt in 1989, but has since declined to zero following a United Nations moratorium on industrial-scale drift-netting in 1989.

Longline fisheries operate throughout the year, although there is a strong seasonal trend in the catch distribution, with the fishery operating in southern latitudes (south of 35° S) during late summer and autumn, moving northwards during winter. Surface fisheries are highly seasonal, occurring mainly from December-April.

4 Data compilation

Data used in this South Pacific albacore assessment consist of fishery-specific catch, effort and length-frequency data, tag release-recapture data, and conditional age-length observations. Details of these data and their stratification are described below.

4.1 Spatial stratification

Hoyle et al. (2012) provides a detail history of the various spatial structures considered in south Pacific albacore tuna assessments so here we will just focus on the approach used in the current assessment and how this differs to the previous one (Harley et al., 2015). Two regional structures were considered in the 2018 assessment; an updated structure ('2018 regions'; Figure 3), which is a simplification of the 2015 configuration, and the structure used in 2015 ('2015 regions'; Figure 4), used in the earlier stages of model development before transiting to the 2018 structure for final outputs, as agreed at the PAW (Pilling and Brouwer, 2018). The recommendation by PAW to switch to a simpler region structure was underpinned by the relative lack of information to inform MULTIFAN-CL on movement between regions, in part due to many of the tag releases occurring on or near the border of the old region structures (Figure 5). These modifications and the consequences for fisheries definitions are covered by Tremblay-Boyer and McKechnie (2018) although we note herein that the difference between the structures consists of a reduction in region number from eight to five with each pair of regions 1 and 4, 2 and 5, and 3 and 6 from the 2015 regions being combined into single regions under the 2018 regions. In parallel, the definition for the longline fleets was refined compared to the 2015 version (see Section 4.3). The albacore catch for the 2018 region structure is shown in Figure 6 and data availability for each fishery is summarized in Figure 7.

4.2 Temporal stratification

The time period covered by this assessment is the first quarter of 1960 to final quarter of 2016. Within this period, data were compiled into quarters (Jan-Mar, Apr-Jun, Jul-Sep, and Oct-Dec). This period and the quarterly time-step is consistent with the 2015 assessment except with the addition of data for the years 2014–2016.

As occurred in the 2015 albacore assessment and the 2017 bigeye and yellowfin assessments, we excluded data for the most recent year as provisional estimates for the catch and effort data for longline fisheries available at the time of the assessments have generally been subject to significant revision either during or shortly after the completion of the assessment.

4.3 Fisheries definitions

MULTIFAN-CL requires all catch and effort to be allocated to fisheries. Ideally, the fisheries are defined to have selectivity and catchability characteristics that do not vary greatly over time. For most pelagic fisheries assessments, fisheries can be defined according to gear type, fishing method and region or sub-region.

The fisheries definitions for the 2015 assessment were a significant simplification from the previous assessment, with just a single fishery for each gear type (e.g. data was aggregated over all flags) in each region where that gear-type was present. The changes to the fisheries definitions under the 2018 regions are detailed in Tremblay-Boyer and McKechnie (2018) and 2018 fleet structure is summarised in Table 1. In brief, despite the reduction in region number, the total number of fisheries has slightly increased since 2015 as the resolution for the longline fleets was increased to reflect different selectivity patterns by longline fleets operating over now larger regions. Longline fleets in each region were split between those flagged to distant-water fishing nations, Pacific Island Countries and Territories and, where applicable (regions 2 and 3), Australia and New Zealand, adding two extra fisheries in total. The troll and gillnet fisheries were maintained as "all flags" fisheries.

The second modification in moving between the 2015 and 2018 regional structures was the addition of Index fisheries to which standardised combined-fleet CPUE time series were applied. This approach allows a fleet-combined, overall index of abundance to be applied to a region instead of to an individual fleet, and an improved modelling of the variation in size of the underlying population. This is described in more detail in the section below.

Details of the flags, and their respective catches within each longline fishery are provided in detail in Tremblay-Boyer and McKechnie (2018). The geographic distribution of the recent catch is presented in Figure 1.

4.3.1 Index fisheries

In most WCPO assessments an index of relative abundance by region is introduced by fixing catchability across regions and years for a set of longline fleets (one per region to avoid conflicts) such that their CPUE indexes abundance over space and time. In this assessment, we have taken a different approach to previous assessments in defining index longline fisheries. The methodology adopted for this assessment is as follows:

- We defined one Index fishery per region, for which catchability was assumed constant across years and regions. These Index fisheries were constructed from the full, multi-fleet longline CPUE analyses (both 'geostatistical' and 'traditional', see Section 4.4.1), but were assigned a trivial catch (of one fish per time period) so that they are in effect non-extractive fisheries. The effort for each time step was adjusted such that the original standardised CPUE from the supporting analysis was preserved.
- The regular capture longline fisheries were based on the same data set, but disaggregated by fleet categories according to the fisheries definitions in Table 1, and otherwise defined as usual – catch represented the total estimated albacore catches of the fisheries (in numbers of fish) and effort was based on nominal CPUE. However, the catchability of these fisheries was allowed to vary over time and across regions within the assessment model.
- The length-frequency data for the regular capture fisheries were constructed as usual. Size data from individual 5-degree-month (or other) strata were weighted by the catch in the process of aggregating the data to represent the fisheries at the spatial (region) and temporal (quarter) resolution of the model. This method ensures that the size data are most representative of the removals from the population by the fisheries in each time period and region and follows the approach described in McKechnie (2014).
- By contrast, the length-frequency data for the Index fisheries was subjected to the same aggregation process, but with the size data weighted by CPUE (rather than by catch). Weighting by CPUE attempts to make the size data more representative of the abundance of the underlying albacore population in each region and time period.
- Because the size data for the index and respective capture fisheries are effectively being used twice (but weighted differently), we adjusted the likelihood weighting (effective sample sizes) of the size data for both Index and capture fisheries such that the original intended weight (effective sample size) in the likelihood was preserved.

We regard this new method as preferable because:

- Given the dynamic and patchy effort of longline fleets in the South Pacific over time, there are distinct advantages to developing CPUE indices from combined-fleets datasets. Index fisheries make maximum use of the fully integrated, multi-fleet standardised CPUE analyses by providing the best possible spatial and temporal coverage for the indices of relative abundance in the assessment, and avoids assigning the multi-fleet standardised CPUE time series to only one fleet component within the assessment.
- It allows the size data to be weighted by CPUE for the Index fisheries, thus better representing the albacore population, while maintaining a catch-based weighting for the capture fisheries, providing aggregated size data more representative of the catch of those fisheries.

4.4 Catch and effort data

Catch and effort data were compiled according to the fisheries defined in Table 4. All catches were expressed in numbers of fish, with the exception of the driftnet fishery, where catches were expressed in weight (metric tonnes). For longline fisheries, effort was standardized as described below, while for troll and driftnet fisheries, the number of vessel days of fishing activity was used.

Overall annual catches by gear type, and then further broken down by region are provided in Figures 2 and 6. Catch has been decreasing from a historical high in 2010 as mentioned in Section 3.2, and most of the recent catch has occurred in region 2, the area almost exclusively comprised of EEZs between 10-25° S and west of 150° W. The increasing regional trend to 2010 can be attributed to increased catch in PICT EEZs and by the Chinese fleet since the 1990s. Troll catches are exclusively in the southern regions, primarily region 3. Region 3 has had the most sustained catches for albacore tuna since the 1960s, and with the recent decrease in catch, which happened exclusively in region 2, region 3 accounted for a sizeable proportion of the catch in the most recent years.

4.4.1 Longline effort and CPUE

Two approaches to CPUE standardisation were examined within this assessment, the 'geostatistical' approach, and the 'traditional' approach. These are outlined briefly below, with full details of the analyses undertaken to calculate the standardized CPUE indices and regional weights used in this assessment provided in Tremblay-Boyer and McKechnie (2018).

All analyzes were conducted with the available Pacific-wide operational (i.e., set-by-set) longline catch and effort data[3], classified by the assessment boundaries. This dataset was first described in McKechnie et al. (2015) and has been annually updated since then. Individual CPUE standardisations were performed by region under the traditional approach, but for the geostatistical approach we were able to apply the model to the entire assessment area. Under the traditional approach region-specific trends were therefore not influenced by those in other regions, while under the geostatistical approach a South Pacifc-wide trend was estimated to which regional interactions were then applied. We summarise the two approaches below.

The geostatistical approach to CPUE standardisation was used for the diagnostic case model. Geostatistics explicitly models the spatial structure in the response variable, that is, the fact that observations closer in space are more likely to be similar. This allows the spatial autocorrelation to be accounted for, which increases the precision in estimates and in some instances makes it easier to identify a relationship between response and candidate explanatory variables. Targeting clusters defined from the relative proportion of albacore tuna, bigeye tuna, yellowfin tuna, and swordfish catch were also used as covariates. The models were run in TMB (Kristensen et al., 2016) which meant the final indices could be constructed directly within the estimating algorithm, instead of post-hoc as done usually, such that we were able to extract region-specific time-series of standard errors directly as model outputs, instead of having to perform an additional step *via* the canonical method. The final indices (Figure 8) were mean-standardized and rescaled according to regional weights (see below), following the same approach as for traditional CPUEs.

The analysis to derive the regional weights was also based upon the analysis of fleet-combined operational longline catch and effort data. The aim of the analysis was to standardize the data in such a way that spatial differences in CPUE across the entire model domain reflects differences in relative abundance. The geostatistical models (Tremblay-Boyer and McKechnie, 2018) produce an abundance surface over the entire stock assessment region from which it is straightforward, even for multiple regional structures, to compute relative estimates of abundance among regions. These regional weights (or regional scaling factors) were then used to scale the mean-centered standardised

[3]the data set was similar to that used for the Pacific-wide analysis of McKechnie et al. (2015) except Japan did not authorize the inclusion of any data held only by them (i.e., not otherwise held by SPC) in that analysis

indices between regions. We therefore used the geostatistical model outputs aggregated for the period 1975-2016 to estimate the regional scaling factors. This was consistent with the approach adopted in the bigeye and yellowfin assessments of 2017, except that we did not use oceanographical covariates in the present analysis due to the challenges in separating their impact on relative abundance *vs.* catchability.

For the 'traditional CPUE' approach, the final indices used in the assessment were based on negative binomial regression models incorporating vessel effects and cluster as a factor (where data for multiple clusters were included), and were developed following Tremblay-Boyer et al. (2015b). Temporal CV's were estimated using the canonical method of Francis (1999), which estimates CV's for all time periods in the standardization model, including the reference period. These CVs underestimate the variation represented in the standardized effort component of MULTIFAN-CL's likelihood and so they are rescaled for each region separately so that they have a mean of 0.2 over the time periods 1998–2015 (the period for which CPUE were available for all regions). The final mean-centered indices under this approach are shown in Figure 9. The regional weights used in the early steps of the model progression to the diagnostic case were those developed in Tremblay-Boyer et al. (2015a).

The regional multi-fleet longline CPUE time series developed *via* the two approaches described here were then applied to the Index fisheries in each region, depending on the CPUE scenario. The time-series for these two indices are compared in Figure 10.

4.5 Size data

Available length-frequency data for each of the defined fisheries were compiled into 100, 1-cm size classes (30–129 cm). Data were collected from a number of sources, and can be summarized as follows.

4.5.1 Longline

Albacore catch size composition data have been routinely collected from the fishery since the early 1960's. These data are characterized by inconsistent temporal and spatial resolution, may be subject to very small sample sizes and consequently exhibit high variability in some periods. In addition the spatial and temporal distribution of length sampling has not always reflected that of the fishery. As a consequence, some samples may have very different size compositions to the majority of the catch and are representative only of periods and locations where very small catches have been made. Further details of the breakdown by flag and time of length-frequency samples for different fisheries is provided in Tremblay-Boyer et al. (2015a) and Scott and McKechnie (2015).

In previous assessments, a data re-weighting approach has been applied to improve the consistency of the size frequency data and to ensure that it is as representative as possible of catches across the full spatial and temporal extent of the fishery. Following the recommendations of the external review of the bigeye assessment (Ianelli et al., 2012), a revised re-weighting method (McKechnie, 2014) was developed and applied for key tuna assessments conducted since 2014. The revised method re-weights the size composition data according to the proportion of temporally smoothed catch taken within each 10° x 20° spatial cell within a region in a given year-quarter. In addition, a minimum weighting threshold was imposed on the lowest allowable weighting to reduce the influence

of size data from cells with very little catch. Re-scaled length frequency data based on an 11 year-quarter moving average for catch scaling and a minimum weighting threshold of 0.1 were used for the assessment (Scott and McKechnie, 2015).

4.5.2 Troll and other surface fisheries

New Zealand domestic troll data (fishery in region 3) were collected from port sampling programmes conducted by the New Zealand Ministry of Fisheries and, more recently, the New Zealand National Institute of Water and Atmospheric Research (NIWA).

Length-frequency data from troll fishing operations in the sub-tropical convergence zone (STCZ) (fisheries 13 and 14, regions 3 and 5) were collected and compiled through the Albacore Research Tagging Project (1991-1992) and by port sampling programmes in Levuka, Fiji; Pago Pago, American Samoa; and Papeete, French Polynesia; and, during the 1990–1991 and 1991–1992 seasons, by scientific observers.

Driftnet data were provided by the NRIFSF for Japanese driftnet vessels. Data from Japanese vessels were also collected by observers and by port sampling in Noumea, New Caledonia. It is assumed that these data are representative of all driftnet activity.

4.6 Tagging data

Limited tagging data were available for incorporation into the assessment. Data consisted of tag releases and returns from a South Pacific Albacore Research Group tagging programme in the mid-1980s and OFP albacore tagging programmes conducted during the austral summers of 1990–1992 and 2009–2010 (Figure 5, see also Hoyle et al., 2012). Albacore were captured primarily by trolling and tagged using standard tuna tagging equipment and techniques by trained scientists and scientific observers. During the 1980s and 1990s, the majority of tag releases were made by scientific observers on-board New Zealand and US troll vessels fishing in New Zealand waters and in the central South Pacific sub-tropical convergence zone region. The more recent tagging was conducted in New Zealand waters.

For the albacore assessment, tag releases were stratified by release region (all albacore releases occurred in 2018 structure regions 3 and 5, or regions 3, 6 and 8 under the 2015 structure), time period of release (quarter) and the same size classes used to stratify length-frequency data. Releases were classified into 24 tag release groups (region, year and quarter). Release numbers were modified to account for returns that could not be classified to recapture fisheries and/or time periods, and for tagging-related effects on the survival of tagged fish using the most recent methodology outlined in McKechnie et al. (2016b) and McKechnie et al. (2017b) (see Section 5.4). Following adjustment, the total effective number of releases was 6,879. Returns from each size class of each tag release group (138 tag returns in total) were then classified by recapture fishery and recapture time period (quarter).

Tag releases principally comprised juvenile fish (aged 1–4 years); few fish larger than 80 cm (FL) were tagged (Figure 13 from Hoyle et al., 2012). The length composition of fish from tag recoveries was comparable to the length at release, albeit slightly larger, allowing for growth during the period at liberty. Many of the tag recoveries were from longline fisheries in the southern regions (3 and 5) (Figure 13 from Hoyle et al., 2012). Relatively few tags were returned from the troll fisheries.

Most tag recoveries occurred during the five years following release although there were several in excess of nine years after release.

Note that there were no additional tag releases subsequent to the 2015 assessment although an additional 7 recaptures were included in the 2018 data. These relate to fish tagged around New Zealand in 2009 that have been recaptured in longline fisheries after 2013, which was the terminal year of the 2015 assessment.

4.7 Conditional age-at-length data

Observations from otolith readings were available from an ageing study of South Pacific albacore by Farley et al. (2013) which comprised $n = 1969$ ages-at-length (males, females and unknown, combined), with age expressed as the decimal year, collected throughout the South Pacific with a focus on the sub-tropical region between 10° S and 25° S (Figure 11). These observations were stratified according to the fishery definitions, spatial and temporal structures used in the assessment model, based upon the individual sample details (method, flag, date and latitude/longitude). Samples were collected over the years 2009 and 2010, but were aggregated into the single year of 2010, as no inter-annual variation in growth was to be considered in the model (constant growth is assumed in MULTIFAN-CL). Samples were aggregated in fishery-quarter strata and only those containing more than 50 age-length observations were retained, resulting in 10 samples under the 2018 region structure (14 under the 2015 region structure). The two samples from troll fisheries were subsequently excluded from input to the model. The region 2 "troll" sample could not be attributed to a capture fishery in the model as it had been collected by scientists during a biological sampling cruise. The region 3 sample was excluded because of conflict between the modal structure of the troll length composition data with the other growth information available to the model (this is discussed further in the Discussion section), but we performed a sensitivity analysis where it was included (Section 6.2). The ages expressed in decimal years were translated into quarters to be consistent with the temporal structure assumed in the model. The remaining 8 samples made up a total of $n = 1572$ age-length observations input to the model.

5 Model description

5.1 General characteristics

The model can be considered to consist of several components, (i) the dynamics of the fish population; (ii) the fishery dynamics; (iii) the dynamics of tagged fish; (iv) the observation models for the data; (v) the parameter estimation procedure; and (vi) stock assessment interpretations. Detailed technical descriptions of components (i)–(iv) are given in Hampton and Fournier (2001) and Kleiber et al. (2017). In addition, we describe the procedures followed for estimating the parameters of the model and the way in which stock assessment conclusions are drawn using a series of reference points. In this section, model settings primarily refer to those used within the 'diagnostic case' model.

5.2 Population dynamics

The model partitions the population into five spatial regions (under the 2018 regional structure) and 48 quarterly age-classes. The last age-class comprises a 'plus group' in which mortality and other characteristics are assumed to be constant. The population is 'monitored' in the model at quarterly time steps, extending through a time window of 1960–2016. The main population dynamics processes are as follows.

5.2.1 Recruitment

Recruitment is defined as the appearance of age-class 1 fish (i.e. fish averaging $\sim$ 35-50 cm given estimated growth curves) in the population. In contrast to the tropical tunas, spawning of South Pacific albacore occurs during the Austral summer. Recruitment was allowed to occur in each quarter although the nature of the data sources were expected to result in recruitment mainly occurring during the expected time periods. It was assumed that recruitment occurs instantaneously at the beginning of each quarter. This is a discrete approximation to continuous recruitment, but provides sufficient flexibility to allow a range of variability to be incorporated into the estimates as appropriate.

Spatially-aggregated (over all model regions) recruitment was assumed to have a weak relationship with spawning potential *via* a Beverton and Holt stock-recruitment relationship (SRR) with a fixed value of steepness (h). Steepness is defined as the ratio of the equilibrium recruitment produced by 20% of the equilibrium unexploited spawning potential to that produced by the equilibrium unexploited spawning potential (Francis, 1992; Harley, 2011). Typically, fisheries data are not very informative about the steepness parameter of the SRR parameters (ISSF, 2011); hence, the steepness parameter was fixed at a moderate value (0.80) and the sensitivity of the model results to the value of steepness was explored by setting it to lower (0.65) and higher (0.95) values.

In the diagnostic case model, it was assumed that annual recruitment was related to annual mean spawning potential, as recommended by the 2011 Bigeye Tuna Peer Review (Ianelli et al., 2012) and implemented for the 2015 South Pacific albacore assessment (Harley et al., 2015) and most recent WCPO tropical tuna assessments (McKechnie et al., 2016a, 2017a; Tremblay-Boyer et al., 2017).

The SRR was incorporated mainly so that yield analyses and population projections could be undertaken for stock assessment purposes, and the determination of equilibrium- and depletion-based reference points. We therefore applied a weak penalty (equivalent to a CV of 2.2) for deviation from the SRR so that it would have negligible effect on recruitment and other model estimates (Hampton and Fournier, 2001), but still allow the estimation of asymptotic recruitment. This approach was recommended (recommendation 20) by the review of the 2011 bigeye stock assessment (Ianelli et al., 2012). The SRR was calculated over the period from 1970–2015 to prevent the early recruitments (which appear to be part of a different 'regime' to subsequent estimates and may not be well estimated in any case), and the terminal recruitments (which are not freely estimated), from influencing the relationship, which is consistent with the approach of the 2015 assessment.

The distribution of recruitment among the model regions was estimated within the model and allowed to vary over time in a relatively unconstrained fashion. We investigated model structures in which all recruitment was assumed to originate in the southern regions (3 and 5), but found that, when the average distribution of recruitment among regions was estimated, the southern regions

dominated the distribution in any case. We therefore allowed all models to estimate the average regional distribution of recruitment, but used initial values for these estimates that put the bulk of the recruitment in the southern regions. In contrast, the 2015 assessment's starting values had $\sim$ 30% of the recruitment in the tropical regions (2015 regions 1 and 4), based on predictions from a SEAPODYM study (Harley et al., 2015), although young albacore are rarely caught outside of the southern-most regions. The spatial pattern of recruitment in the current assessment is therefore felt to be an improvement over previous assessments.

5.2.2 Initial population

The population age structure in the initial time period in each region was assumed to be in equilibrium and determined as a function of the average total mortality during the first 20 quarters. This assumption avoids having to treat the initial age structure, which is generally poorly determined, as independent parameters in the model.

5.2.3 Growth

The standard assumptions for WCPO assessments were made concerning age and growth: 1) the lengths-at-age are normally distributed for each age-class; 2) the mean lengths-at-age follow a von Bertalanffy (VB) growth curve; 3) the standard deviations of length for each age-class are a log-linear function of the mean lengths-at-age; and 4) the probability distributions of weights-at-age are a deterministic function of the lengths-at-age and a specified weight-length relationship. These processes are assumed to be regionally and temporally invariant.

For the diagnostic case model, growth was estimated within the model through fitting to the available age-at-length information from the longline fleet and the size data. Following the previous assessment, age-at-length data from the troll fleet were discarded due to the known conflicts between these and other data (Section 4.7, see also Harley et al., 2015). The L1 parameter, the length at which individuals first enter the fishery, was fixed at 34.2 cm based on the estimated parameters from a sex-combined von Bertalanffy function fitted to the full age-at-length data by Williams et al. (2012). This allows L1 to be associated with a specific age, in this case 0.5 years.

The growth curve is a significant focus of the current assessment and represents one of the major uncertainty axes in the model grid. The alternative growth hypotheses considered in the assessment to assess the impact of this uncertainty will be described in Section 6.2.

5.2.4 Movement

Movement was assumed to occur instantaneously at the beginning of each quarter *via* movement coefficients that connect regions sharing a common boundary. Note that fish can move between non-contiguous regions in a single time step due to the 'implicit transition' computational algorithm employed (see Hampton and Fournier, 2001 and Kleiber et al., 2017 for details). Movement is parameterised as the proportion of fish in a given region that move to the adjacent region. Across each inter-regional boundary in the model, movement is possible in both directions for the four quarters, each with their own movement coefficients. Thus, the number of movement parameters is 2 $\times$ no.region boundaries (6) $\times$ 4 quarters. The seasonal pattern of movement persists from year to year with no allowance for longer-term variation in movement. Usually there are limited data

available to estimate age-specific movement and the movement coefficients are normally invariant with respect to age. A prior of 0.1 is assumed for all movement coefficients, inferring a relatively high mixing rate between regions. A low penalty is applied to deviations from the prior.

5.2.5 Natural mortality

Our modelling of natural mortality was consistent with the 2015 assessment whereby a fixed, age-invariant M of 0.3 was set in the diagnostic case. This was formulated to be consistent with other albacore stock assessments, e.g., ICCAT (Dr L Kell, pers. comm.) and a previous North Pacific assessment (ISC Albacore Working Group, 2011).

We consider M to be a key source of uncertainty and therefore alternative natural mortality scenarios were examined (see Section 6.2).

5.2.6 Sexual maturity, or reproductive potential-at-age

Reproductive output at age, which is used to derive spawning potential, attempts to provide a measure of the relative contribution of fish at different ages to the next generation. For this assessment, we used a new feature of MULTIFAN-CL allowing the relative reproductive potential to be specified by length class, with internal conversion to age class using the growth parameter estimates of the model. Relative reproductive potential was computed as the multiple of length-specific vectors for the proportions of females in the population (based on a large number of albacore sexed and measured by observers) and the proportions of females mature (Farley et al., 2014). This input is displayed in Figure 12. This curve is updated from that of the 2015 assessment to account for the declining availability of females at larger lengths.

5.3 Fishery dynamics

The interaction of the fisheries with the population occurs through fishing mortality. Fishing mortality is assumed to be a composite of several separable processes - selectivity, which describes the age-specific pattern of fishing mortality; catchability, which scales fishing effort to fishing mortality; and effort deviations, which are a random effect in the fishing effort - fishing mortality relationship.

5.3.1 Selectivity

In many stock assessment models, selectivity is modelled as a functional relationship with age, e.g. using a logistic curve to model monotonically increasing selectivity and various dome-shaped curves to model fisheries that select neither the youngest nor oldest fish. Modelling selectivity with separate age-specific coefficients (with a range of 0-1), constrained with smoothing penalties, allows more flexibility but has the disadvantage of requiring a large number of parameters. In most cases we have instead used the same methods as the 2015 assessment which was based on cubic spline interpolation techniques. This is a form of smoothing, but the number of parameters for each fishery is the number of cubic spline 'nodes' that are deemed to be sufficient to characterise selectivity over the age range. We used five nodes, which seemed to be sufficient to allow for reasonably complex selectivity patterns. All selectivities were constrained such that the selectivity of the last two age

classes was equivalent. Selectivity coefficients for the longline fisheries were computed over age-class ranges of 5–48, except for fleets in the southernmost regions which were allowed to catch younger fish (age-class ranges of 3–48), for troll fisheries over ranges of 3–46 and for driftnet fisheries over ranges of 5–46. Coefficients outside these ranges were set to zero.

In a previous South Pacific albacore assessment (Hoyle et al., 2012), the albacore population was modelled in a single spatial region, requiring that seasonal selectivity for the longline fisheries be modelled to account for the movement-driven seasonal availability of different-sized albacore to the different fisheries. In the current assessment, spatial structure and movement is explicit, so this enabled non-seasonal selectivity for longline fisheries to be employed. Explicit spatial structure also allowed simplifying assumptions to be made regarding the form of the selectivity curve for the longline fisheries in each region. For each fishery, we assumed that the oldest albacore were fully recruited. To encourage this behaviour, selectivity coefficients were penalized to be non-decreasing for successively older age-classes. We initially tested the assumption that the Index longline fisheries in all regions shared common selectivity coefficients. However, it was found that this resulted in severe lack of fit to the size data for several of those fisheries and therefore independent selectivity coefficients were allowed.

5.3.2 Catchability

Constant (time-invariant) catchability was assumed for the Index longline fisheries in each region; Table 4). This assumption is similar to assuming that the CPUE for these fisheries indexes the exploitable abundance over time. The Index longline fisheries were assumed to share catchability parameters, thus providing the model with information on the relative population sizes among regions.

For all other fisheries, catchability was allowed to vary slowly over time (akin to a random walk) using a structural time-series approach. Random walk steps were taken every two years, and the deviations were constrained by prior distributions of mean zero and standard deviation of 0.1.

5.3.3 Effort deviations

Effort deviations were used to model the random variation in the effort - fishing mortality relationship, and are constrained by pre-specified prior distributions (on the log-scale). There were several categories of fisheries with respect to the effort deviation penalties applied and these are outlined in Table 4 and presented in Figure 13. The region-specific CPUE indices for the Index longline fisheries represent the principal indices of stock abundance, and the extent to which the model can deviate from the indices is controlled by the penalty weights assigned to the standardised effort series. For these fisheries the prior was set to have a mean of zero and the CV was allowed to be time-variant and based on the variance estimates from the GLMs fitted to each fishery (see Tremblay-Boyer and McKechnie, 2018 for more details on the variance estimates). The average CV for the period 1998–2015 was assumed to be 0.2 and the rest of the time-series CV scaled accordingly. The resulting scaled CVs were transformed to an effort deviate penalty for each CPUE observation in MULTIFAN-CL. Penalties are inversely related to variance, such that lower effort penalties are associated with indices having high variance, consequently these indices are less influential in fitting the model.

Finally, for all other fisheries (including the DWFN, PICT and Australia/New Zealand longline) the nominal effort was used, but to prevent the CPUE of these fisheries from influencing population dynamics they received effort deviation penalties equivalent to a CV of about 0.4 for the average effort (Table 4). The penalties for these fisheries were scaled according to the square root of the observed effort (normalised to an average of 1) such that low penalties are applied for low observed effort and higher penalties are applied for high effort.

5.4 Dynamics of tagged fish

5.4.1 Tag reporting

In principle, tag-reporting rates can be estimated internally within the model. In practice, experience has shown that independent information on tag-reporting rates for at least some fisheries tends to be required for reasonable model behaviour to be obtained. Reporting rates were allowed to vary across fisheries, but were assumed to be common across tag release groups. We adjusted tag release numbers to account for tag returns that could not be included in the data because of insufficient recapture information. This is an important source of non-reporting, particularly for models where the tag return data need to be stratified by spatial regions. This adjustment was made to preserve the observed rate of tag recapture by release group in the original data (Berger et al., 2014).

We also further adjusted the tag release numbers downwards by a factor of 0.5 to account for likely mortality of albacore due to the stress of capture, handling and tagging. Initial tagging mortality (being a type 1 tag loss) operates in a similar fashion to non-reporting and was therefore dealt with by adjusting the releases. The choice of 0.5 as the adjustment factor was somewhat arbitrary, but was influenced by recent work on tagger effects on tagged fish survival and associated correction factors in what are thought to be more robust tropical tunas (Berger et al., 2014). In that study it was found that the median correction factors for tagger effects were 0.68–0.76 for the tropical tunas. Given that albacore are believed to be more sensitive to capture and handling, and were captured by trolling rather than pole-and-line fishing (as used for tropical tuna tagging), it was felt that a stronger correction was appropriate in this case. The 2015 stock assessment also tested a factor of 0.7 and found that this resulted in relatively minor impacts on model results.

5.4.2 Tag mixing

The population dynamics of the fully recruited tagged and untagged populations are governed by the same model structures and parameters. The populations differ in respect of the recruitment process, which for the tagged population is the release of tagged fish, i.e. an individual tag and release event is the "recruitment" for that tagged population. Implicitly, we assume that the probability of recapturing a given tagged fish is the same as the probability of catching any given untagged fish in the same region and time period. For this assumption to be valid either the distribution of fishing effort must be random with respect to tagged and untagged fish and/or the tagged fish must be randomly mixed with the untagged fish. The former condition is unlikely to be met because fishing effort is almost never randomly distributed in space. The second condition is also unlikely to be met soon after release because of insufficient time for mixing to take place.

Depending on the distribution of fishing effort in relation to tag release sites, the probability of

capture of tagged fish soon after release may be different to that for the untagged fish in that model region. It is therefore desirable to designate one or more time periods (quarters) after release as "pre-mixed" and compute fishing mortality for the tagged fish based on the actual recaptures, corrected for tag reporting, rather than use fishing mortalities based on the general population parameters. This in effect de-sensitises the likelihood function to tag recaptures in the pre-mixed periods while correctly removing fish from the tagged population for the recaptures that occurred. We assumed that albacore mix fairly slowly with the untagged population at the region level and that this mixing process is complete by the end of the eighth quarter after release. We investigate the robustness to this assumption in sensitivity analyses. This is a longer period than typically employed for tropical tuna assessments, and was in part motivated by a desire to make the tagging data, for which recapture rates have been typically of the order of only 1%, less influential in the estimation of fishing mortality and abundance.

Tagged fish are modelled as discrete cohorts based on the region, year, quarter and age at release for the first 30 quarters after release. Subsequently, the tagged fish are pooled into a common group. This is to limit memory and computational requirements.

5.5 Likelihood components

There are four data components that contribute to the log-likelihood function for this assessment: the total catch data, the length-frequency data, the tagging data and the conditional age-at-length data.

The observed total catch data are assumed to be unbiased and relatively precise, with the SD of residuals on the log scale being 0.002. Note that this is close to the 'catch conditioned' approach often used in other integrated assessments.

The probability distributions for the length-frequency proportions are assumed to be approximated by robust normal distributions, with the variance determined by the effective sample size (ESS) and the observed length-frequency proportion. Size frequency samples are assigned an ESS lower than the number of fish measured. Lower ESS values recognise that (i) length-frequency samples are not truly random (because of non-independence in the population with respect to size), and would have higher variance as a result; and (ii) the model does not include all possible process error, resulting in further under-estimation of variances. We examined likelihood profiles for all data sources with respect to overall biomass scaling in the assessment (see further details in Section 7.2.6) and found that there was substantial conflict between the size data and other data in the model. In particular, the size data tended to favour higher population scaling than other data sources. In such cases, it is usually considered preferable for stock assessment models to provide the best fit possible to the CPUE indices that to other data sources. For this reason we made the decision to down-weight the size data in the diagnostic case such that the maximum ESS was 20. Alternative specifications of maximum ESS were explored in sensitivity analyses.

A log-likelihood component for the tag data was computed using a negative binomial distribution which provides flexibility for specifying (or estimating) the degree of overdispersion relative to the Poisson distribution. For this assessment, in view of the small amount of tagging data, we simply assumed approximate Poisson equivalence for all models. Trial fits with more overdispersed settings were not influential on the main model results.

A further log-likelihood component is included for models that include the conditional age-at-length

dataset (Harley et al., 2015; McKechnie et al., 2017a). These data are included in the assessment to assist in estimating growth parameters *via* direct observations of fish ages within length classes. The observed age composition within each length interval is assumed to be multinomially distributed, and this forms the basis of the likelihood component for this data source.

5.6 Parameter estimation and uncertainty

The parameters of the model were estimated by maximizing the log-likelihood of all data components plus the log of the probability density functions of the priors and various penalties specified in the model. The maximization to a point of model convergence was performed by an efficient optimization using exact derivatives with respect to the model parameters (auto-differentiation, Fournier et al., 2012). Estimation was conducted in a series of phases, the first of which used relatively arbitrary starting values for most parameters. A bash shell script, "doitall", implements the phased procedure for fitting the model. Some parameters were assigned specified starting values consistent with available biological information. The values of these parameters are provided in the *alb.ini* input file.

In this assessment two approaches were used to describe the uncertainty in key model outputs. The first estimates the statistical uncertainty within a given assessment model, while the second focuses on the structural uncertainty in the assessment by considering the variation among a suite of models.

For the first approach, the Hessian was calculated for the diagnostic case model, and other models of interest, to obtain the estimated covariance matrix, which is used in combination with the delta method to compute approximate confidence intervals for parameters of interest (for example, the biomass trajectories). For the second approach, a factorial grid of model runs was undertaken which incorporated many of the options of uncertainty explored in one-off sensitivity analyses. This procedure attempts to describe the main sources of structural and data uncertainty in the assessment.

For highly complex population models fitted to large amounts of often conflicting data, it is common for there to be difficulties in estimating absolute abundance. Therefore, a likelihood profile analysis (see also above) was conducted for the marginal posterior likelihood in respect of the total average population biomass as a measure of population scaling, following the procedure outlined by McKechnie et al. (2017a) and Tremblay-Boyer et al. (2017) for the 2017 bigeye and yellowfin tuna assessments.

Retrospective analyses are also undertaken as a general test of the stability of the model, as a robust model should produce similar output when rerun with data for the terminal year/s sequentially excluded (Cadigan and Farrell, 2005). The retrospective analyses for the 2018 diagnostic case model are presented in the Appendix (Section 11.1).

5.7 Stock assessment interpretation methods

Several ancillary analyses using the fitted model/suite of models were conducted in order to interpret the results for stock assessment purposes. The methods involved are summarized below and further details can be found in Kleiber et al. (2017).

5.7.1 Yield analysis

The yield analysis consists of computing equilibrium catch (or yield) and biomass, conditional on a specified basal level of age-specific fishing mortality (F_a) for the entire model domain, a series of fishing mortality multipliers (*fmult*), the natural mortality-at-age (M_a), the mean weight-at-age (w_a) and the SRR parameters. All of these parameters, apart from *fmult*, which is arbitrarily specified over a range of 0–50 (in increments of 0.1), are available from the parameter estimates of the model. The maximum yield with respect to *fmult* can easily be determined using the formulae given in Kleiber et al. (2017), and is equivalent to the MSY. Similarly the spawning potential at MSY (SB_{MSY}) can also be determined. The ratios of the current (or recent average) levels of fishing mortality and biomass to their respective levels at MSY are determined for all models of interest, including those in the structural uncertainty grid, and so alternative values of steepness were assumed for the SRR in many of them.

Fishing mortality-at-age (F_a) for the yield analysis was determined as the mean over a recent period of time (2012–2015). We do not include 2016 in the average as fishing mortality tends to have high uncertainty for the terminal data year of the analysis and the terminal recruitments in this year are constrained to be the average over the full time-series, which affects F for the youngest age-classes.

MSY was also computed using the average annual F_a from each year included in the model (1960–2015). This enabled temporal trends in MSY to be assessed and a consideration of the differences in MSY levels under historical patterns of age-specific exploitation.

5.7.2 Depletion and fishery impact

We assess fishery depletion by computing the unexploited spawning potential time series (at the region level) using the estimated model parameters, but assuming that fishing mortality was zero. Because both the estimated spawning potential SB_t (with fishing), and the unexploited spawning potential $SB_{F=0[t]}$, incorporate recruitment variability, their ratio at each quarterly time step (t) of the analysis, $SB_t/SB_{F=0[t]}$, can be interpreted as an index of fishery depletion. The computation of unexploited biomass includes an adjustment in recruitment to acknowledge the possibility of reduction of recruitment in exploited populations through stock-recruitment effects. To achieve this the estimated recruitment deviations are multiplied by a scalar based on the difference in the SRR between the estimated fished and unfished spawning potential estimates.

A similar approach was used to estimate depletion associated with specific fisheries or groups of fisheries. Here, fishery groups of interest, Tropical longline (region 1), Sub-tropical longline (regions 2 and 4), southern longline (regions 3 and 5), troll and driftnet fisheries, are removed in-turn in separate simulations. The changes in depletion observed in these runs are then indicative of the depletion caused by each of the removed fisheries.

5.7.3 Reference points

The unfished spawning potential ($SB_{F=0}$) in each time period was calculated given the estimated recruitments and the Beverton-Holt SRR. This offers a basis for comparing the exploited population relative to the population subject to natural mortality only. The WCPFC adopted $20\%SB_{F=0}$ as a limit reference point (LRP) for the albacore stock, where $SB_{F=0}$ is calculated as the average over the period 2006–2015. Stock status was referenced against these points by calculating $SB_{recent}/SB_{F=0}$

and $SB_{latest}/SB_{F=0}$, where SB_{latest} and SB_{recent} are the estimated spawning potential in 2016, and the mean over 2013–2016, respectively (Table 3), consistent with decisions taken at SC13.

The other key reference point, $F_{recent}/F_{\text{MSY}}$ (Table 3), is the estimated average fishing mortality over the full assessment area over a recent period of time (F_{recent}; 2012–2015 for this stock assessment) divided by the fishing mortality producing MSY (as produced by the yield analysis and detailed in Section 5.7.1).

5.7.4 Majuro and Kobe plots

For the standard yield analysis (Section 5.7.1), the fishing mortality-at-age, F_a, is determined as the average over some recent period of time (2012–2015 herein). In addition to this approach the MSY-based reference points (F_t/F_{MSY}, and SB_t/SB_{MSY}) and the depletion-based reference point ($SB_t/SB_{F=0[t]}$) were also computed using the average annual F_a from each year included in the model (1960–2015, with no value calculated for the terminal year) by repeating the yield analysis for each year in turn. This enabled temporal trends in the reference point variables to be estimated taking account of the differences in MSY levels under varying historical patterns of age-specific exploitation. This analysis is presented in the form of dynamic Kobe plots and "Majuro plots", which have been presented for all WCPO stock assessments in recent years.

6 Model runs

6.1 Developments from the last assessment

The progression of model development from the 2015 reference case to the model proposed as the diagnostic case in 2018 was incremental, with stepwise changes to the model made in-turn to ensure that the consequences of each modification could be assessed. Changes made to the previous assessment model include additional input data for the years 2014–2016, modified methods in producing the input files, new regional structures, updated biological information and data, updated default settings for the diagnostic case (Tremblay-Boyer and McKechnie, 2018), and implementation of new features of MULTIFAN-CL (Davies et al., 2018). The progression through the models is as follows:

- The 2015 reference case model
- **Step 2** Update 2015 assessment with the new MULTIFAN-CL executable (2.0.4).
- **Step 3** Update analyses with new data, reproducing 2015 methods.
- **Step 4** Include Japanese longline data to the CPUE, as they were not available in 2015.
- **Step 5** Remove filtering on targeting clusters in CPUE standardization, and treat targeting cluster as a covariate instead.
- **Step 6** Switch from 2015 to 2018 region structure.
- **Step 7** Based on model diagnostics of the previous step, the tag mixing period was increased from 4 to 8 quarters, and selectivity for southern longline fleets (regions 3 and 5) adjusted to allow selection of younger fish.

- **Step 8** Shift the initial values for recruitment distribution from all regions to southern regions only to allow for more biologically realistic recruitment, but let the model estimate for all regions.
- **Step 9** Switch CPUE standardized index from traditional to geostatistical model.
- **Step 10** Include index longline fisheries to track CPUE and trends in size data of the population.
- **Step 11** Increase the default divisor on the size composition likelihood from 20 to 50.
- **Step 12** Update to new maturity-at-length ogive to account for the disappearance of females at larger lengths, and use the new MULTIFAN-CL capability to estimate maturity-at-age directly from maturity-at-length (Davies et al., 2018).

6.2 Sensitivity analyses

Several hundred runs were undertaken in conducting the 2018 South Pacific albacore assessment, but in terms of presenting information on the bounds of plausible model sensitivity we have focused on a small set of uncertainty axes which are described in further detail below. These axes were used for 'one-off' changes from the diagnostic case model and, depending on the results of these alternative runs, several of the settings in these one-off models were used in the structural sensitivity analyses (after Hoyle et al., 2008a). The latter process involves constructing a grid of model runs where all-possible combinations of the assumptions are explored (see Section 6.3).

The recommendations of the 2018 PAW formed the basis for several of the one-off sensitivity analyses undertaken from the diagnostic case, but several others were undertaken in order to provide a better understanding of the impact of some of the changes in modelling assumptions. Each of the one-off sensitivity runs was carried out by making a single change to the diagnostic case, and it should again be reinforced that these model runs are not carried out to provide absolute estimates of management quantities but to demonstrate the *relative* changes that result from the various changed assumptions, and for that reason the reference points are presented in the Appendix (Tables 11–12).

6.2.1 Steepness [*h0.65, h0.95*]

Steepness is a particularly difficult parameter to estimate in stock assessment models, but if it is fixed in the model, the choice of value may have significant influence on most reference points used in management. As was the case in other tropical tuna and albacore tuna assessments, we assumed a value of 0.8 for the diagnostic case, but examined values of 0.65 (*h0.65*) and 0.95 (*h0.95*) in sensitivity runs. This choice of values is consistent with the results of the meta-analysis conducted on tuna stock-recruitment data and has been well established in previous Scientific Committees.

6.2.2 Relative weighting of size-frequency data [*Size10, Size20, Size80*]

The difficulties in assigning weighting to the length frequency data were discussed in Section 5.5. To assess the sensitivity of model results to the weighting of these data, three alternative models were considered as sensitivities beyond that in the diagnostic case model. Two levels (divisors of 10

and 20) upweight the data relative to the diagnostic case (corresponding to a maximum effective sample size of 100 and 50 fish, respectively), while the other downweights the data (divisor of 80, corresponding to a maximum effective n of 12.5 fish).

6.2.3 Alternative growth functions [*Chen-Wells*]

Given the uncertainty regarding South Pacific albacore growth, the impact on model outputs of an alternative fixed growth assumption was examined. That alternative scenario fixed growth at the parameter values of the sex-combined 'Chen-Wells' growth model (Xu et al., 2014), which was also used within the 2017 North Pacific albacore reference case model run. This model is a composite of two growth curves estimated for the North Pacific Albacore (Wells et al., 2013; Chen et al., 2012) and was used here to have a lower growth alternative to the K from the Williams growth model fitted to the age-at-length data or estimated by MULTIFAN-CL. Both of the latter estimates have high K compared to those estimated for albacore stocks worldwide (Nikolic et al., 2017), and also give extremely poor fit to the clear presumed annual modes observed in the troll fisheries.

6.2.4 Natural mortality [*M0.2, M0.4, M0.5*]

The level of natural mortality was considered a key area of uncertainty within this assessment. In addition to the value of 0.3 used for the diagnostic case, one-off analyses examined the sensitivity of the assessment to the assumption of values of M of 0.2, 0.4 and 0.5.

We also conducted sensitivity analyses using two alternatives to assess the impact of non-constant mortality at age:

- a sex-combined version of the North Pacific natural mortality settings, noting that the M used in that assessment was in the high range of those typically used for albacore tuna assessments. The M-at-age used in the 2017 assessment of North Pacific albacore (ISC Albacore Working Group, 2017) was specified by sex. In order to use equivalent values in this one-off sensitivity, it was necessary to convert these sex-specific values to a sex-aggregated series. This was done by averaging the male and female values, weighted by the sex ratio for each age class.
- A Lorenzen-based approach (Lorenzen, 1996) which assumes a monotonically declining relationship between M with age class a, such that $M_a = f(l_a, b, c)$, where f is the Lorenzen function with parameters b and c, l_a is the mean length-at-age. We set b such that M declined as a function of l_a, and set c so that M for the oldest age class was $0.3yr^{-1}$.

6.2.5 Alternative standardised CPUE indices [*CPUE-Trad*]

The geostatistical approach to standardising CPUE data as used within the diagnostic case model is an update from previous tuna assessments, and also implies faster stock-mixing through the assessment area than the 'traditional' approach which estimates standardized CPUE for each region independently of the other. The impact of this approach on model estimates was examined by comparison to a model fit incorporating the 'traditional' CPUE approach, as outlined in Section 4.4.1 and further described in Tremblay-Boyer and McKechnie (2018).

6.2.6 Excluding tagging data [*No tag data*]

Given the relative paucity of tagging data available for South Pacific albacore, a sensitivity was performed where these data were excluded from the model. This was used to examine the influence the relatively limited quantity of data was having on model outputs.

6.2.7 Tag mixing period of 4 quarters [*Tag mix 4*]

Within the diagnostic case model, tag mixing was set to 8 quarters to limit the influence of tag data and reflect understanding of juvenile movement throughout the region (since individuals are typically tagged as juveniles). We examined the impact of this mixing period with an alternate model with tag mixing at 4 quarters, consistent with tropical tuna assessments and as done in the 2015 assessment.

6.2.8 Old maturity [*Old m-at-age*]

The maturity-at-age ogive used in previous assessments assumed that 100% of the older age classes were mature. This was updated within the diagnostic case model to account for much lower proportions of females in the population at those ages, based upon observer estimates. To examine the impact of this on model outputs, a one-off sensitivity assuming the maturity-at-age ogive used in Harley et al. (2015) was performed.

6.2.9 Maturity-at-age from integrated maturity-at-length [*Integr m-at-age*]

New functionality within MULTIFAN-CL allows maturity-at-age to be calculated from maturity-at-length data and also accounting internally for the variability of ages for a given length, unlike the current approach which uses a deterministic model to convert between lengths and ages. This different approach should result in a higher proportion of smaller fish being deemed mature, modifying the spawning potential, so the impact of using this new approach was examined as a one-off sensitivity.

6.3 Structural uncertainty

Stock assessments of pelagic species in the WCPO in recent years have utilised an approach to assess the structural uncertainty in the assessment model by running a 'grid' of models to explore the interactions among selected 'axes of uncertainty'. The grid contains all combinations of two or more parameter settings or assumptions for each uncertainty axis. The axes are generally selected from those factors explored in the one-off sensitivities with the aim of providing an approximate understanding of variability in model estimates due to assumptions in model structure not accounted for by statistical uncertainty estimated in a single model run, or over a set of one-off sensitivities.

The structural uncertainty grid for the 2018 assessment was constructed from 5 axes – steepness (3 settings: *0.65, 0.80, 0.95*), natural mortality (2: *0.3, 0.4*) size data weighting (3: *20, 50, 80*), growth (2: *Chen-Wells, Estimated*) and methods for CPUE indices (2: *Geostatistics, Traditional*), with the settings used directly comparable to those presented in Section 6.2 through identical notation. The final grid thus consisted of 72 models (Table 5).

7 Results

7.1 Consequences of key model developments

The progression of model development from the 2015 reference case model to the 2018 diagnostic case model is outlined in Section 6.1 and results are displayed in Figure 14 showing changes in the spawning potential compared to its unfished equivalent ('depletion') and in Figure 15 showing changes in the spawning potential. A summary of the consequences of this progression through the models is as follows:

- The 2015 reference case model refitted with the latest version of MULTIFAN-CL (grey line; Figure 14, left panel) produced very similar results to the 2015 version.
- The model with new data but following 2015 methods (blue line) showed more optimistic depletion but otherwise followed the same temporal trends as the previous step.
- The model with traditional CPUE including Japanese data (light blue) scaled biomass down from the previous step to similar levels to 2015 reference case model, especially in the first half of the time-series. Depletion was also more pessimistic.
- The model with traditional CPUE including Japanese data and targeting cluster as a covariate instead of a filter (aquamarine) had more pronounced depletion in the first half of the time-series but was otherwise similar to previous steps.
- The switch from 2015 to 2018 region structure (ochre) scaled the biomass up by a large amount with concurrent more optimistic depletion levels. Depletion at the start of the time-series was very low ($\sim$ 5% of unfished spawning potential).
- The longer tag mixing period and separate selectivities for southern longline fleets (burnt yellow) had minimal effects on depletion or spawning potential estimates, but improved some of the diagnostics (not shown here).
- The change in starting estimates for recruitment distribution between regions (bright yellow) brought depletion and spawning estimates back to similar levels to models with the 2015 region structure (i.e. step 2 through to step 5), though with more optimistic depletion levels.
- The switch to the geostatistical model for CPUE standardization (orange line, Figures 14 and 15, right panel) did not have a strong effect on early depletion levels, but did lead to more pessimistic depletion from the late 1970s onwards, resulting in similar depletion estimates to those from models with 2015 region structure at the end of the time series. The decline in the spawning potential estimates was also more pronounced. This model indicated a recovery of the stock in the most recent period (less depletion), consistent with the geostatistical CPUE time series.
- Using Index fisheries to track CPUE and trends in size data in the population (purple) led to more pessimistic depletion levels by a few percentage points and slightly lowered predicted spawning potential in the early period of the time-series.
- Additional downweighting of the size composition likelihood (orchid) led to the most pessimistic depletion estimates in this stepwise progression, but had minimal impact on the spawning potential estimates, indicating that there was less of a predicted decline in unfished spawning potential.

– Diagnostic case: The updated maturity-at-length ogive and direct estimation of maturity-at-age from maturity-at-length (dark blue) reduced depletion estimates in the last part of the time-series due to the increased contribution of younger age classes to the spawning potential.

7.2 Model fit for the diagnostic case model

This section discusses the model results for the diagnostic case model, defined by the final step in the stepwise model development (*Diagnostic case*; Figure 14), in particular the fit to the various sources of data, and the biological and fisheries-related parameters.

7.2.1 Catch data

Very high penalties were applied to the catch data for all fisheries and so the residuals of the observed and model-predicted catches were very small (Figure 16).

7.2.2 Standardised CPUE

There was very high variation in the first two decades of the standardised indices in each region Figure 17 and there appears to have been some decrease in CPUE over that period. On the whole the model fits the data well although there is a tendency for the model to underestimate CPUE somewhat during this early period, but it should be noted that penalties for fitting CPUE in that period are also lower (Figure 13). This can be attributed partly to the inability of the model to replicate the significant variation between time steps, that is, it tends to fit those data points with lower CPUEs well over that period (Figure 17), but struggles to simultaneously fit the very high CPUEs, which are often adjacent. The model predicted moderate seasonal variation in CPUE in each region, though the magnitude was less than observed in the standardised indices.

The plots of effort deviates for each fishery over time indicate an adequate fit to the CPUE indices (Figure 18), with no systematic departures from a distribution around zero.

7.2.3 Size frequency data

There was a generally reasonable fit to the time-aggregated length frequency data for fisheries with adequate sample sizes (Figure 19), particularly the longline fisheries in several regions. There was certainly some lack of fit for several fisheries, as occurred during the 2015 assessment, although it seems to be reduced in the current assessment due to the splitting of longline fisheries within regions. The worse fit to several of the fisheries (e.g. DWFN LL 5, PICT LL 3, PICT.AZ LL 5) can often be attributed to small sample sizes and highly variable data with large fluctuations in lengths between years (Figure 20). This suggests the model is not currently specified at the level of detail required to capture the variability seen in these data. In other cases (e.g. combined Australia/New Zealand longline fleet in region 3: AZ LL 3), the moderately poor fits seem to relate to trends in lengths over time that cannot be explained during a period of declining population abundance (Figure 20).

There appears to be improved fit to the troll fisheries data compared to the 2015 assessment, presumably due to the growth function better reflecting the modal progression observed in these

data. The model is still unable to fit the modal structure closely (Figure 19) but the deviations between the observed and model predicted distribution have been much reduced since 2015.

7.2.4 Tagging data

The model appeared to fit the overall tagging data adequately (Figure 21). However, it should be noted that the number of tag returns is significantly lower than the other tuna species assessed by SPC in the WCPO.

The observed and model-predicted tag returns by time-at-liberty across all tag release events for the diagnostic case model were very similar (Figure 22). The tagging reporting rate parameters were estimated to be low for all reporting rate groupings, and in contrast to the 2015 assessment, there were no cases against or close to the upper bound of 0.9 (Figure 23, see also Section 7.3.4).

7.2.5 Conditional age-at-length data

We assess the diagnostic fit to the age-at-length data here, but implications of the fitted growth model are further discussed in Section 7.3.5. The estimated mean age-at-length showed variable fit to the otolith ageing information over the range of ages for which there were data (Figure 24). The model had a tendency to overestimate length for age classes below about 15 quarters, underestimate lengths at higher age classes ($\sim >$ 30 quarters), but fit well for the intermediate ages. It should be noted however that the variation in age-at-length (age-dependent standard deviation) is high across all age classes and that some lengths are only found in certain regions that appear to have different growth signals (e.g. juveniles in the New Zealand troll fisheries). Similar trends were observed during the 2015 assessment, and different growth models were used in the structural grid to account more comprehensively for the uncertainty in growth in this iteration of the assessment. Figure 24 also includes the predicted age-at-length from the Chen-Wells growth model as a reference, but noting that the parameters for this model were fixed and not informed by the conditional age-at-length data.

7.2.6 Likelihood profile

The change in negative log-likelihood relative to the minimum is shown for the total likelihood (black line) and the individual data components (coloured lines) in Figure 25. This displays significant declines as the parameter moves further away from the maximum value of the diagnostic case model, although the curves for the individual components display different levels of support for the mean total biomass. We also included the effort deviation likelihood profile aggregated over catch and Index fisheries (Figure 26 and 27), which shows that the maximum index fishery likelihood coincided with that of the overall model for the effort deviates, and balanced that between catch and Index fisheries for the size data. The total likelihood corresponds with that of the CPUE data which was a desirable outcome, but note that the likelihood is relatively flat in the vicinity of the minimum value.

7.3 Model parameter estimates (diagnostic case)

Estimates from the diagnostic case are presented here in a detailed form, e.g. by fishery and region, so that model behaviour can be assessed. We do not present these results for all models in the structural uncertainty grid, because of the sheer volume of material that this would entail. However, results for all models are available on request.

7.3.1 Catchability

Time-series changes in catchability were estimated for all fisheries apart from the Index fisheries (Figure 28). Many of the time-series display significant variation in this parameter and often do not show any general trends. These changes in catchability over time can be due to many factors apart from the technical efficiency of the gear in catching fish on a set-by-set basis, e.g. changes in the spatial distribution of the fleet(s) within the region and changes in the composition of the fleet(s) over time. Of particular note is the declining trend early in the time series for the longline fisheries in the northern regions (DW LL 1 and DW LL 4) perhaps reflecting an early change in targeting away from albacore towards the tropical tunas.

7.3.2 Selectivity

The estimated selectivity functions for each fishery were largely as expected, and are displayed in Figure 29. The driftnet and troll fisheries were estimated to have very narrow dome-shaped selectivities, with very few fish older than about 10 quarters being selected. All longline fisheries showed asymptotic, or near-asymptotic selectivity, however some differences among these fisheries were evident. The longline fisheries in the southern regions showed a tendency to select fish of a younger age and in some cases this included fish well below 10 quarters of age (e.g. AZ LL 3, PICT LL 3, DWFN LL 3 and 5). The subtropical and tropical fisheries tended to only select fish once they were at least about 15 quarters of age, with perhaps the most extreme examples being in region 2 (e.g. AZ LL 2, PICT LL 2). There was evidence for moderate differences in selectivity between longline fisheries in the same region (e.g. AZ LL 2 vs DWFN LL 2), which may reflect differences in operational characteristics or the spatial coverage of the respective fleets. The shape of the selectivity curves for the Index fisheries also show differences among regions. We initially attempted to fit the model with selectivity shared across these fisheries; however the fits to the size data were poor and this assumption was subsequently relaxed.

7.3.3 Movement

Figure 30 provides a graphical representation of the seasonal movement coefficients for the diagnostic case model among model regions. There is strong movement into region 2 from all other regions during the 3rd quarter and to a lesser extent in the 4th quarter, consistent with the generally higher CPUE in region 2 longline fisheries in those quarters. Similarly, there is high movement from region 2 to region 3 in the first quarter, again consistent with the seasonal occurrence of fisheries in this region.

7.3.4 Tag Reporting Rates

The estimated tag reporting rates by fishery are displayed in Figure 23. The reporting rates are have relatively diffuse priors because there is no means of independently assessing the reporting rate, or other related tag losses, such as initial tagging mortality, that would be reflected here. The estimates therefore reflect which fisheries reported the tag recaptures, and as a result the tagging data are not strongly influential in determining fishing mortality rates and abundance.

7.3.5 Growth

For the diagnostic case, a standard von Bertalanffy (VB) growth curve is estimated internally by the assessment model, with information on growth derived from length frequency data and age-at-length data, compiled into quarterly age classes. These latter data were reported by Williams et al. (2012). The estimated VB curve fits the age-at-length data well and indicates rapid growth for the youngest age-classes – growth of approximately 20 cm over two years from an initial size of 50 cm. Sizes close to the maximum length (approximately 100 cm) are attained at around six years (24 quarters) of age. The estimated standard deviation of age-at-length increases with age and is approximately 6.2 cm for the final age class (Figure 24). This is necessary to fit the size frequency data observed for the longline fisheries (maximum size of around 115 cm) and is also supported by the high apparent variation in age-at-length observed in the otolith dataset.

The rapid growth of 50-70 cm albacore estimated by the fitted VB growth curve is inconsistent with inferred annual modes in the length frequency data for the troll and driftnet fisheries (Figure 31). These modes are presumed to represent annual cohorts because reproductive biology studies clearly demonstrate strongly seasonal spawning for albacore, peaking during the austral summer (Farley et al., 2014). The spacing of the three clearest modes in the 50-70 cm size range would suggest annual growth rates of approximately 10 cm per year, rather than 20 cm per year inferred from the fitted VB curve. We attempted many trial fits to simultaneously fit the troll/driftnet fishery size data and age-at-length data, but these attempts were unsuccessful—there seems to be a fundamental inconsistency that cannot be resolved with the current data but could be due to:

- The lack of otolith data for fish < 70 cm;
- The possibility of a regional difference in growth, slower in the southern regions where the troll fishery and smaller individuals occur, than in the subtropical regions to the north where the majority of the otolith sampling took place (Figure 11).

Additional otolith analysis, ideally from fish taken from the distinctive modes in the troll fishery, may help resolve this issue (see Research recommendations). Meanwhile for this assessment, albacore growth remains a significant uncertainty, leading us to include an alternative, externally-specified growth model used for North Pacific albacore (Xu et al., 2014) in the structural uncertainty grid. A similar model ensemble approach to addressing growth uncertainty was also recommended by Kolody et al. (2016) in a recent review on modelling tuna growth for t-RFMO assessments.

7.4 Stock assessment results

7.4.1 Recruitment

For the diagnostic case, recruitment is estimated to occur primarily in the southern regions 3 and 5 (Figures 32 and 35). This is consistent with where small albacore first appear in the troll fishery, and also where smaller albacore occur in longline fisheries.

Overall, recruitment is estimated to have declined during the 1960s and 1970s, and to have then gradually increased to a moderate level thoughout the 1980s and 1990s. The estimated initial decline in recruitment should be interpreted with caution, because it is responding to sharply declining longline CPUE during this period that cannot be explained by fishing mortality due to the relatively small level of catch. It is more likely that the initial decline is a catchability effect, as it occurs during a period when the Japanese longline fleet was transitioning to target tropical tunas. Recruitment shows considerable inter-annual variation, thought to be influenced positively by La Niña conditions and negatively by El Niño conditions (Lehodey et al., 2015).

The estimated SRR for the diagnostic case model is presented in Figure 33.

7.4.2 Biomass

The temporal pattern in spawning potential at the regional scale is consistent with the results presented for the 2015 stock assessment (Figures 34 and 35). Spawning potential declines from an initial high in the 1960s and stays relatively constant from the 1990s onwards, with a slight increase in recent years. This initial decline is recruitment driven, which as noted earlier, should be interpreted with caution. The absolute spawning potential is scaled up compared to the 2015 assessment, largely as a result of additional younger age classes being included in the spawning potential with the incorporation of the relative maturity at length data.

Region 2 is estimated to support the highest proportion of the spawning potential, with region 3 also being important, and regions 1, 4, 5 representing smaller proportions. Compared to the 2015 assessment (and accounting for the change in region structure), the tropical regions contain less spawning potential in this assessment and there is more of the biomass between 25° S and 10° S (region 2).

These patterns are mirrored in the estimates of longline vulnerable (exploitable) biomass (Figure 36), which show initial declines followed by episodic increases and decreases. For regions 2 and 3, there has been a strong increase in vulnerable biomass during the final 5 years of the assessment period (2011-2016). A similar general trend can be seen in the vulnerable biomass of the Index fleets (Figure 37), with vulnerable biomass increasing over a similar period in region 2 after a period of decline from the late 1980s to around 2010, while in region 3 vulnerable biomass has increased since the 1990s. Note the horizontal red lines indicate the regional weights, which also scale the vulnerable biomass presented in Figure 36.

7.4.3 Fishing mortality

A steady increase in fishing mortality of adult age-classes is estimated to have occurred over most of the assessment period (Figures 38 and 39), accelerating since the 1990s but declining following

the decline in catch since 2010. Juvenile fishing mortality increased until around 1990, with a large spike in the late 1980s due to the driftnet fishery, and has remained stable at a comparatively low level since that time.

The fishing mortality-at-age estimates by region (Figure 40) highlight patterns that match the distribution of fleets by region. Where longliners are most active there is an increase over time in fishing mortality on large age classes, matching the aggregated pattern. Region 4 is distinctive for high fishing mortality on the oldest age classes, consistent with the selectivity estimates for fisheries in that region. In regions with troll and driftnet fleets (3 and 5), fishing mortality on juveniles is higher (with the distinct peak in 1989 from driftnet catch), and is highly seasonal.

7.5 Multimodel inference - stepwise model development, sensitivity analyses and structural uncertainty

7.5.1 One-off changes from the structural uncertainty analysis

Comparisons of the spawning potential, and depletion trajectories for the diagnostic case and one-change sensitivity runs from the structural uncertainty analysis are provided in Figures 41–42. The key reference points are compared in Appendix Tables 11–12 (one-off sensitivity models) and Tables 7–10 (structural uncertainty grid), and the likelihood components are provided in Appendix Tables 13–14. In addition to discussions from PAW, the results from these one-off sensitivities informed the selection of the grid axes and levels therein.

Steepness [*h0.65, h0.95*]

Low penalties on fitting the SRR relationship means that the value of steepness specified in the model has a negligible effect on fit and time-series estimates of spawning potential. Given steepness is more influential when levels of depletion are high, and since under the diagnostic case the stock tends to remain above 40% depletion, the impact of steepness was limited. Slightly different predictions of spawning potential depletion were estimated, with the low (h0.65) and high (h0.95) steepness models suggesting a stock that is more or less depleted, respectively, consistent with previous assessments of tuna in the WCPO: low and high steepness values lead to more pessimistic and optimistic estimates of stock status, respectively. This is particularly the case for MSY and MSY-based reference points ($F_{recent}/F_{\text{MSY}}$ for the diagnostic case, *h0.65* and *h0.95* were 0.29, 0.38 and 0.21, respectively) while the depletion-based reference points tend to be less sensitive to assumed steepness (Appendix Table 12).

Weighting of the size-frequency data [*Size10, Size20, Size80*]

The three models with alternative size frequency data weighting (divisors of 10, 20 and 80) had differing impacts on model outputs. With the divisor of 10, spawning potential depletion was more optimistic by ∼15% and there was a pronounced scaling upward of both the fished and unfished (not shown) spawning potential. Trends were less pronounced with the alternative divisors, with the divisor of 20 scaling upward the spawning potential and lowering the depletion slightly (slightly more optimistic) compared to the diagnostic case, and the divisor of 80 having the opposite effect. This effect of the size data weighting is likely due to the lack of trend in the length data, which is interpreted by the model as a lack of fishing impact (as otherwise we would expect older, larger fish to progressively disappear from the population).

Alternative growth functions [*Chen-Wells*]

The alternative scenario fixing growth at the Chen-Wells parameters (as used in the 2017 North Pacific reference case, (ISC Albacore Working Group, 2017) resulted in a decrease in the spawning potential, especially in the first half of the time-series, and a concurrently more pessimistic depletion estimate by about 8% ($SB_{F=0} \sim 38\%$ in 2016). This trend is expected given the much lower K of the Chen-Wells model (~ 0.25 compare to about 0.47 in the estimated model), which for the given level of natural mortality would result in higher sensitivity to fishing pressure.

Alternative natural mortality M [*M0.2, M0.4, M0.5*]

Assuming a natural mortality value $M = 0.4$ or $M = 0.5$ led to much more optimistic depletion estimates, and increased spawning potential, indicative of a more productive stock. Conversely, under $M = 0.2$ the terminal depletion was ∼25% with starting values ∼80%, and spawning potential was also lower, especially in the earlier part of the time-series.

Alternative natural mortality-at age from North Pacific M [*NP m-at-age*]

Use of the sex-combined version of the North Pacific albacore natural mortality settings, noting that the M used in that assessment was in the high range of those typically used for albacore assessments, led to much more optimistic depletion estimates, and increased spawning potential. Given that the scaling resembles that found with the $M = 0.5$ alternative, this increase is likely driven by the increased overall natural mortality *vs.* the age-specific estimates.

Alternative natural mortality-at age estimated with the Lorenzen function M [*Lorenzen*]

The temporal trends under the Lorenzen estimates were similar but depletion estimates were more optimistic especially in the early 1990s, by up to 10%. The spawning potential was scaled up for the first part of the time-series.

Alternative standardised CPUE indices [*CPUE-Trad*]

Using the 'traditional' approach to standardizing CPUE instead of the geostatistical method led to more pessimistic depletion estimates for the diagnostic case at the start of the time-series only, with the starting depletion about 9% lower. The estimates of spawning potential are scaled down throughout the time-series, and do not show an abrupt decline in the 1960s seen in the diagnostic case. The traditional CPUE generally predicts less pronounced drops in abundance earlier in the time-series (when catch was relatively low) with relatively constant abundance thereafter, so the model might not have to scale up the population as much to sustain the higher catches in later decades. Of note, the traditional CPUE sensitivity also predicts a steady increase in unfished spawning potential since the 1980s to levels about one fifth higher what they were at the start of the time-series (not shown).

Excluding the tagging data [*No tag data*] The model excluding the tagging data scaled the population up slightly, especially in earlier decades, and also had slightly more optimistic depletion estimates. Temporal trends were otherwise maintained compared to those in the diagnostic case.

Tag mixing period of 4 quarters [*Tag mix 4*] The model with the mixing period reduced to four quarters (repeating the 2015 model default level) had minimal impacts on both depletion and estimates of spawning potential.

Old maturity [*Old m-at-age*] The maturity-at-age ogive used in previous assessments assumed that 100% of the older age classes were mature. This was updated to account for a much lower proportion of females in the population at those ages, based on observer estimates (Figure 12). Using the original maturity-at-age resulted in more pessimistic depletion estimates, with $SB_{F=0}$

about 37% in the final year. The spawning potential estimates were otherwise similar but slightly less variable.

Maturity-at-age from integrated maturity-at-length [*Integr m-at-age*] This sensitivity uses the new approach to calculate maturity-at-age from maturity-at-length data. It accounts for variability of ages for a given length and typically results in a higher proportion of younger fish being deemed mature. It had minimal impacts on depletion estimates.

7.5.2 Structural uncertainty analysis

The results of the structural uncertainty analysis are summarised in several forms – time-series plots of fisheries depletion for all models in the grid (Figures 43, 44 and 45), boxplots of $F_{recent}/F_{\text{MSY}}$ and $SB_{latest}/SB_{F=0}$ for the different levels of each of the five axes of uncertainty (Figure 46), Majuro and Kobe plots showing the estimates of $F_{recent}/F_{\text{MSY}}$ and $SB_{latest}/SB_{F=0}$ (and $SB_{recent}/SB_{F=0}$ for comparison) across all models in the grid (Figures 47 and 48), and averages and quantiles across the full grid of 72 models (and specific subsets of models) for all the reference points and other quantities of interest (Tables 6–10) that have also been presented for the diagnostic case model and one-off sensitivity models.

Many of the results of the structural uncertainty analysis are consistent with the results of previous assessments of tuna stocks in the WCPO that used the same uncertainty axes, notably for M and steepness. However, additional axes have been included in this assessment and these have significant consequences for summaries of stock status and resulting management implications. In addition, the transition from diagnostic case to grid-derived metrics of stock status requires thoughtful selection of the grid levels included when building the summary statistics, especially in instances where a level shifts estimates up or down in a predictable manner (e.g. M, see below).

The general features of the structural uncertainty analysis are as follows:

- The grid contains 72 models showing a wide range of estimates of stock status, trends in abundance and reference points. The uncertainty identified is higher than for previous assessments for this albacore stock, but none of the runs fell below the LRP of 20% $SB_{F=0}$. The terminal depletion (2016) ranges from 0.30 to 0.77 of $SB_{F=0}$ (0.32 to 0.72 for $SB_{recent}/SB_{F=0}$), with distinct patterns under some axes.
- The most influential axis was that of natural mortality. The median depletion for runs with M=0.4 was on average 20% more optimistic than that for runs with M=0.3. There was no overlap between the 90% quantile bands for the two levels (Figure 45). This result is significant for management considerations as the 2015 management advice was developed solely using M=0.3.
- The subset of models with M=0.3 have a median terminal depletion of 42.4%, ranging between 29.5% and 54.8%. The subset of models with M=0.4 have a median depletion of 62.0%, ranging between 48.2% and 76.9%.
- The next most influential axis is the growth which further subsets the runs into two distinct categories in terms of depletion trends, with virtually no overlap from 1980 onwards. For a given model configuration, the estimated growth always predicts a more optimistic depletion (average +6.8%) except for a few runs under the highest size downweighting level (80), which also have the lowest estimated K for the runs where growth was estimated.

- CPUE is the next most influential axis. Overall the geostatistical CPUE results in a slightly higher median depletion but the traditional CPUE runs are more variable in terms of the initial depletion. In general, traditional CPUE start from a more depleted state in the 1960s but the depletion rates match those from the geostatistical runs from the 1980s to recent years. The geostatistical runs almost all show a switch towards more optimistic depletion estimates starting in 2012, whereby the traditional CPUE runs predict ongoing increases in the depletion of the spawning potential.
- Size weighting was not a main driver for grid trends, with a change from size weighting of 80, through the diagnostic case weighting of 50, to 20 indicating small increases in depletion, but variable impacts on fishing mortality (see Section 7.5.1 for discussion of weighting under the divisor of 10). However, the impact of the size weighting was very model configuration specific. This can be especially seen when tracking the trajectory of depletion from the initial depletion stage, with in some instances a size weighting of 20 resulted in more optimistic depletion estimates, while in other cases the opposite pattern occurred.
- The steepness axis had minimal influence on the grid for runs predicting lower, more optimistic depletion estimates, but runs approaching 40% depletion had a clear pattern with 0.65 and 0.95 steepness resulting in more pessimistic and more optimistic terminal depletion, respectively. This is expected as a shallower SRR should only become influential once the spawning potential reaches lower levels.

7.5.3 Further analyses of stock status

There are several ancillary analyses related to stock status that are typically undertaken on the diagnostic case model (dynamic Majuro analyses, fisheries impacts analyses etc.). The shift towards relying more on multimodel inference for the 2018 assessment makes it more difficult to present these results over a large number of model runs. In this section we rely heavily on the tabular results of the structural uncertainty grid (Tables 6–10). Where space allows, diagnostic plots are presented for example models from the grid with different estimates of stock status.

Fishery impacts for example models

It is possible to attribute the fishery impact (with respect to depletion levels) to specific fishery components (grouped by gear-type), in order to estimate which types of fishing activity have the most impact on spawning potential (Figure 49). The majority of the fisheries depletion in each region over the entire assessment period can be attributed to longline fisheries, and in the terminal years of the assessment this is almost entirely the case. The sub-tropical longline fleets (region 2 and 4) have the most impact overall, though in region 3 the temperate longline fleet has most of the impact. In region 1 the longline impact is mostly split between that of the tropical and sub-tropical fleets, though in earlier years the temperate longline fleet also had a significant impact. The driftnet fishery is estimated to have had a moderate impact on depletion over the years it operated and this impact occurred in all regions to a degree, despite the fishery only occurring in region 3, owing to the movement of fish among regions. The troll fisheries has a relatively low impact on the stock, being most notably in regions 3 and 5 where this fishery operates.

Yield analysis and equilibrium estimates across the grid

The yield analyses conducted in this assessment incorporates the spawner recruitment relationship (Figure 33) into the equilibrium biomass and yield computations. Importantly, in the diagnostic

case model, the steepness of the SRR was fixed at 0.8 so only the scaling parameter was estimated. Other models in the one-off sensitivity analyses and structural uncertainty analyses assumed steepness values of 0.65 and 0.95.

The ratio of SB_{MSY} to SB_0 was estimated to be between 0.07 and 0.23 (median = 0.16), and the ratio of SB_{MSY} to $SB_{F=0}$ was estimated to be between 0.06 and 0.22 (median = 0.15). While this uncertainty appears much wider than in the 2015 assessment, a wider range of uncertainties were examined in the current assessment, and these estimates are in particular notably sensitive to the growth and mortality configurations (see Tables 7 to 10).

A plot of the yield distribution under different values of fishing effort relative to the current effort are shown in Figure 50 for models representing different parts (e.g. more optimistic vs pessimistic outcomes) of the structural uncertainty grid. For the diagnostic case model it is estimated that MSY would be achieved by increased fishing mortality by a significant amount, although the resulting increase in yield would be relatively minor. The right-hand arm of the yield curve displays a very gradual decline in yield with increasing in fishing mortality. The different example models shown display a similar pattern over the scale of fishing mortality although the absolute value of the yield curve differs quite significantly, along with the level of fishing mortality that would achieve MSY – the more optimistic models with $M = 0.4$ estimate that MSY would occur at a much higher fishing mortality multiplier, but the relative gains in yield would again be minimal.

The yield analysis also enables an assessment of the MSY level that would be theoretically achievable under the different patterns of age-specific fishing mortality observed through the history of the fishery (Figure 51). For the diagnostic case model the MSY level was estimated to be relatively stable (in comparison to other WCPO tunas) with a moderate reduction in MSY over the middle years of the assessment when troll and driftnet fisheries selecting for smaller fish contributed more (proportionally) to the overall catch levels.

Dynamic Majuro and Kobe plots and comparisons with Limit Reference Points

The section summarising the structural uncertainty grid (Section 7.5.2) presents terminal estimates of stock status in the form of Majuro plots. Further analyses can estimate the time-series of stock status in the form of Majuro and Kobe plots, the methods of which are presented in Section 5.7.4. The large number of model runs in the structural uncertainty grid precludes undertaking and presenting this process for all runs, however an example for the diagnostic case model is presented in Figure 52. The equivalent dynamic Kobe plots are displayed in Figure 53. At the beginning of the assessment period the stock was almost at unexploited levels though over the first several decades stock status declined steadily on both the Majuro and Kobe plots. Since about 1990 the stock has fluctuated around a similar region, well away from the regions of concern on both plots. The exception was for a short period of time around the operation of the driftnet fishery at the end of the 1980s when the very high fishing mortalities of small fish and reduced estimates of MSY pushed the stock towards, but not into, the region of overfishing in the case of the diagnostic case model.

8 Discussion

8.1 General remarks on the assessment

As noted in previous assessments, South Pacific albacore is a challenging stock to assess for a number of reasons. The main underlying source of difficulty concerns the basic structure of the fishery: exploitation is focused on the oldest segment of the population with relatively little exploitation of pre-adult fish. This means that there is relatively little information in the model to inform on recruitment variability. Also, with the majority of the exploitation focused on fish that are growing very slowly, or have essentially ceased growing, estimating the age composition of catches from length composition, regardless of the quality of growth estimates, is subject to considerable uncertainty. As a result, the information in the data to support estimation of absolute population size is weak, and some of the different data sources, e.g. the size and CPUE data, are conflicting in this regard (Figure 25). In particular, in spite of declines in longline CPUE, mainly during the 1960s, there is little evidence in the data for any decline in either average size, or the disappearance of the largest fish, in the longline catch. This may be a result of the fishery structure noted above, but model misspecification, e.g. unaccounted for changes in selectivity or incorrect growth specification, could also be a factor (Maunder and Piner, 2017; Wang and Maunder, 2017). With regards to selectivity, more detailed analysis of longline setting operations, how they have changed over time, and their interaction with albacore vertical distribution and its environmental determinants, is required for a better understanding of size distribution of the longline catch.

The existence of such data conflicts in integrated stock assessment models is not uncommon. While further investigation of the data conflicts evident in this assessment is necessary, it was reassuring that the overall negative log-likelihood was minimised at an average biomass consistent with the minimum for the CPUE data, which is a desirable feature of integrated stock assessments. Also, alternative weighting of the size composition data was not overly influential regarding key stock assessment results (Figure 46), indicating some degree of robustness to the data weighting assumptions within the structural uncertainty grid.

8.2 Improvements in the assessment

While ongoing work is required, it is worth noting a number of improvements in this assessment from that conducted in 2015. Firstly, following recommendations from PAW we switched to a simplified region structure and refined the definition for the longline fleets. This resulted in improved model diagnostics, especially with the fit to the length data over time. In addition, given the paucity of information on movement, more complex regional structures are hard to justify for this stock.

Second, we introduced a length-based specification of relative reproductive potential which combined length-based information on female maturity and the proportion of females in the population. The length-based specification allowed the transformed estimates of reproductive potential-at-age to respond more readily to different growth estimates during model fitting. Also, the incorporation of the latest maturity-at-length data resulted in the inclusion of additional younger age classes in the estimates of population reproductive potential, which had an impact on the estimates of depletion.

Third, we developed a new approach of specifying 'Index fisheries' to provide the main information on albacore relative abundance over time and among spatial regions. These fisheries included data

from all significant longline fleets operating in the fishery and thus provided the most comprehensive spatial and temporal coverage possible. The definition of essentially non-extractive 'Index fisheries' also allowed size data associated with these fisheries to be compiled in such a way to be more representative of the underlying population than of the catch.

Fourth, the construction of 'Index fisheries' and DWFN longline fisheries benefited from the new availability of additional operational-level longline data provided by fishing nations. These data resulted in a better spatial and temporal coverage of the longline fishery than in any previous albacore assessments.

Finally, we included a geostatistical approach to estimating relative abundance indices for albacore for the first time. The geostatistical approach potentially better recognises the spatial relationships of data than the traditional GLM approach to CPUE standardisation, and it was noteworthy that the two approaches (with both included in the structural uncertainty grid) provided different estimated relative abundance time-series, once growth and natural mortality were accounted for. In particular, the geostatistical approach results in more similar trends across regions, inferring a greater degree of stock mixing than in previous assessments based on the traditional GLM approach.

8.3 Uncertainty

As with other WCPFC tuna assessment conducted in recent years, we have attempted to characterise uncertainty across a number of key axes. The most influential sources of uncertainty in the stock assessment results are the assumed level of natural mortality and growth (Figure 46). For the diagnostic case, we assumed age-invariant M of 0.3 consistent with the 2015 assessment, and used a level of 0.4 yr^{-1} as the alternative setting in the structural uncertainty grid. As expected, the higher setting results in substantially more optimistic assessment outcomes. We also tested age-dependent M settings using a Lorenzen approach (with asymptotic $M = 0.3yr^{-1}$ increasing for younger age classes inversely proportional to mean age-at-length) and a setting equivalent to that used in the 2017 assessment of north Pacific albacore (ISC Albacore Working Group, 2017). Neither of these age-dependent settings resulted in any appreciable differences in key assessment results relative to models with the invariant 0.4 and 0.5 yr^{-1} settings, respectively. Natural mortality remains a key uncertainty in this assessment, and it is appropriate that such uncertainty continue to be reflected in the overall stock assessment results.

Growth was also a major source of uncertainty in this assessment. A considerable amount of work on South Pacific albacore growth has been conducted in recent years (Williams et al., 2012) and, as was the case for the 2015 assessment, the conditional age-at-length data resulting from this work have been incorporated into the diagnostic case model for this assessment. However there is an unresolved inconsistency in the growth rates indicated by the VB curve fitted to the age-at-length data (approximately 20 cm per year for fish in the size range 50-70 cm) and presumed annual modes having a spacing of approximately 10 cm that consistently appear in the troll size composition data, and historically in the driftnet size composition data (Figure 31). As noted in Section 7.3.5, additional analysis of otoliths taken from 50-70 cm albacore in the troll fishery is required to identify the reason for this inconsistency. If such samples are found to have age estimates consistent with the modal structure, this would indicate that albacore in the southern region (or smaller albacore generally) genuinely have slower growth than those further north, in addition to the east-west patterns in K (both sexes) and in L_∞ (males only) reported by Williams et al. (2012). To our knowledge, no integrated assessment packages currently exist that can account

for spatial variations in growth rates over the range of a stock. When we tried fitting the assessment with growth curves consistent with the 10 cm troll modes Figure 31, diagnostics other than that for the growth data were extremely poor, and predictions made by the model otherwise seemed very unlikely.

If, on the other hand, the ages from 50-70 cm albacore in the troll fishery are found to be consistent with the VB estimates fitted to the age-at-length data currently in the assessment, other avenues to investigate would include the age estimates themselves, or the potential for temporal variation in juvenile growth. This is work that needs to be undertaken with high priority. Integrated growth models fitted externally to MULTIFAN-CL might also be useful to identify drivers of estimated growth parameters, since it can be challenging to untangle drivers of growth fit when growth is fitted directly within MULTIFAN-CL as part of the stock assessment.

8.4 Main stock assessment conclusions

For most of the models investigated, estimates of spawning potential, and biomass vulnerable to the various longline fisheries, have been stable or possibly increasing slightly over the past 20 years. This has been influenced mainly by the estimated recruitment, which has generally been somewhat higher since 2000 than in the two decades previous. Most models also estimate an increase in spawning and longline vulnerable biomass since about 2011, driven by some high estimated recruitments, particularly around 2009. For example, for the diagnostic case model, this has led to the spawning potential depletion ratio increasing from slightly less than 0.4 in 2011 to close to 0.5 in 2016.

While the key stock assessment results across all models in the structural uncertainty grid of this assessment show a wide range of estimates, all models indicate that South Pacific albacore is above the limit reference point (of $0.2SB_{F=0}$), with overall median depletion for 2016 ($SB_{latest}/SB_{F=0}$) estimated at 0.52 (80 percentile range 0.37-0.69). Likewise, recent average fishing mortality is estimated to be well below F_{MSY} (median $F_{recent}/F_{\text{MSY}} = 0.20$, 80 percentile range 0.08-0.41), reflecting the very flat yield curves in the vicinity of the maximum (Figure 50). We can thus conclude that South Pacific albacore is not currently overfished, nor is overfishing occurring.

8.5 Research recommendations

A number of key research needs have been identified in undertaking this assessment. In summary these are:

- To obtain additional estimates of age from otoliths taken from troll-caught albacore (in the New Zealand fishery, or in the subtropical convergence zone fishery further east) over a size range of at least 50-70 cm. These estimates would then be compared for consistency with the existing age-at-length data originating mainly from longline-caught albacore further north, and with relative ages inferred from the modal structure of the troll fishery size composition data. Furthermore noting that spatial patterns in growth have become increasingly prevalent for a number of tuna stocks in the WCPO and elsewhere, a cross t-RFMO workshop on modelling variations in growth through space should be considered.
- To explore alternatives to the Von Bertalanffy model when modelling albacore growth within MULTIFAN-CL.

- To undertake more detailed analysis of albacore size-related vulnerability to longline fishing, examining the interaction of albacore depth distribution, longline fishing depth and the environmental impacts on these variables, to indicate possible changes in selectivity of longline fisheries operating in different regions.
- To acquire and analyse detailed information on the size-sampling of albacore, to potentially inform decisions on appropriate effective sample size settings in integrated stock assessments.
- Continue to refine the geostatistical analysis of operational-level CPUE data to provide indices of relative abundance for future assessments. There are also a number of methodological changes that should be explored, and potentially included in future assessments, including:
- Further development of the method of converting relative reproductive potential-at-length to age-based parameters fully incorporating the model estimates of the variability of age-at-length.
- Development of a sex-specific assessment model for South Pacific albacore, allowing sex-specific settings for key demographic parameters, such as natural mortality and growth.
- Implementation of the 'orthogonal polynomial recruitment' approach (Davies et al., 2018) to provide additional structure to recruitment estimation to potentially improve model stability and estimation properties.
- Improve the weighting of the size data component of the likelihood through use of new methods to estimate effective sample size.
- Investigate more flexible estimation of selectivity, in particular for the longline fisheries, that might be a source of current model misspecification.

8.6 Acknowledgements

We thank the various fisheries agencies for the provision of the catch, effort and size frequency data used in this analysis, and gratefully acknowledge the hard work of observers working throughout the region. From SPC, Peter Williams and his team provided exhaustive assistance in collating and interpreting catch statistics for this species, Sylvain Caillot helped with database extracts for the tagging data and Thomas Peatman provided feedback on analyses and the final draft. Jessica Farley and Paige Evenson from CSIRO gave insights on the interpretation and analyses of growth data.

9 Tables

Table 1: Definition of fisheries for the MULTIFAN-CL South Pacific albacore tuna stock assessment.

Fishery	Nationality	Gear	Region	Longline.group
1. DWFN LL 1	Distant-water Fishing Nations	Longline	1	Tropical
2. PICT.AZ LL 1	Pacific Island Countries and Territories	Longline	1	Tropical
3. DWFN LL 2	Distant-water Fishing Nations	Longline	2	Sub-tropical
4. PICT LL 2	Pacific Island Countries and Territories	Longline	2	Sub-tropical
5. AZ LL 2	Australia/New Zealand	Longline	2	Sub-tropical
6. DWFN LL 3	Distant-water Fishing Nations	Longline	3	Temperate
7. PICT LL 3	Pacific Island Countries and Territories	Longline	3	Temperate
8. AZ LL 3	Australia/New Zealand	Longline	3	Temperate
9. DWFN LL 4	Distant-water Fishing Nations	Longline	4	Sub-tropical
10. PICT.AZ LL 4	Pacific Island Countries and Territories	Longline	4	Sub-tropical
11. DWFN LL 5	Distant-water Fishing Nations	Longline	5	Temperate
12. PICT.AZ LL 5	Pacific Island Countries and Territories	Longline	5	Temperate
13. All TR 3	All nationalities	Troll	3	–
14. All TR 5	All nationalities	Troll	5	–
15. All DN 3	All nationalities	Driftnet	3	–
16. All DN 5	All nationalities	Driftnet	5	–
17. Index LL 1	Index fishery	Longline	1	–
18. Index LL 2	Index fishery	Longline	2	–
19. Index LL 3	Index fishery	Longline	3	–
20. Index LL 4	Index fishery	Longline	4	–
21. Index LL 5	Index fishery	Longline	5	–

Table 2: Summary of the number of release events, tag releases and recoveries by region and program

Prog		RTTP			SPATP	
Years		1986–1992			2009–2010	
Category	Grps	Rel	Rec	Grps	Rel	Rec
1	0	0	0	0	0	0
2	0	0	0	0	0	0
3	13	4154	95	2	1019	21
4	0	0	0	0	0	0
5	9	1706	30	0	0	0
Total	22	5861	125	2	1019	21

Table 3: Description of symbols used in the yield and stock status analyses. For the purpose of this assessment, 'recent' is the average over the period 2012–2015 for fishing mortality, and the average over the period 2013–2016 for spawning potential, and 'latest' is 2016.

Symbol	Description
C_{latest}	Catch in the last year of the assessment (2016)
MSY	Equilibrium yield at F_{MSY}
F_{recent}	Average fishing mortality-at-age for a recent period (2012–2015)
fmult	Multiplier on current effort required to achieve MSY
F_{MSY}	Fishing mortality-at-age producing the maximum sustainable yield (MSY)
$F_{recent}/F_{\mathrm{MSY}}$	Average fishing mortality-at-age for a recent period (2012–2015) relative to F_{MSY}
SB_{MSY}	Spawning potential that will produce the MSY
SB_0	Equilibrium unexploited spawning potential
SB_{MSY}/SB_0	Spawning potential that will produced the MSY relative to the equilibrium unexploited spawning potential
$SB_{F=0}$	Average spawning potential predicted to occur in the absence of fishing for the period 2006–2015
$SB_{\mathrm{MSY}}/SB_{F=0}$	Spawning potential that will produce MSY relative to the average spawning potential predicted to occur in the absence of fishing for the period 2006–2015
$SB_{latest}/SB_{F=0}$	Spawning biomass in the latest time period (2016) relative to the average spawning biomass predicted to occur in the absence of fishing for the period 2006–2015
$SB_{latest}/SB_{\mathrm{MSY}}$	Spawning biomass in the latest time period (2016) relative to that which will produce the maximum sustainable yield (MSY)
$SB_{recent}/SB_{F=0}$	Spawning biomass in for a very recent period (2013–2016) relative to the average spawning biomass predicted to occur in the absence of fishing for the period 2006–2015
$SB_{recent}/SB_{\mathrm{MSY}}$	Spawning biomass in for a very recent period (2013–2016) relative to the average spawning biomass predicted to produce the MSY

Table 4: Summary of the groupings of fisheries within the assessment for estimation of selectivity and catchability (used for the implementation of regional weights, see also Section 5.3.3). See Table 1 for further details on each fishery.

Fishery	Region	Selectivity	Catchability	SeasCat	TimVarCat	TimVarCatCV	EffPen	EffPenCV
F1 DWFN LL 1	1	1	1	N	Y	0.1	scaled	0.41
F2 PICT.AZ LL 1	1	2	2	N	Y	0.1	scaled	0.41
F3 DWFN LL 2	2	3	3	N	Y	0.1	scaled	0.41
F4 PICT LL 2	2	4	4	N	Y	0.1	scaled	0.41
F5 AZ LL 2	2	5	5	N	Y	0.1	scaled	0.41
F6 DWFN LL 3	3	6	6	N	Y	0.1	scaled	0.41
F7 PICT LL 3	3	7	7	N	Y	0.1	scaled	0.41
F8 AZ LL 3	3	8	8	N	Y	0.1	scaled	0.41
F9 DWFN LL 4	4	9	9	N	Y	0.1	scaled	0.41
F10 PICT.AZ LL 4	4	10	10	N	Y	0.1	scaled	0.41
F11 DWFN LL 5	5	11	11	N	Y	0.1	scaled	0.41
F12 PICT.AZ LL 5	5	12	12	N	Y	0.1	scaled	0.41
F13 All TR 3	3	13	13	Y	Y	0.1	scaled	0.41
F14 All TR 5	5	14	14	Y	Y	0.1	scaled	0.41
F15 All DN 3	3	15	15	Y	Y	0.1	scaled	0.41
F16 All DN 5	5	16	16	Y	Y	0.1	scaled	0.41
F17 Index LL 1	1	17	17	N	N	–	time-variant	0.20
F18 Index LL 2	2	18	17	N	N	–	time-variant	0.20
F19 Index LL 3	3	19	17	N	N	–	time-variant	0.20
F20 Index LL 4	4	20	17	N	N	–	time-variant	0.20
F21 Index LL 5	5	21	17	N	N	–	time-variant	0.20

Table 5: Description of the structural sensitivity grid used to characterise uncertainty in the assessment. Levels used under the diagnostic case are starred.

Axis	Levels	Option
Steepness	3	0.65, 0.80*, or 0.95
Natural mortality	2	0.3*, 0.4
Growth	2	Estimated* (K, L_∞) or fixed (Chen-Wells)
Size frequency weighting	3	Sample sizes divided by 20, 50*, or 80
CPUE	2	Geostatistical*, Traditional

Table 6: Summary of reference points over all 72 individual models in the structural uncertainty grid

	Mean	Median	Min	10%	90%	Max
C_{latest}	61719	61635	60669	60833	62704	63180
MSY	100074	98080	65040	70856	130220	162000
$YF_{current}$	71579	71780	56680	62480	80432	89000
fmult	6.2	4.96	1.89	2.44	12.05	17.18
F_{MSY}	0.07	0.07	0.05	0.05	0.09	0.1
$F_{recent}/F_{\text{MSY}}$	0.23	0.2	0.06	0.08	0.41	0.53
SB_{MSY}	71407	68650	26760	39872	100773	134000
SB_0	443794	439800	308800	353870	510530	696200
SB_{MSY}/SB_0	0.16	0.17	0.07	0.1	0.21	0.23
$SB_{F=0}$	469004	462633	380092	407792	534040	620000
$SB_{\text{MSY}}/SB_{F=0}$	0.15	0.15	0.06	0.09	0.2	0.22
SB_{latest}/SB_0	0.55	0.56	0.33	0.42	0.69	0.74
$SB_{latest}/SB_{F=0}$	0.53	0.52	0.3	0.37	0.69	0.77
$SB_{latest}/SB_{\text{MSY}}$	4	3.42	1.45	1.96	7.07	10.74
$SB_{recent}/SB_{F=0}$	0.51	0.52	0.32	0.37	0.63	0.72
$SB_{recent}/SB_{\text{MSY}}$	3.88	3.3	1.58	1.96	6.56	9.67

Table 7: Summary of reference points over the 36 models in the structural uncertainty grid where growth is estimated

	Mean	Median	Min	10%	90%	Max
C_{latest}	61738	61656	60737	61240	62377	62591
MSY	104663	101420	74240	79420	132280	162000
$YF_{current}$	73368	73180	61760	66000	81180	89000
fmult	6.43	5.4	2.25	2.76	11.71	17.18
F_{MSY}	0.08	0.08	0.06	0.07	0.09	0.1
$F_{recent}/F_{\text{MSY}}$	0.21	0.19	0.06	0.09	0.36	0.45
SB_{MSY}	80155	78245	42380	49205	109900	134000
SB_0	482872	474800	378500	411950	565200	696200
SB_{MSY}/SB_0	0.16	0.17	0.1	0.1	0.21	0.21
$SB_{F=0}$	501882	498274	422907	446580	563809	620000
$SB_{\text{MSY}}/SB_{F=0}$	0.16	0.16	0.09	0.1	0.2	0.22
SB_{latest}/SB_0	0.58	0.58	0.4	0.46	0.7	0.73
$SB_{latest}/SB_{F=0}$	0.56	0.55	0.37	0.42	0.72	0.77
$SB_{latest}/SB_{\text{MSY}}$	3.83	3.42	1.86	2.34	6.47	7.13
$SB_{recent}/SB_{F=0}$	0.53	0.54	0.37	0.42	0.64	0.72
$SB_{recent}/SB_{\text{MSY}}$	3.64	3.3	1.86	2.14	6.29	6.61

Table 8: Summary of reference points over the 36 models in the structural uncertainty grid where growth is fixed to the Chen-Wells model

	Mean	Median	Min	10%	90%	Max
C_{latest}	61700	61543	60669	60830	62861	63180
MSY	95484	91380	65040	68280	124660	133680
$YF_{current}$	69790	70740	56680	60980	78140	82600
fmult	5.97	4.66	1.89	2.08	13.45	14.61
F_{MSY}	0.06	0.06	0.05	0.05	0.07	0.07
$F_{recent}/F_{\text{MSY}}$	0.25	0.21	0.07	0.07	0.48	0.53
SB_{MSY}	62659	62675	26760	30225	93075	96830
SB_0	404717	408400	308800	333450	470850	508100
SB_{MSY}/SB_0	0.15	0.16	0.07	0.07	0.22	0.23
$SB_{F=0}$	436126	436627	380092	395940	476264	498241
$SB_{\text{MSY}}/SB_{F=0}$	0.14	0.14	0.06	0.07	0.2	0.21
SB_{latest}/SB_0	0.53	0.52	0.33	0.39	0.66	0.74
$SB_{latest}/SB_{F=0}$	0.49	0.47	0.3	0.35	0.66	0.71
$SB_{latest}/SB_{\text{MSY}}$	4.16	3.4	1.45	1.8	8.93	10.74
$SB_{recent}/SB_{F=0}$	0.49	0.48	0.32	0.35	0.63	0.64
$SB_{recent}/SB_{\text{MSY}}$	4.11	3.37	1.58	1.75	8.95	9.67

Table 9: Summary of reference points over the 36 models in the structural uncertainty grid where natural mortality m is 0.3

	Mean	Median	Min	10%	90%	Max
C_{latest}	61727	61624	60669	60830	62861	63180
MSY	78352	78220	65040	68280	88920	93320
$YF_{current}$	67567	67280	56680	60980	75520	76760
fmult	3.38	3.15	1.89	2.08	4.63	6.06
F_{MSY}	0.07	0.07	0.05	0.05	0.08	0.09
$F_{recent}/F_{\text{MSY}}$	0.33	0.32	0.16	0.22	0.48	0.53
SB_{MSY}	74609	71745	39130	42615	103500	117500
SB_0	413997	409500	308800	333450	492950	551700
SB_{MSY}/SB_0	0.18	0.18	0.12	0.13	0.22	0.23
$SB_{F=0}$	460167	459082	380092	395940	521265	565429
$SB_{\text{MSY}}/SB_{F=0}$	0.16	0.16	0.1	0.11	0.2	0.21
SB_{latest}/SB_0	0.47	0.48	0.33	0.39	0.56	0.61
$SB_{latest}/SB_{F=0}$	0.42	0.42	0.3	0.35	0.52	0.55
$SB_{latest}/SB_{\text{MSY}}$	2.83	2.64	1.45	1.8	4.11	4.39
$SB_{recent}/SB_{F=0}$	0.42	0.42	0.32	0.35	0.48	0.52
$SB_{recent}/SB_{\text{MSY}}$	2.77	2.59	1.58	1.75	3.86	4.33

Table 10: Summary of reference points over the 36 models in the structural uncertainty grid where natural mortality m is 0.4

	Mean	Median	Min	10%	90%	Max
C_{latest}	61711	61653	60737	60991	62588	62830
MSY	121796	118240	102840	109840	133600	162000
$YF_{current}$	75591	74820	65240	68940	82580	89000
fmult	9.02	7.94	4.62	5.34	14.3	17.18
F_{MSY}	0.07	0.07	0.05	0.05	0.09	0.1
$F_{recent}/F_{\text{MSY}}$	0.13	0.13	0.06	0.07	0.19	0.22
SB_{MSY}	68204	65715	26760	30225	98420	134000
SB_0	473592	460050	363100	410850	555550	696200
SB_{MSY}/SB_0	0.14	0.15	0.07	0.07	0.19	0.2
$SB_{F=0}$	477840	463993	407793	426504	553916	620000
$SB_{\text{MSY}}/SB_{F=0}$	0.14	0.14	0.06	0.07	0.2	0.22
SB_{latest}/SB_0	0.63	0.63	0.49	0.56	0.71	0.74
$SB_{latest}/SB_{F=0}$	0.63	0.62	0.48	0.53	0.72	0.77
$SB_{latest}/SB_{\text{MSY}}$	5.16	4.5	2.59	2.93	8.93	10.74
$SB_{recent}/SB_{F=0}$	0.6	0.6	0.51	0.55	0.64	0.72
$SB_{recent}/SB_{\text{MSY}}$	4.98	4.2	2.74	2.88	8.95	9.67

10 Figures

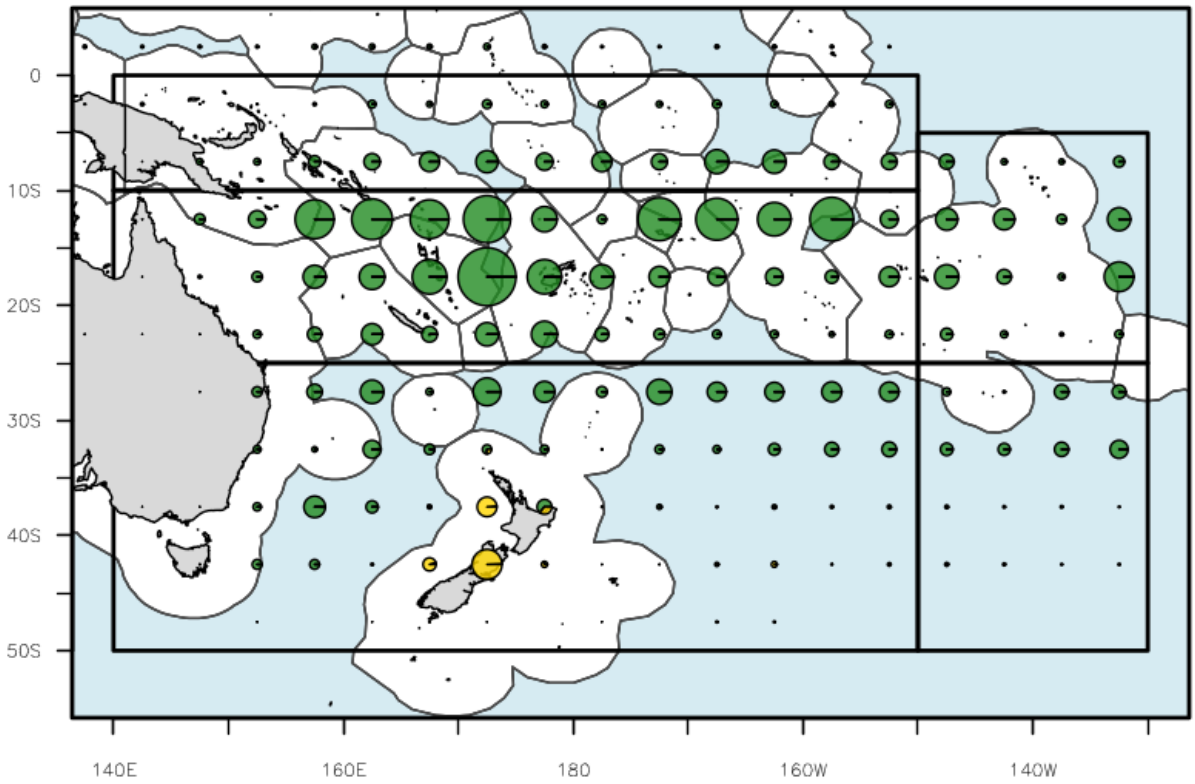

Figure 1: Distribution and magnitude of albacore tuna catches for the most recent decade of the stock assessment (2006-2015) by 5° square and fishing gear: longline (green), pole-and-line (red), purse seine (blue) and miscellaneous (yellow), for the WCPO and part of the EPO. Overlayed are the regional boundaries for the stock assessment (2018 regional structure).

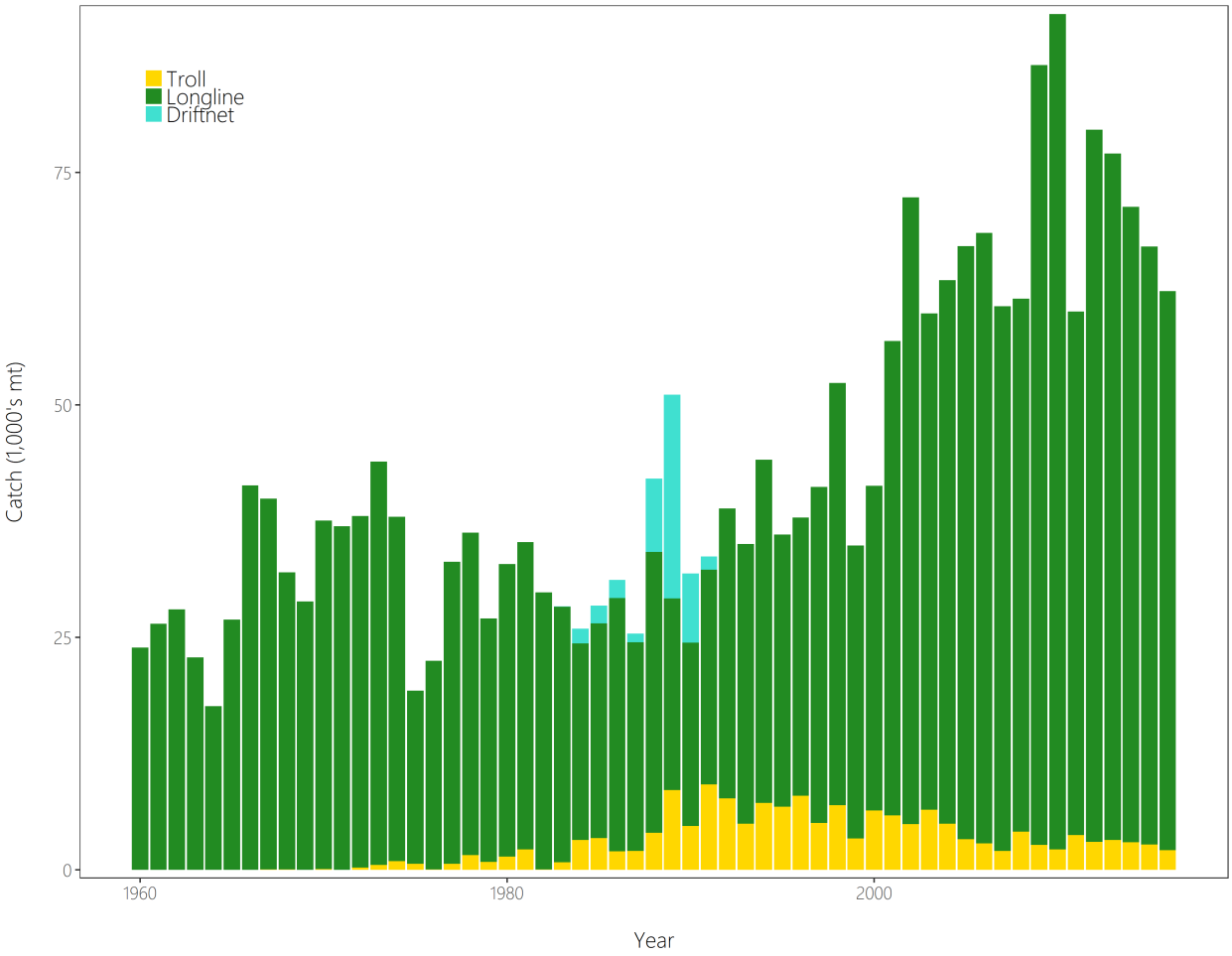

Figure 2: Time series of total annual catch (1000's mt) by fishing gear for the diagnostic case model over the full assessment period. The different colours refer to longline (green), troll (yellow) and driftnet (turquoise). Note that the catch by longline gear has been converted into catch-in-weight from catch-in-numbers and so estimates differ from the annual catch estimates presented in Williams and Reid (2018), however these catches enter the model as catch-in-numbers.

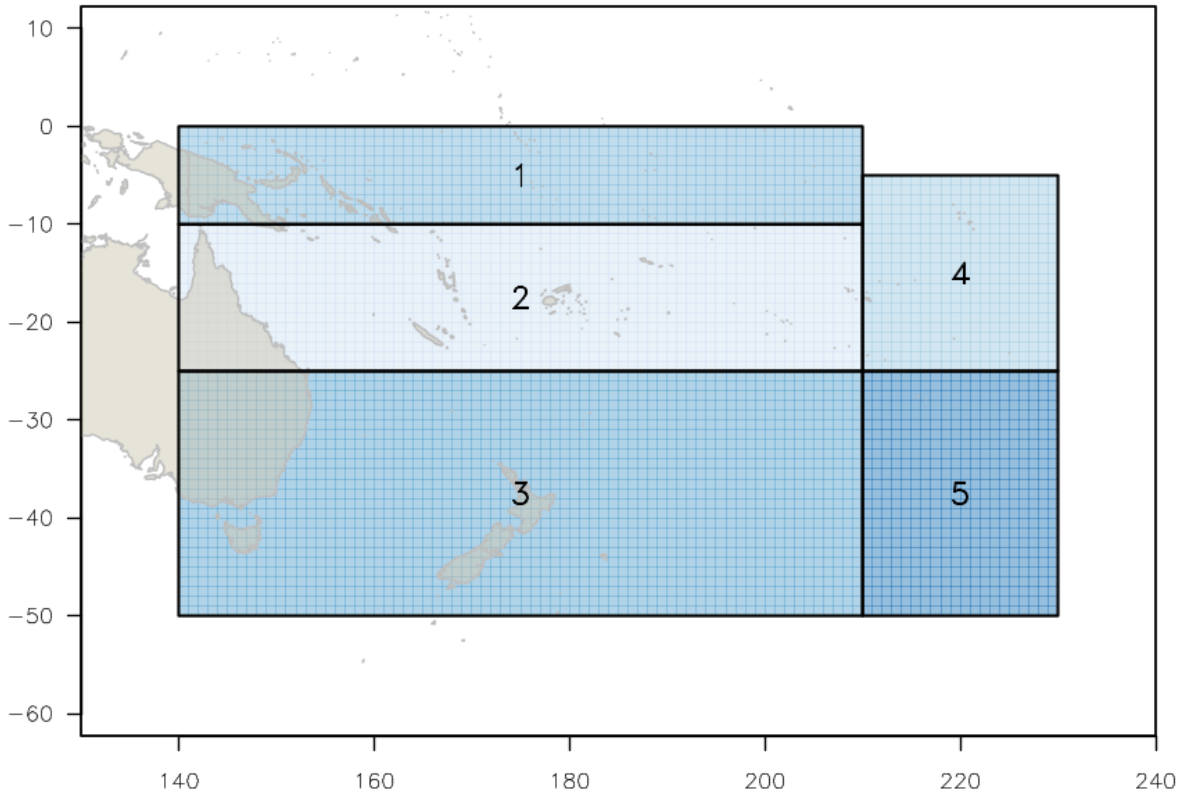

Figure 3: The geographical area covered by the stock assessment and the boundaries for the 5 regions under the updated "2018 regional structure".

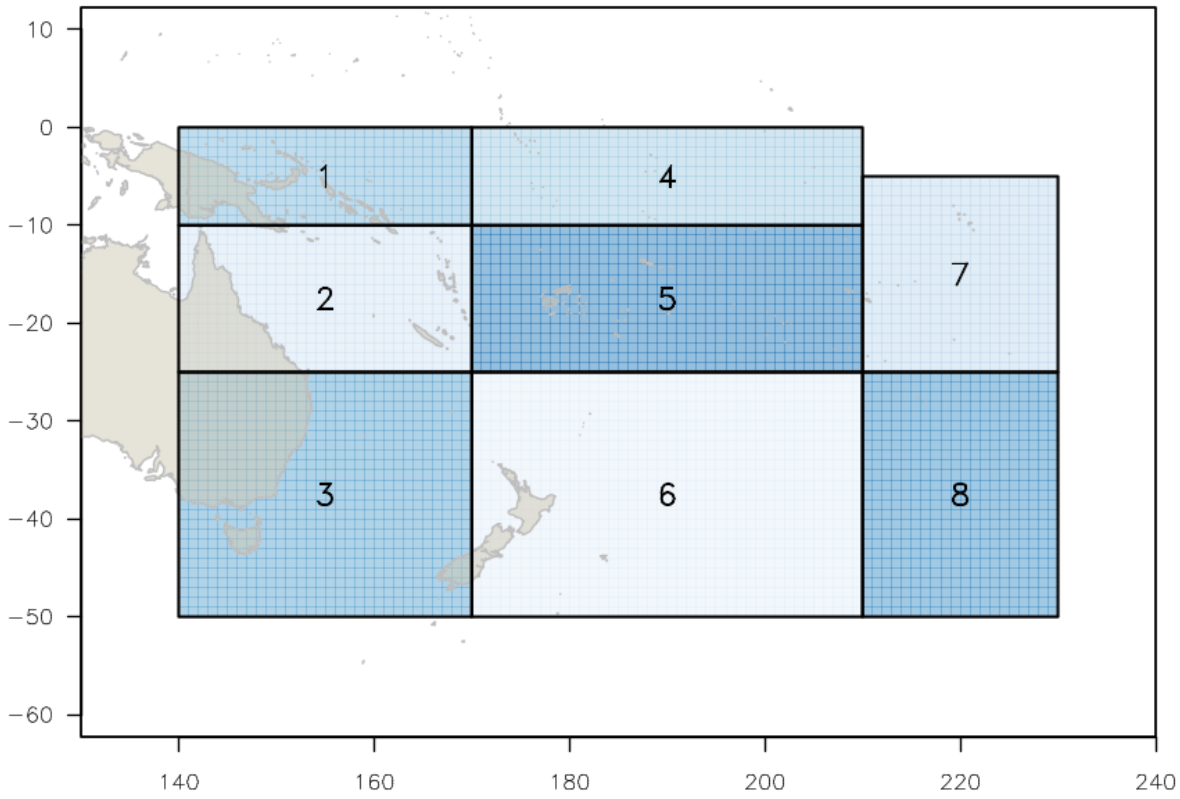

Figure 4: The geographical area covered by the stock assessment and the boundaries for the 8 regions under the "2015 regional structure" which was used in the earlier stages of model development.

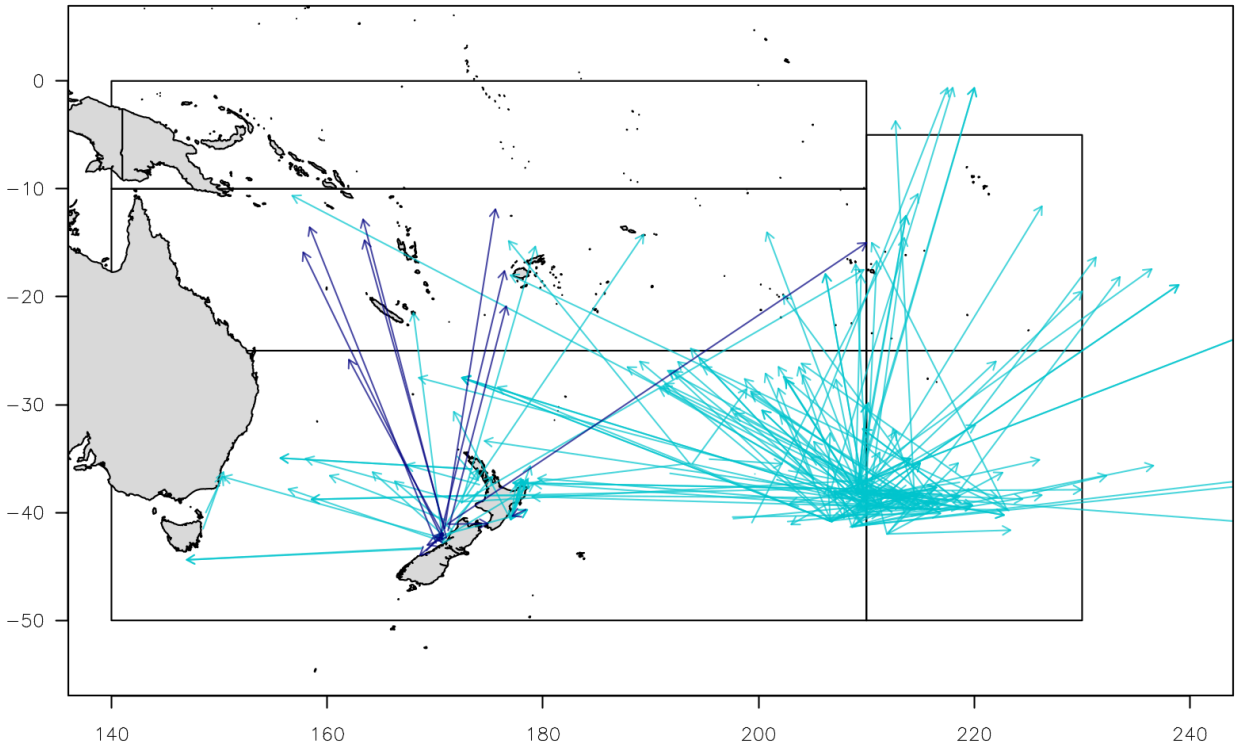

Figure 5: Map of the movements of tagged South Pacific albacore released in the southern WCPFC Convention Area and subsequently recaptured. Dark blue = tagged fish released under the SPATP, light blue = tagged fish released under the RTTP.

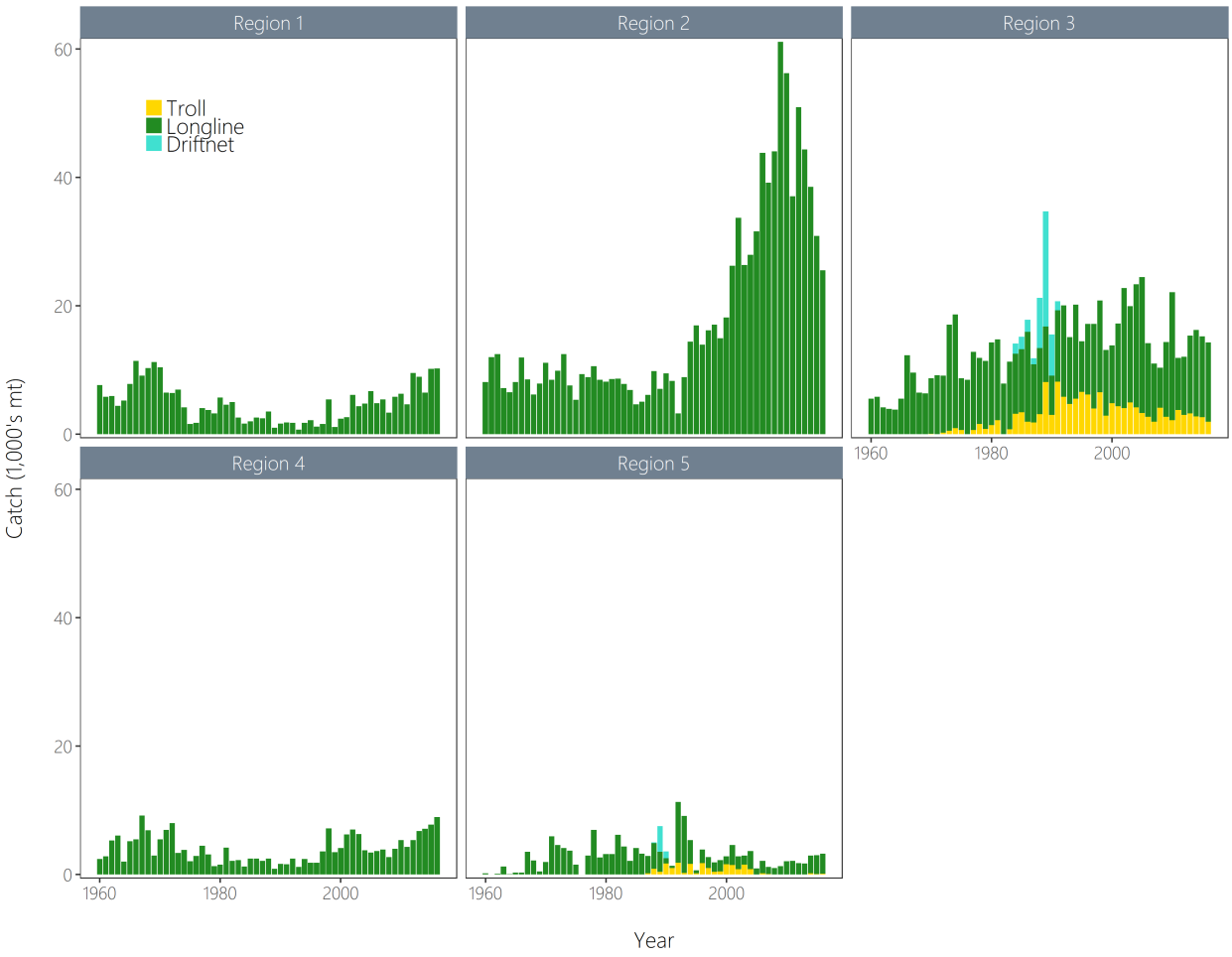

Figure 6: Time series of total annual catch (1000's mt) by fishing gear and assessment region from the diagnostic case model over the full assessment period. The different colours denote longline (green), driftnet (turquoise) and troll (yellow).

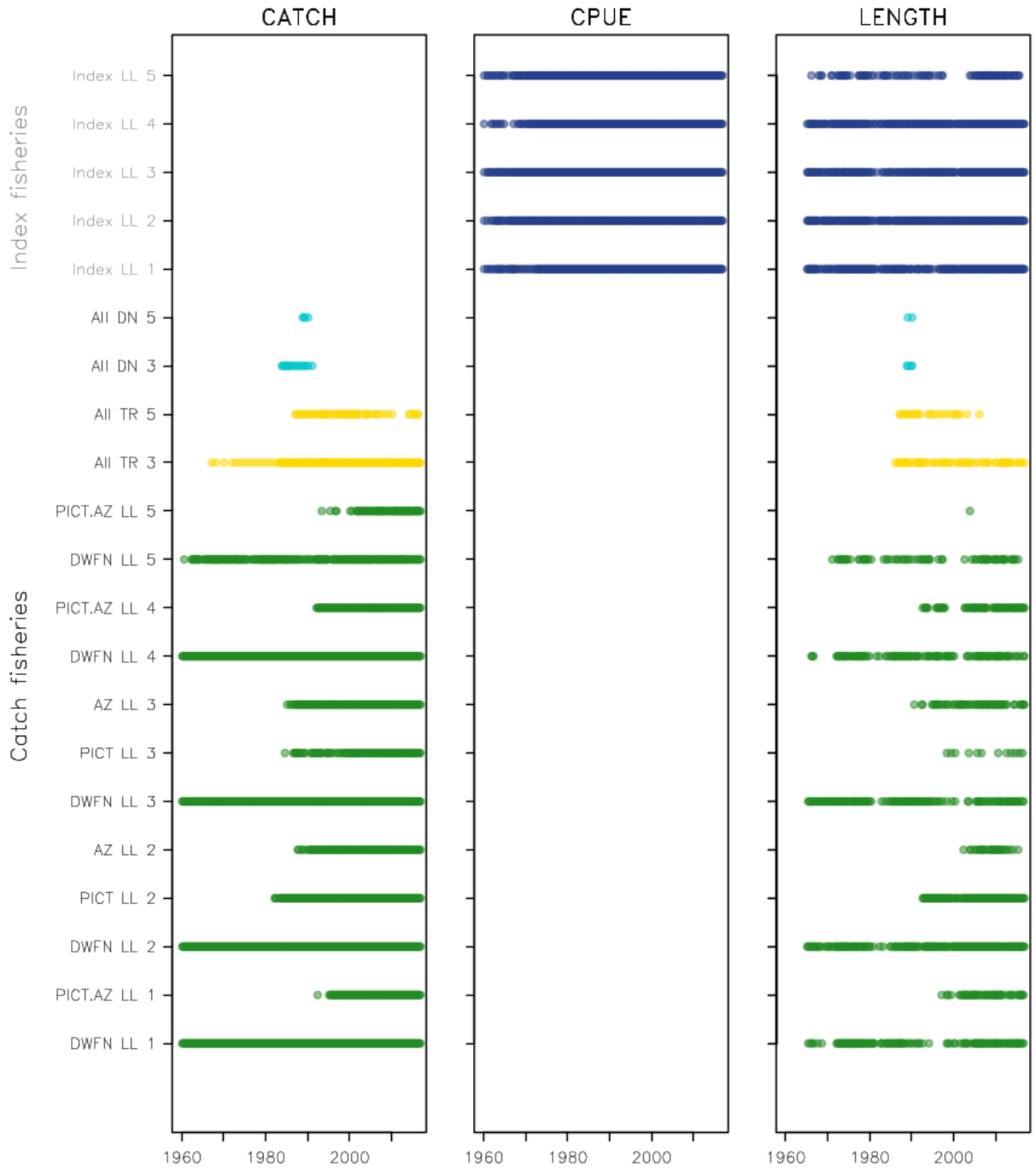

Figure 7: Presence of catch, standardised CPUE and length frequency data by year and fishery for the diagnostic case model (2018 regional structure, hence 16 catch fisheries + 5 index fisheries). The different colours denote gear-type of the fishery: longline (green); troll (yellow); driftnet (turquoise); index (blue).

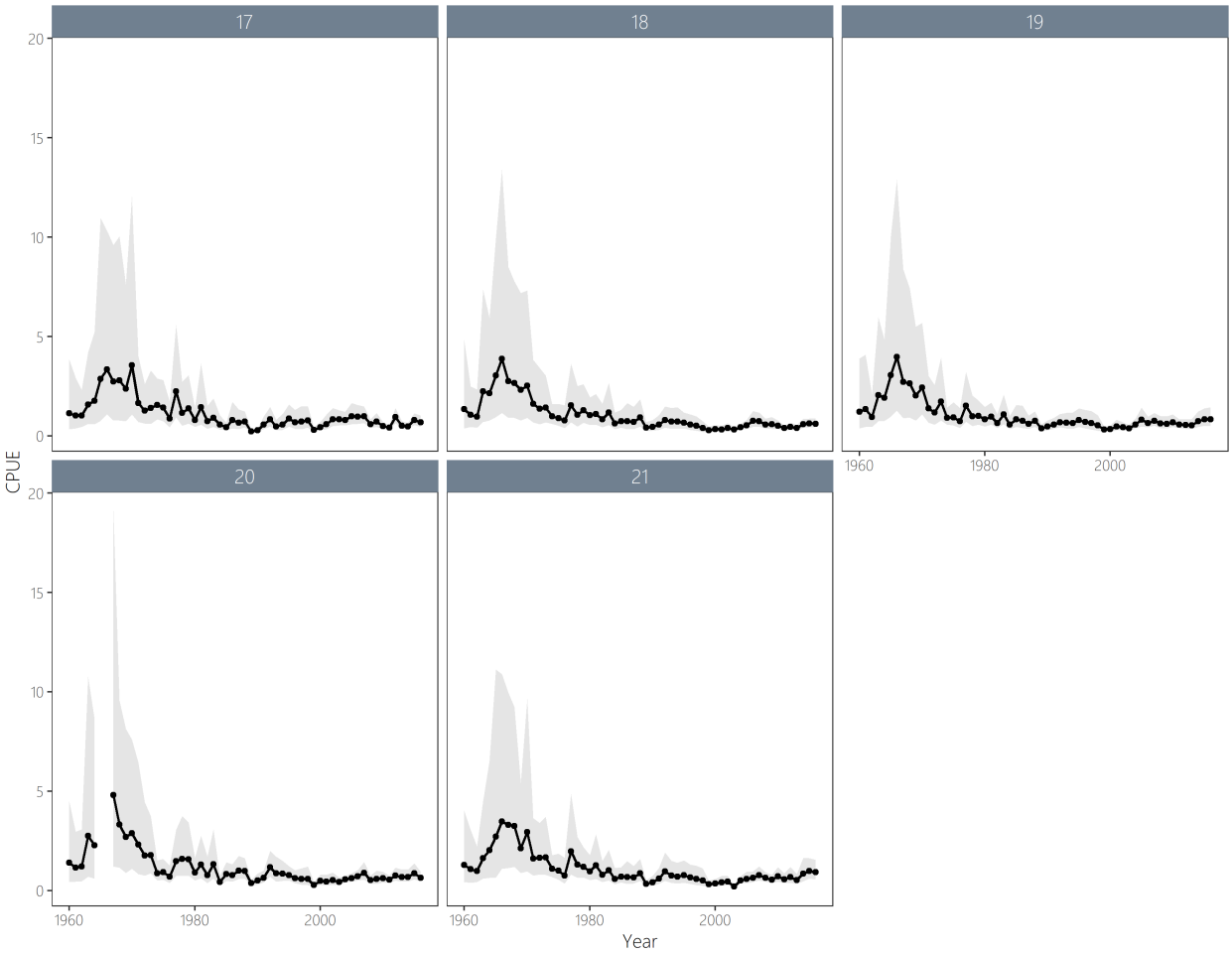

Figure 8: Standardised catch-per-unit-effort (CPUE) indices for the index longline fisheries in regions 1 to 5 under the 'geostatistical' CPUE approach (used in the diagnostic case model). See Tremblay-Boyer and McKechnie (2018) for further details of the estimation of these CPUE indices. The light grey band represent the 95% confidence intervals derived from the effort deviation penalties used in the diagnostic case model.

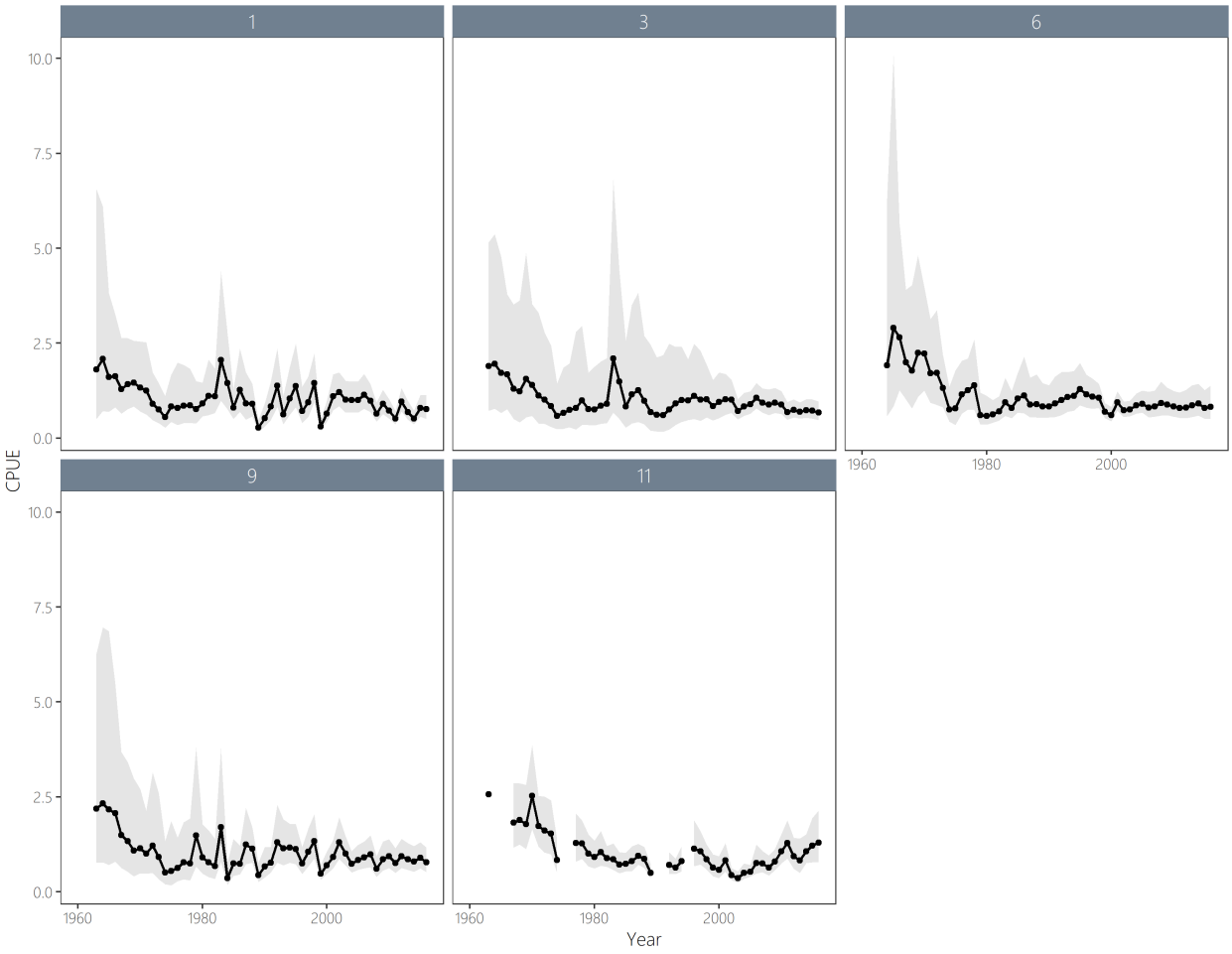

Figure 9: Standardised catch-per-unit-effort (CPUE) indices for the index longline fisheries in regions 1 to 5 under the 'traditional' CPUE approach. See Tremblay-Boyer and McKechnie (2018) for further details of the estimation of these CPUE indices. The light grey band represent the 95% confidence intervals derived from the effort deviation penalties used in the diagnostic case model.

Figure 10: Mean standardised catch-per-unit-effort (CPUE) indices for the index longline fisheries in regions 1 to 5 for the geostatistical *vs.* the traditional approach. See Tremblay-Boyer and McKechnie (2018) for further details of the estimation of these CPUE indices for both approaches.

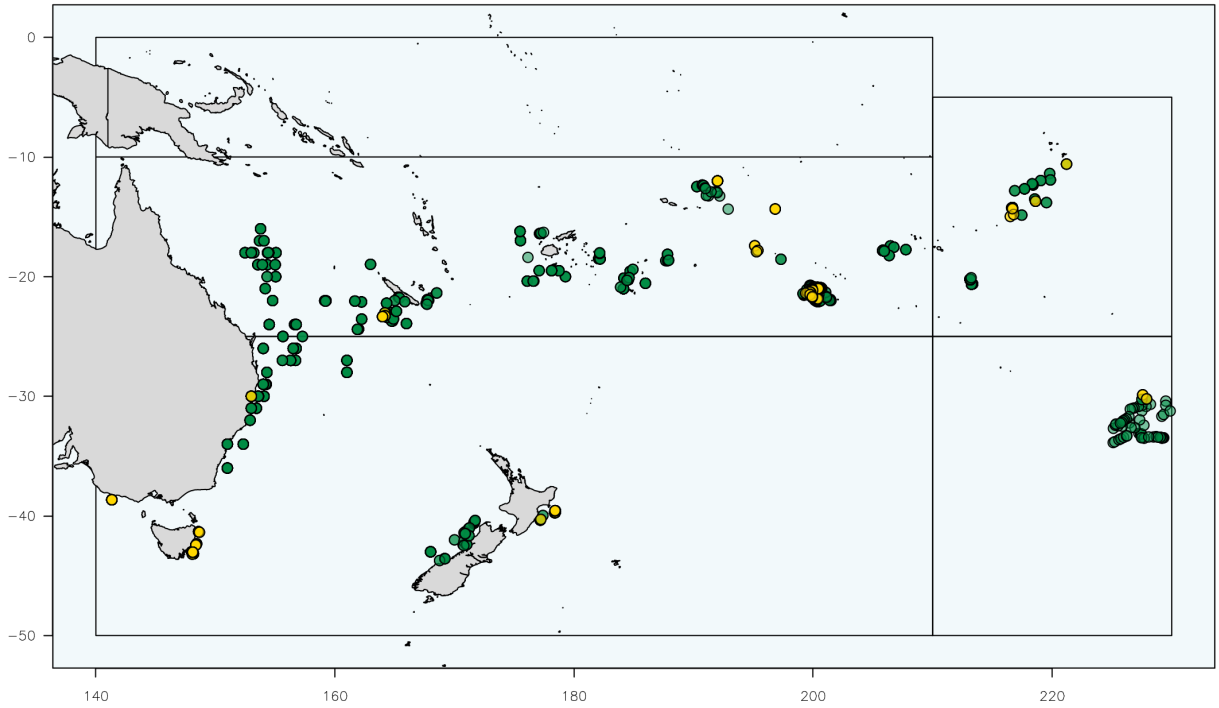

Figure 11: Capture location of South Pacific albacore for which otoliths were considered for the growth analysis, with the 2018 region structure. Longline-caught individuals are in green, troll-caught are in yellow, noting that troll catches in region 2 were taken as part of a biological sampling cruise and not attributable to an extractive fishery.

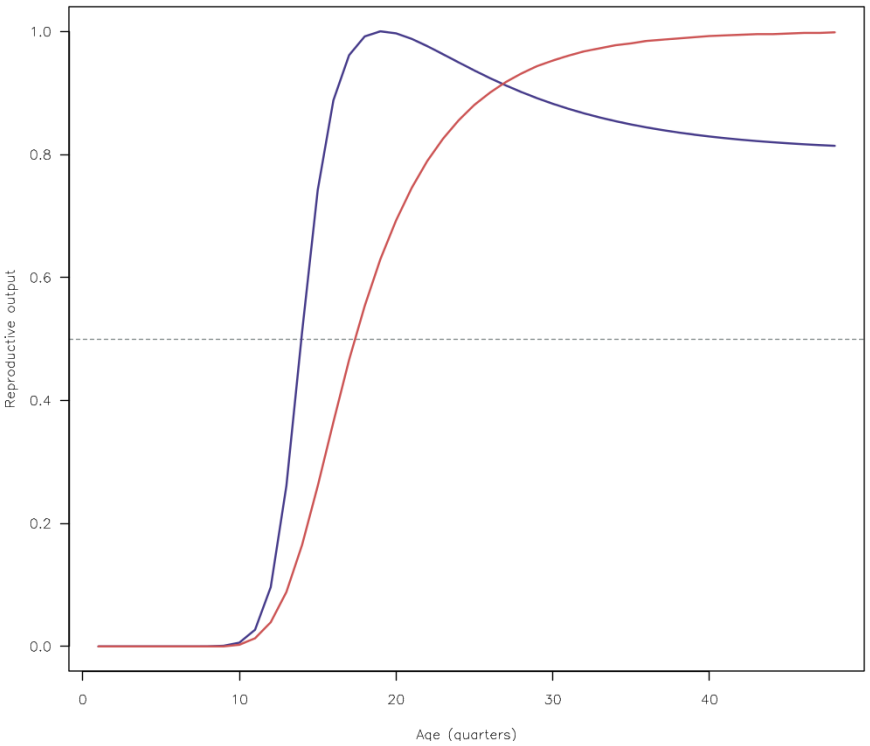

Figure 12: Maturity-at-age as used in the diagnostic case model (black line) and in the 2015 assessment (red line).

Figure 13: Plot of the effort deviation penalties applied to each fishery, by region, with the colours of the lines representing the gear of the fishery. In several cases there is more than one fishery for a given gear-type in a region (e.g. regions 3 and 7 both have two longline fisheries, though only a single fishery receives a standardised CPUE index in both regions). A higher penalty gives more weight to the CPUE of that fishery and so the high weightings applied to the standardised CPUE indices are evident.

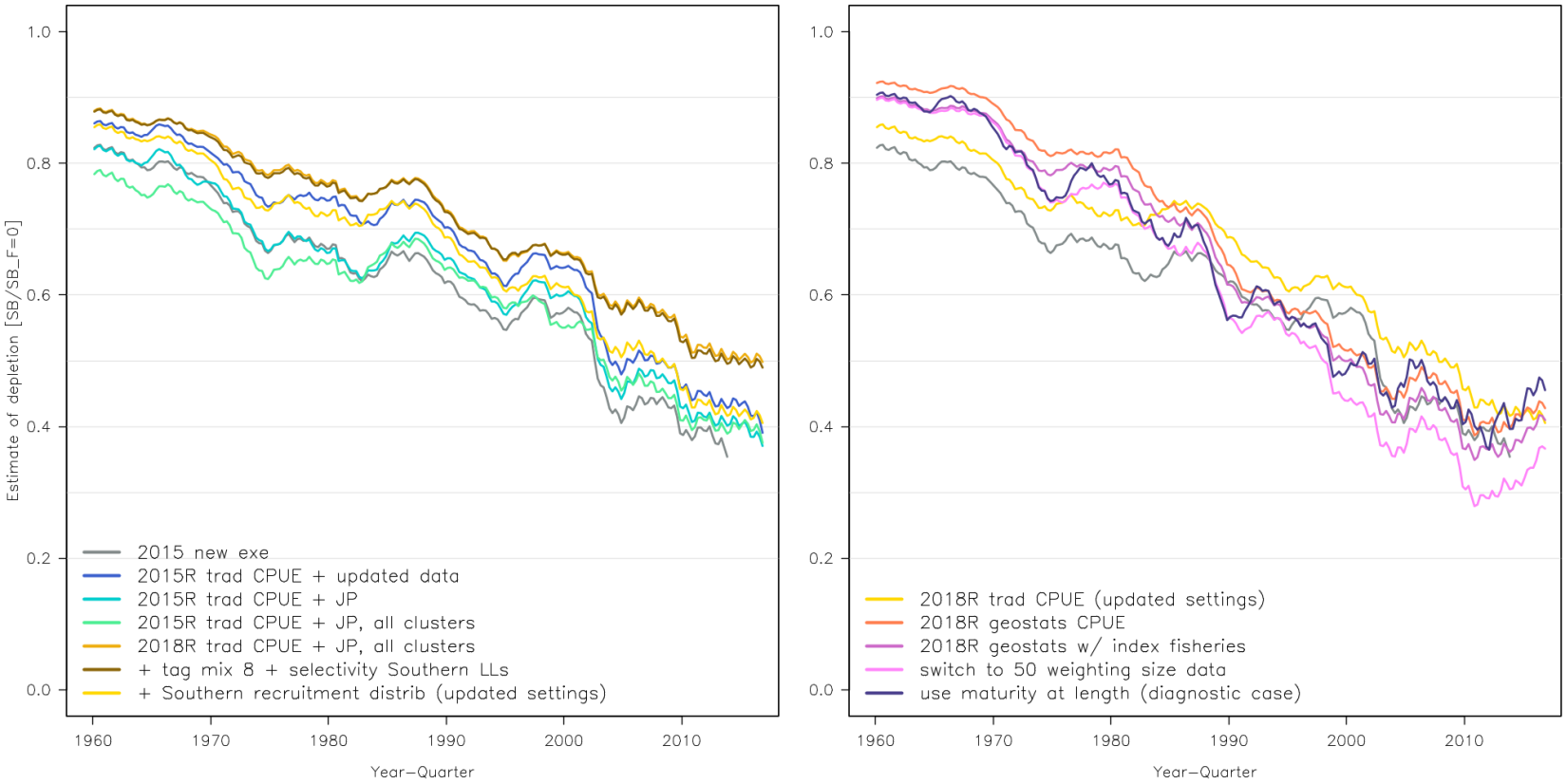

Figure 14: Progression from 2015 to 2018 diagnostic model: depletion

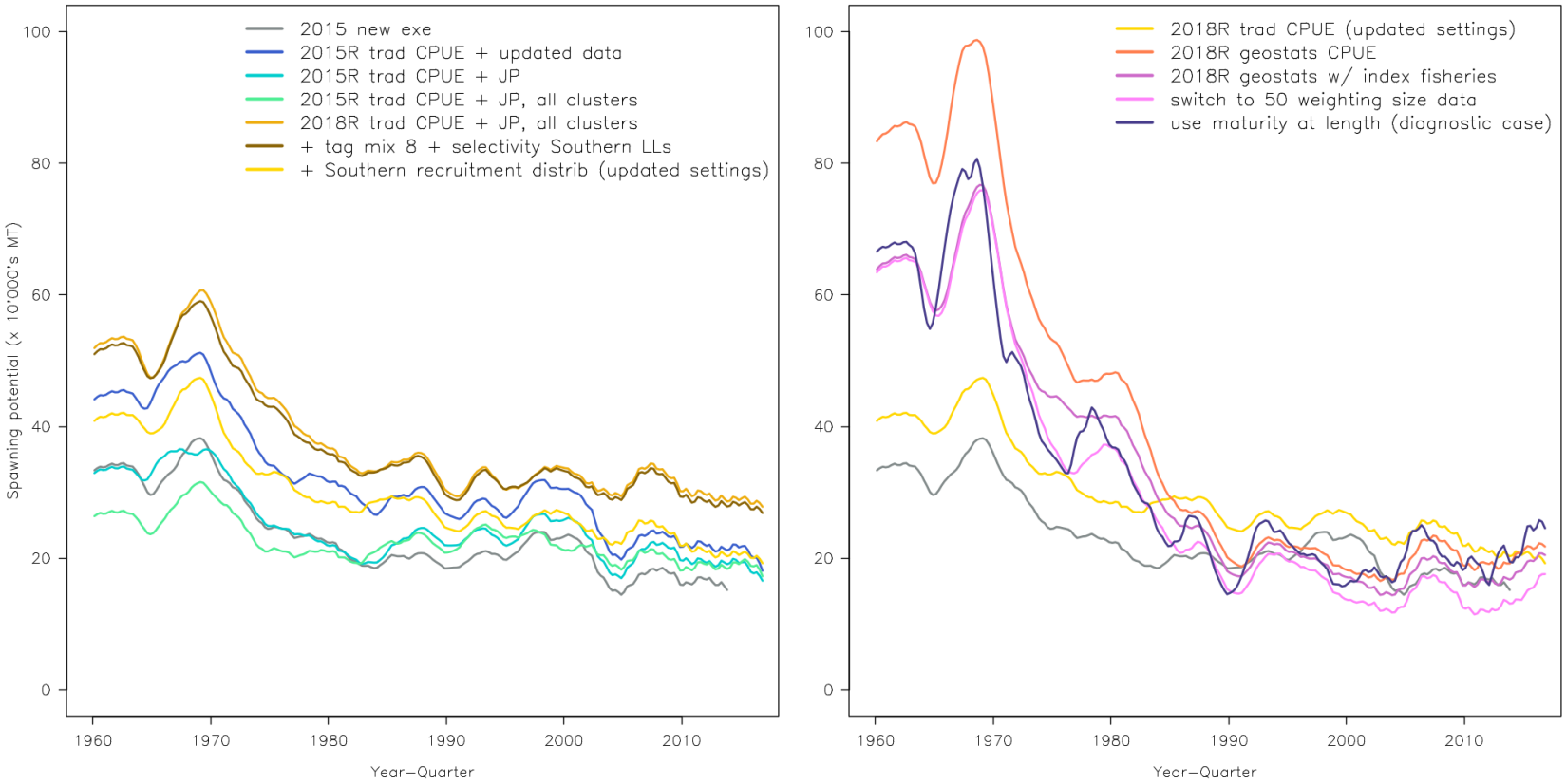

Figure 15: Progression from 2015 to 2018 diagnostic model: spawning potential

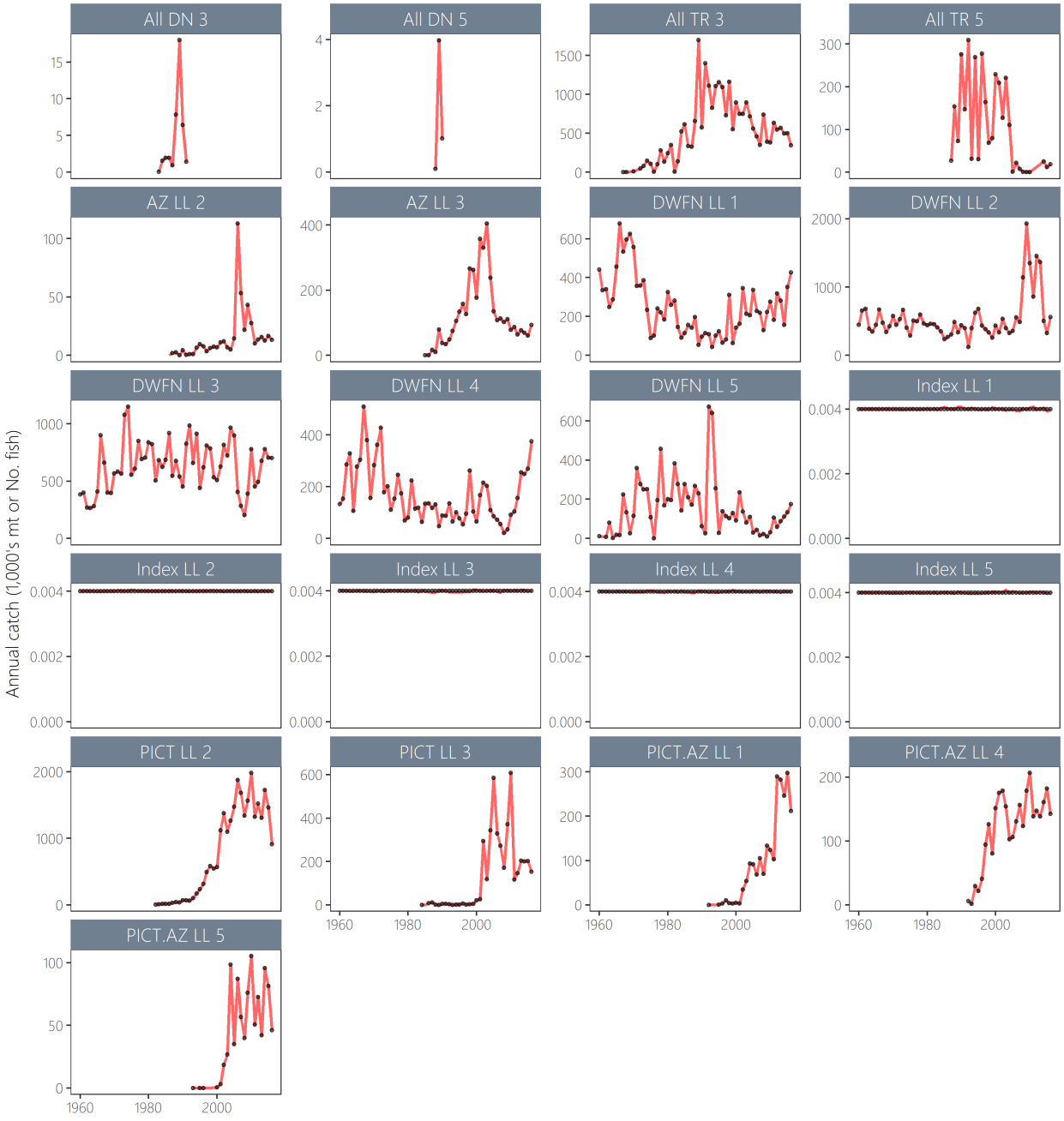

Figure 16: Observed (black points) and model-predicted (red lines) catch for the 21 fisheries in the diagnostic case model. The y-axis is in catch-in-numbers for the longline fisheries and catch-in-weight for the other fisheries, both divided by 1,000.

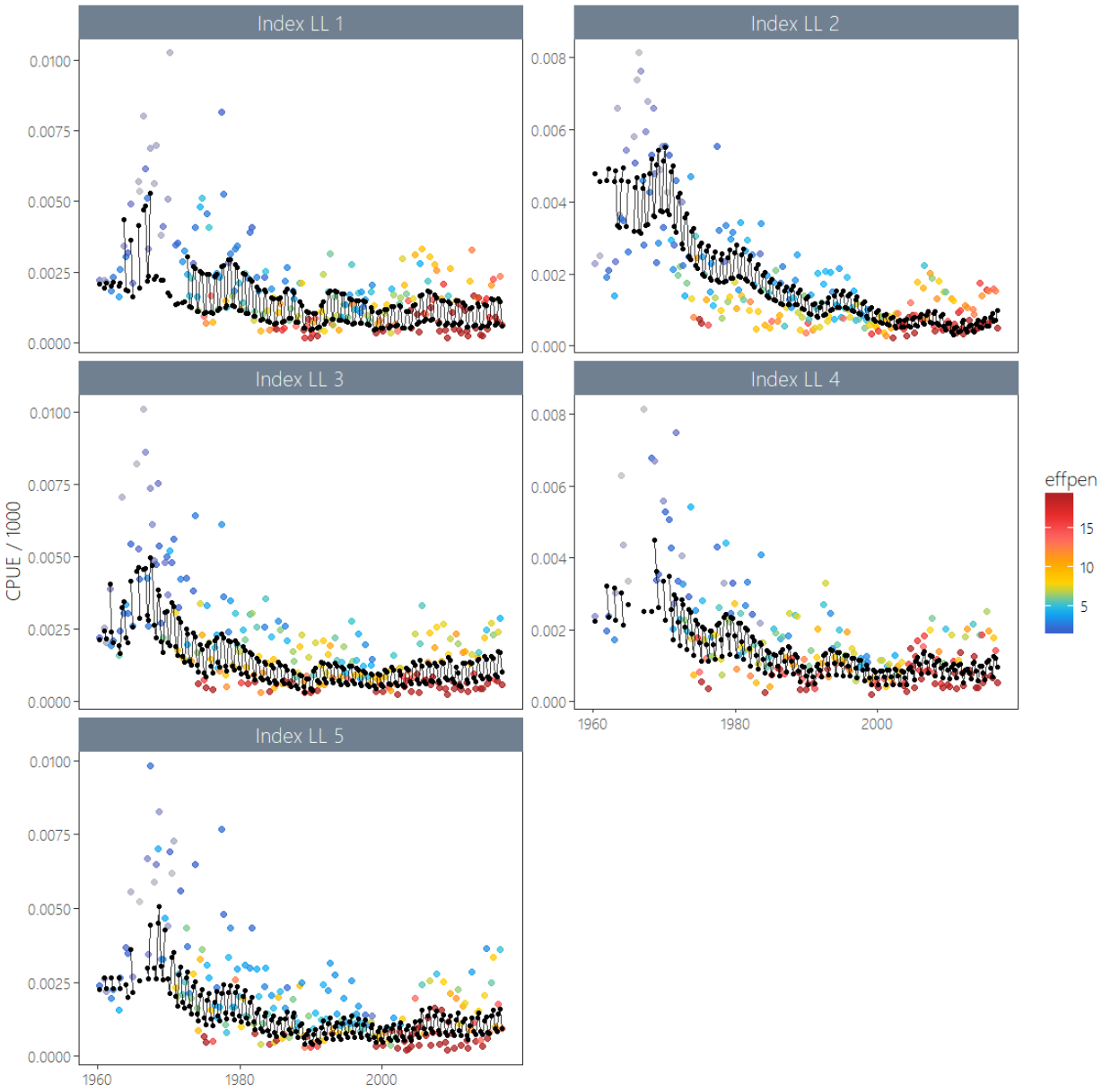

Figure 17: Observed (coloured points) and model-predicted (black points and lines) CPUE for the five fisheries which received standardised CPUE indices in the diagnostic case model. Observed points are coloured as a function of the penalty weight applied on them, going from blue to red as penalty increases.

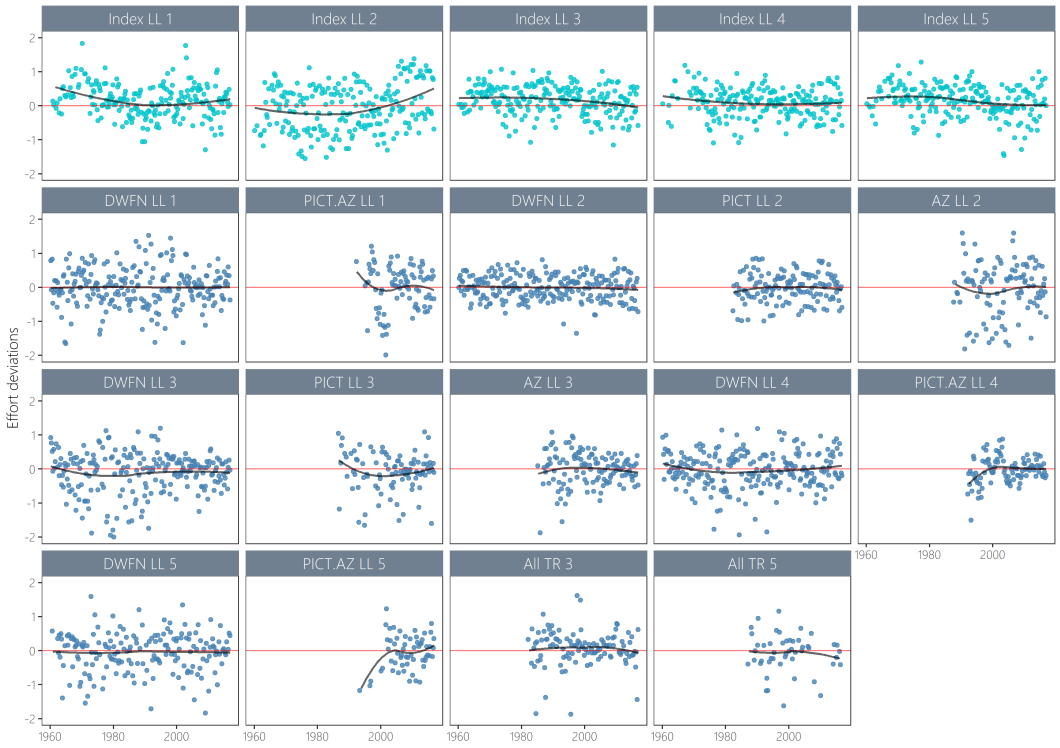

Figure 18: Effort deviations by time period for each of the fisheries receiving standardised CPUE indices in the diagnostic case model. The dark line represents a lowess smoothed fit to the effort deviations.

Figure 19: Composite (all time periods combined) observed (grey histograms) and predicted (coloured lines) catch-at-length for all fisheries with samples for the diagnostic case model. The colours indicate the groupings of the fisheries with respect to selectivity, such that fisheries sharing the same colour in the plot also share selectivity functions in the model.

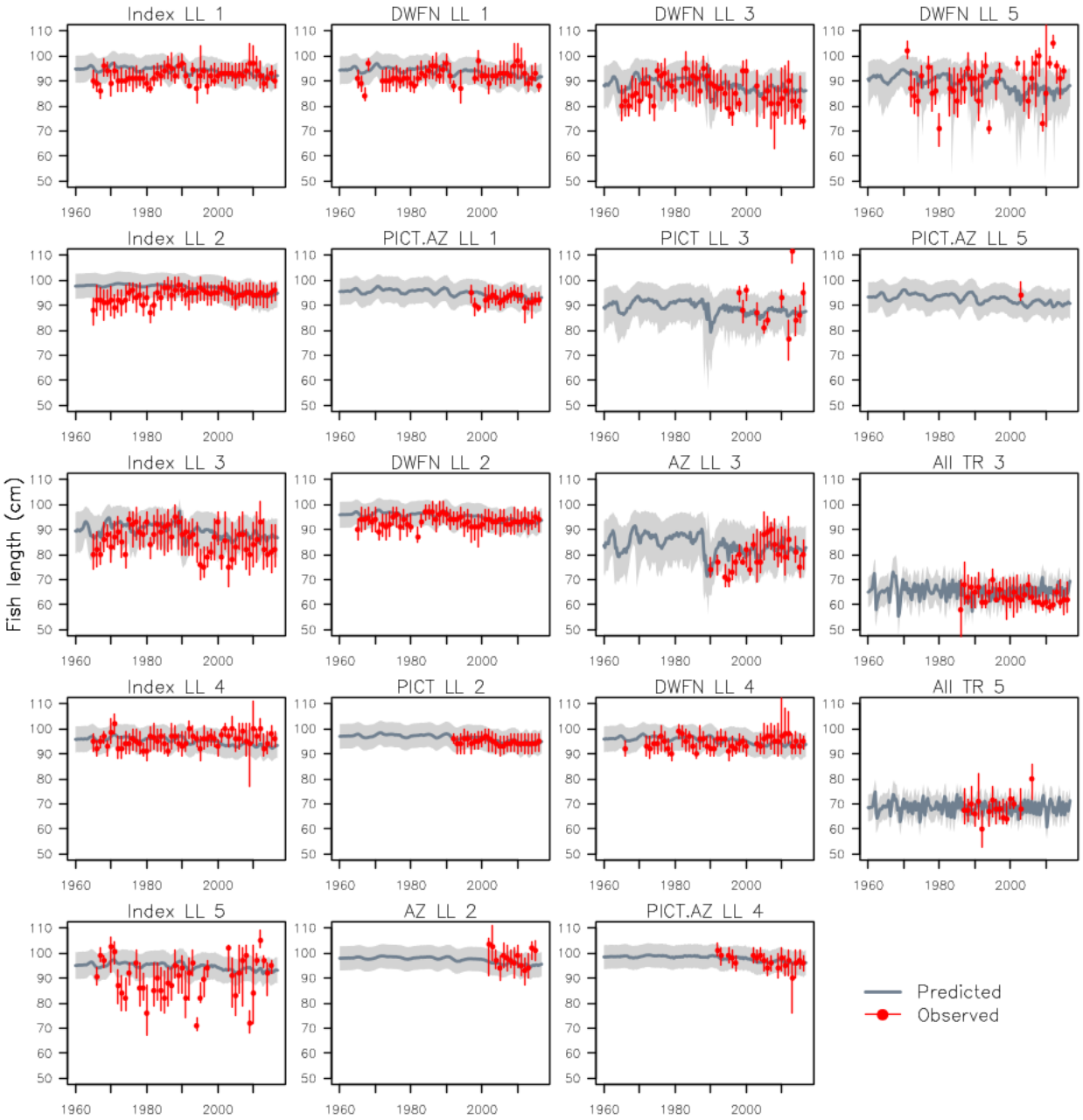

Figure 20: A comparison of the observed (red points) and predicted (grey line) median fish length (FL, cm) for all fisheries with samples for the diagnostic case model. The uncertainty intervals (grey shading) represent the values encompassed by the 25% and 75% quantiles. Sampling data are aggregated by year and only length samples with a minimum of 30 fish per year are plotted.

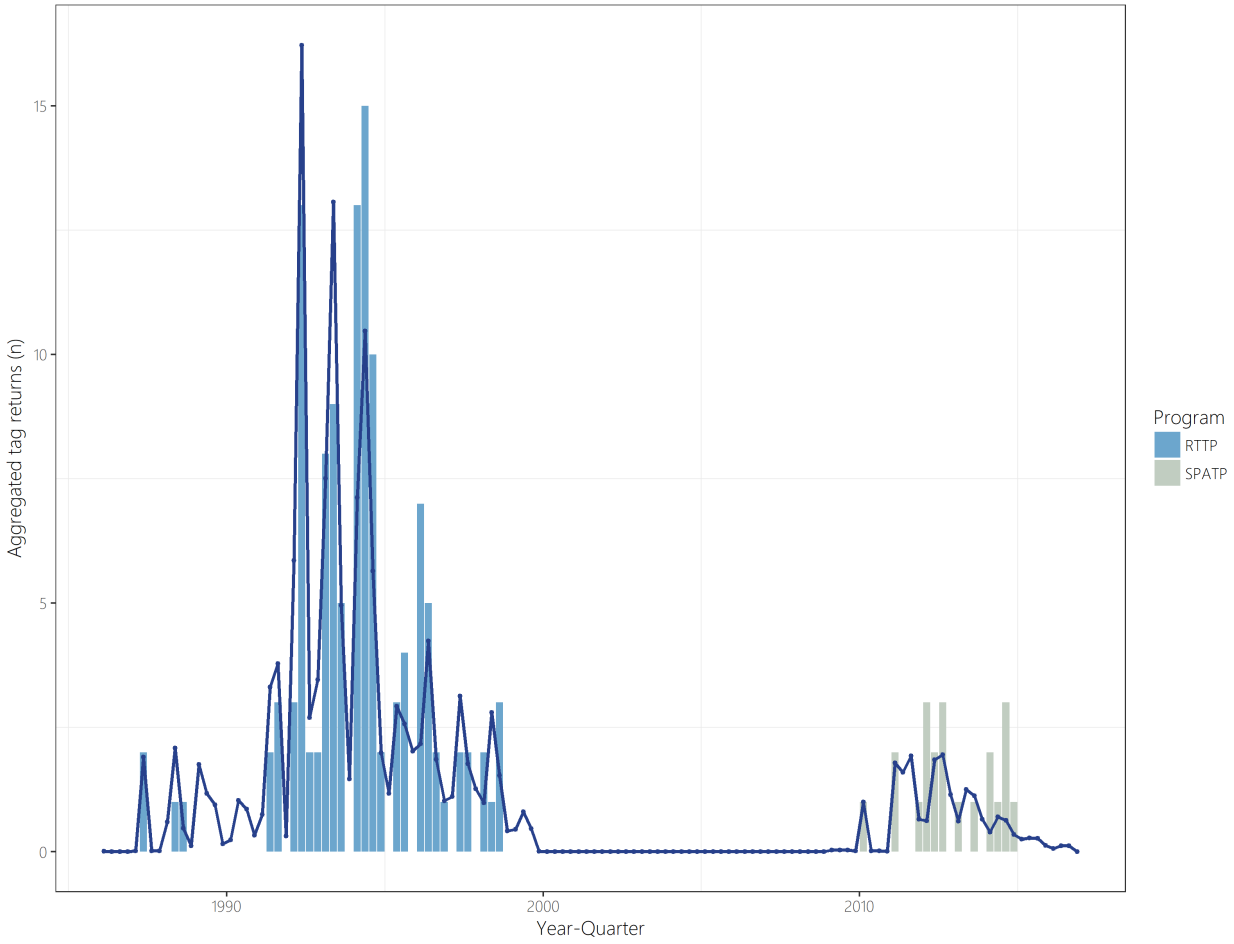

Figure 21: Observed (coloured bars) and model-predicted (blue line) tag returns over time for the diagnostic case model across all tag release events with all tag recapture groupings aggregated. The colour of the bars denotes the tagging programme from which the recaptured fish were released.

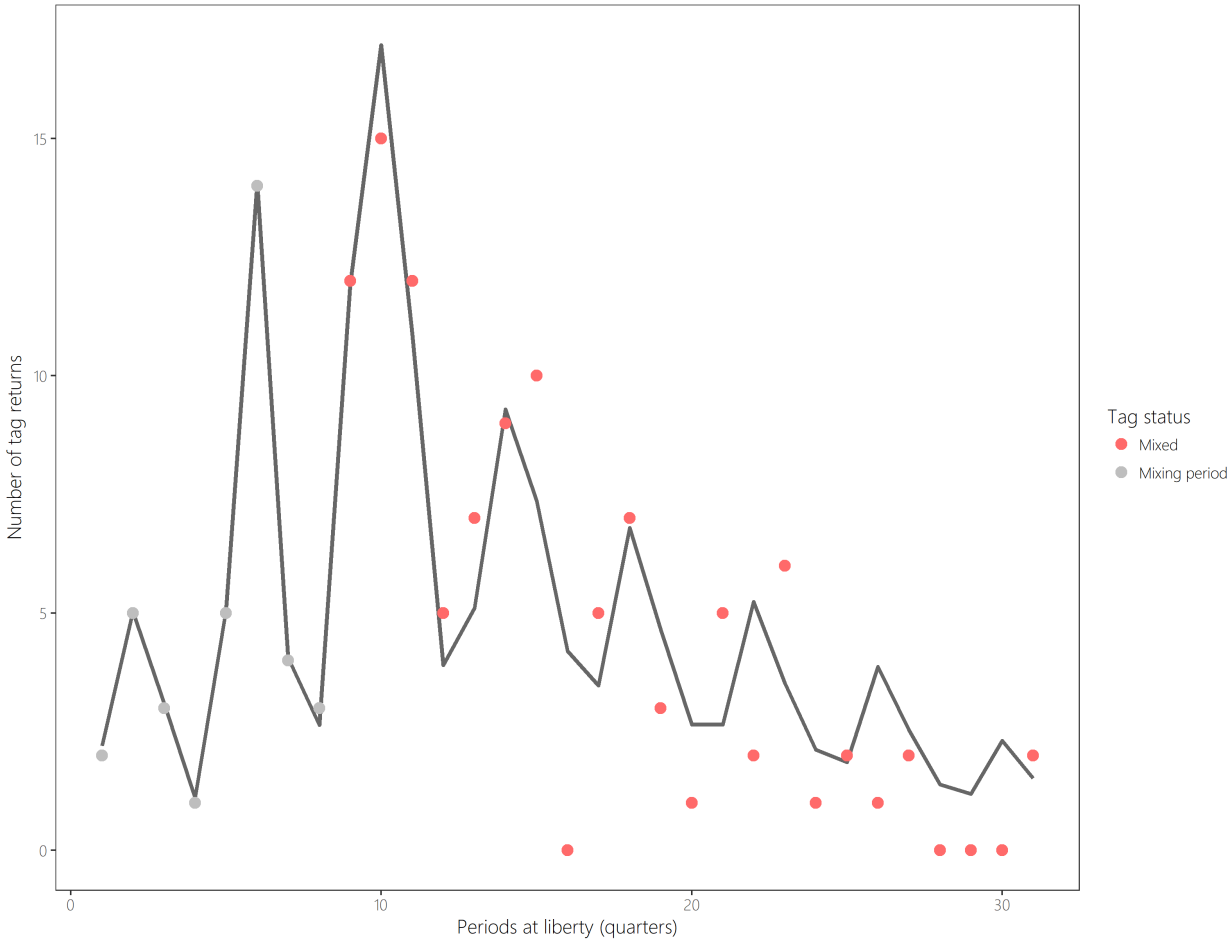

Figure 22: Observed and model-predicted tag attrition across all tag release events for the diagnostic case model.

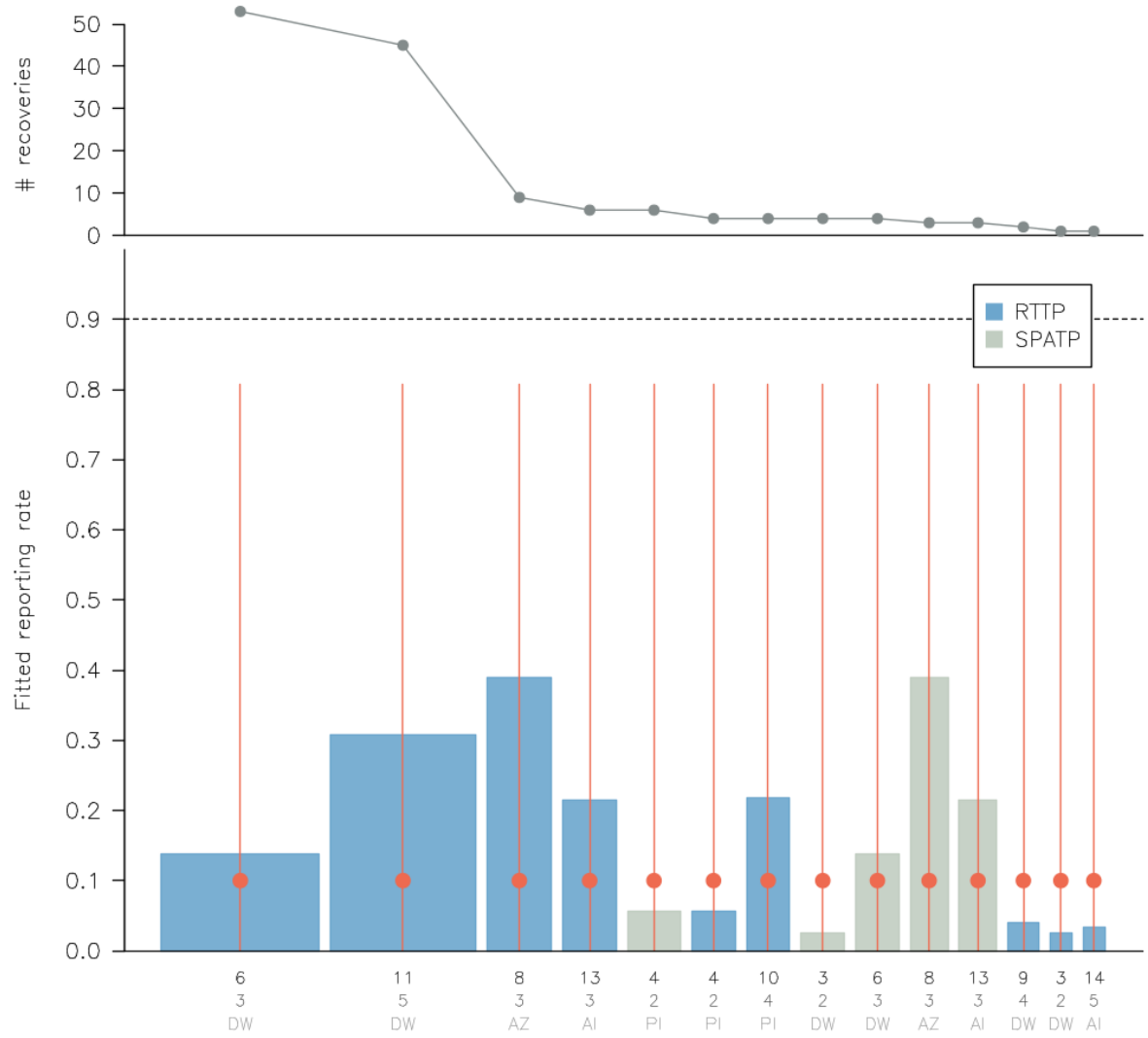

Figure 23: Estimated reporting rates for the diagnostic case model by tagging group with the prior distribution in red for each reporting rate group. The imposed upper bound (0.9) on the reporting rate parameters is shown as a dashed line. The number of recoveries per group is indicated in the top panel. Reporting rates can be estimated separately for each release program and recapture fishery group but in practice are aggregated over some recapture groups to reduce dimensionality.

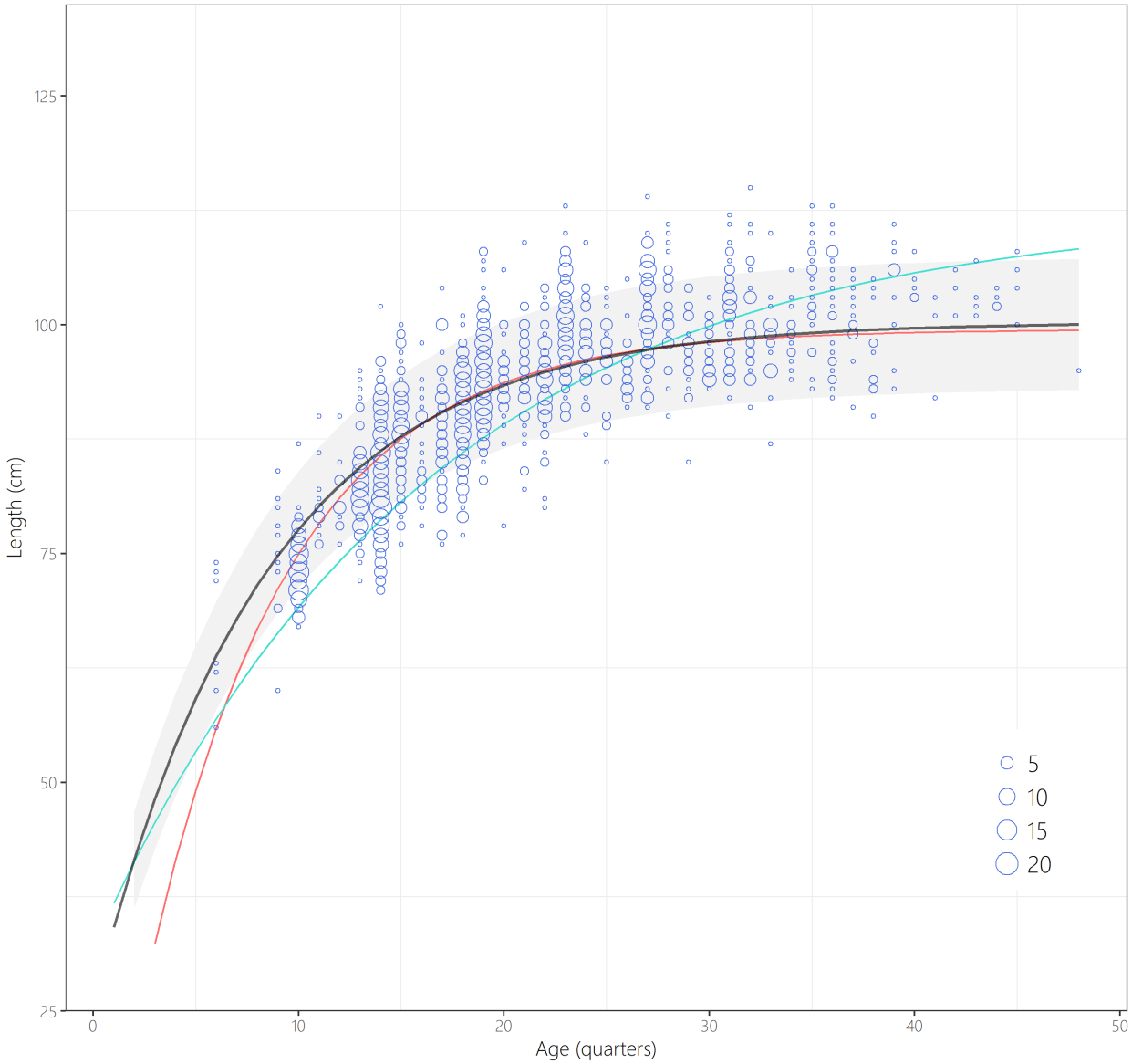

Figure 24: Estimated growth for the diagnostic case model vs. age-at-length samples included in the model. The blue line represents the estimated mean fork length (cm) at-age and the blue region represents the length-at-age within one standard deviation of the mean, for the diagnostic case model. The green line is the growth for the Chen-Wells growth scenario and the red line represents the fitted growth from the 2015 stock assessment.

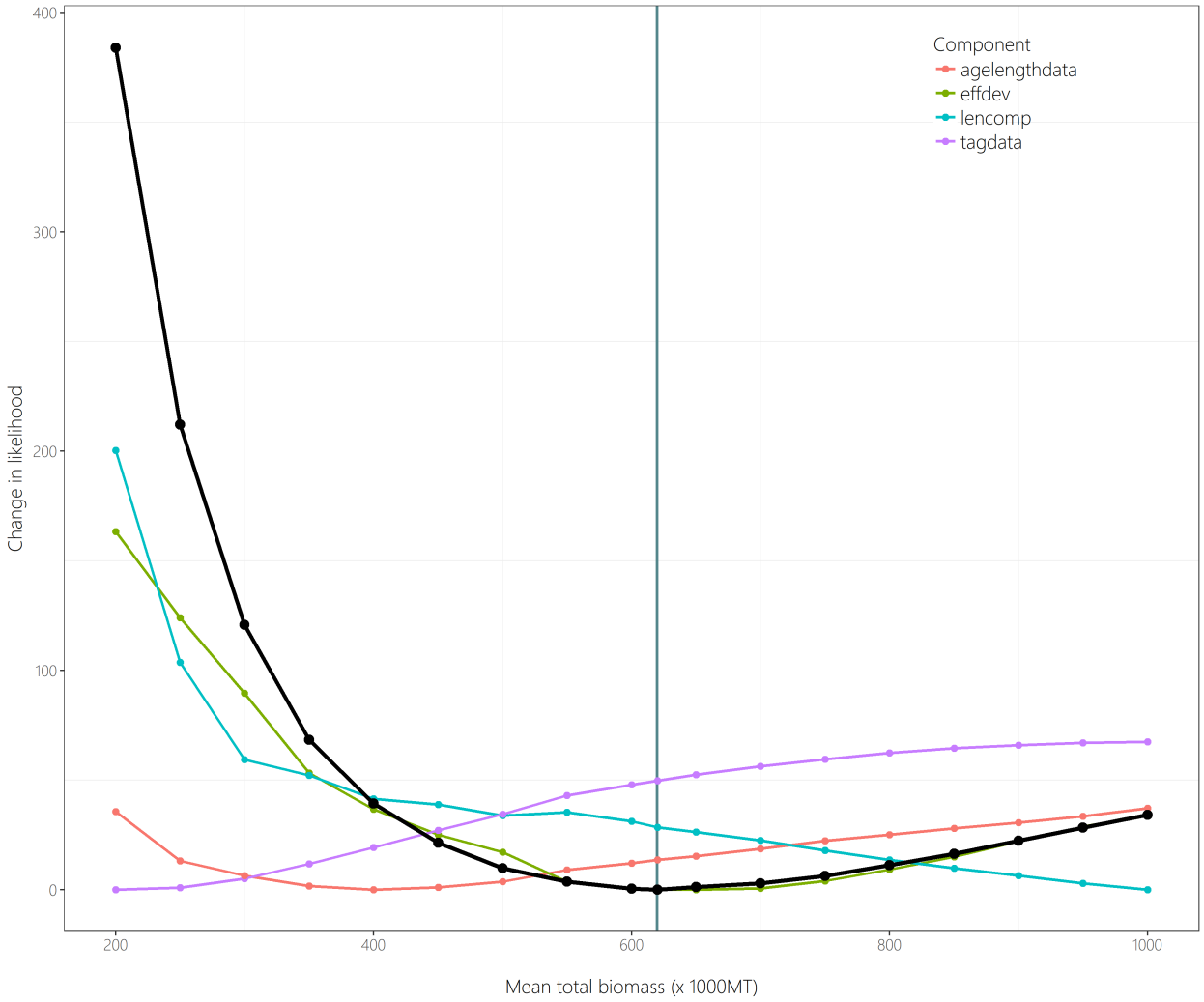

Figure 25: Change in the total, and individual data component log-likelihoods with respect to the derived parameter, mean total biomass over the assessment period, across a range of values at which this parameter was penalised to fit, for the diagnostic case model.

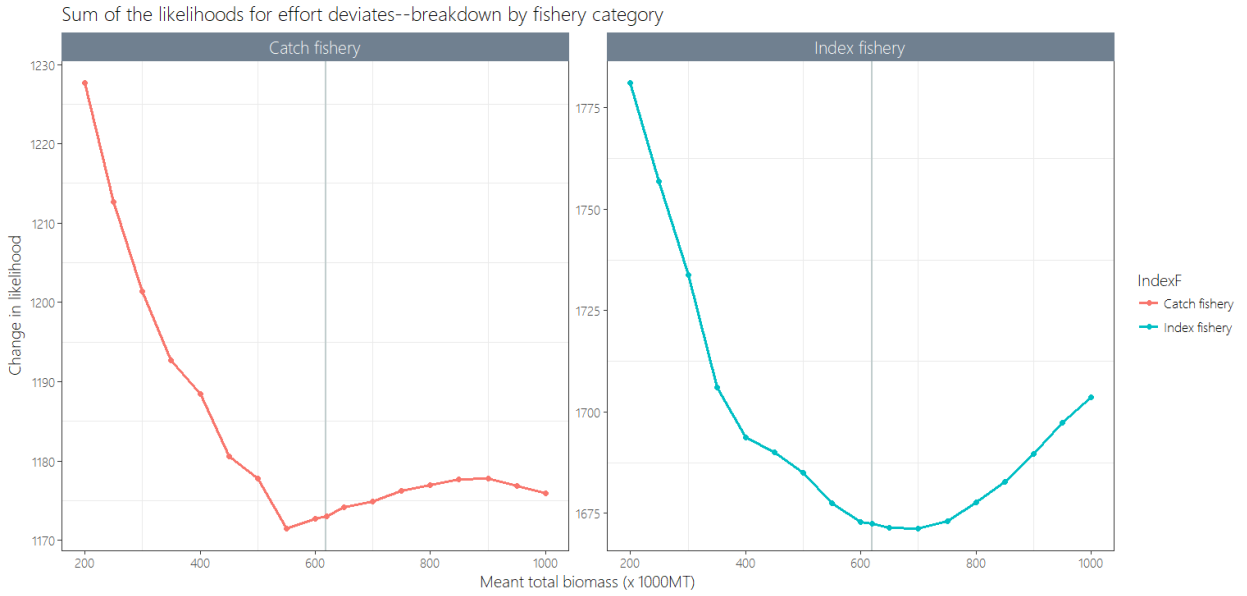

Figure 26: Change in the log-likelihoods for the effort deviates for the catch *vs.* index fisheries as a function of the derived parameter, mean total biomass over the assessment period, across a range of values at which this parameter was penalised to fit, for the diagnostic case model.

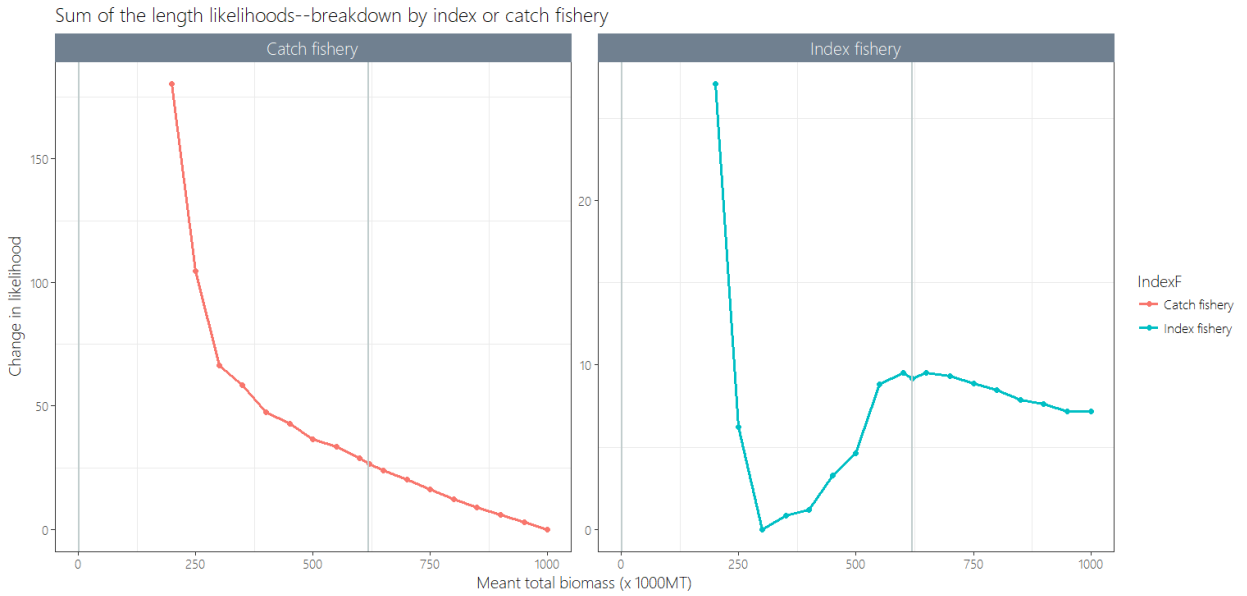

Figure 27: Change in the log-likelihoods for the size (length) data for the catch *vs.* index fisheries as a function of the derived parameter, mean total biomass over the assessment period, across a range of values at which this parameter was penalised to fit, for the diagnostic case model.

Figure 28: Estimated time series of catchability for those fisheries assumed to have random walk in these parameters. Values shown are the annual means which removes seasonal variability.

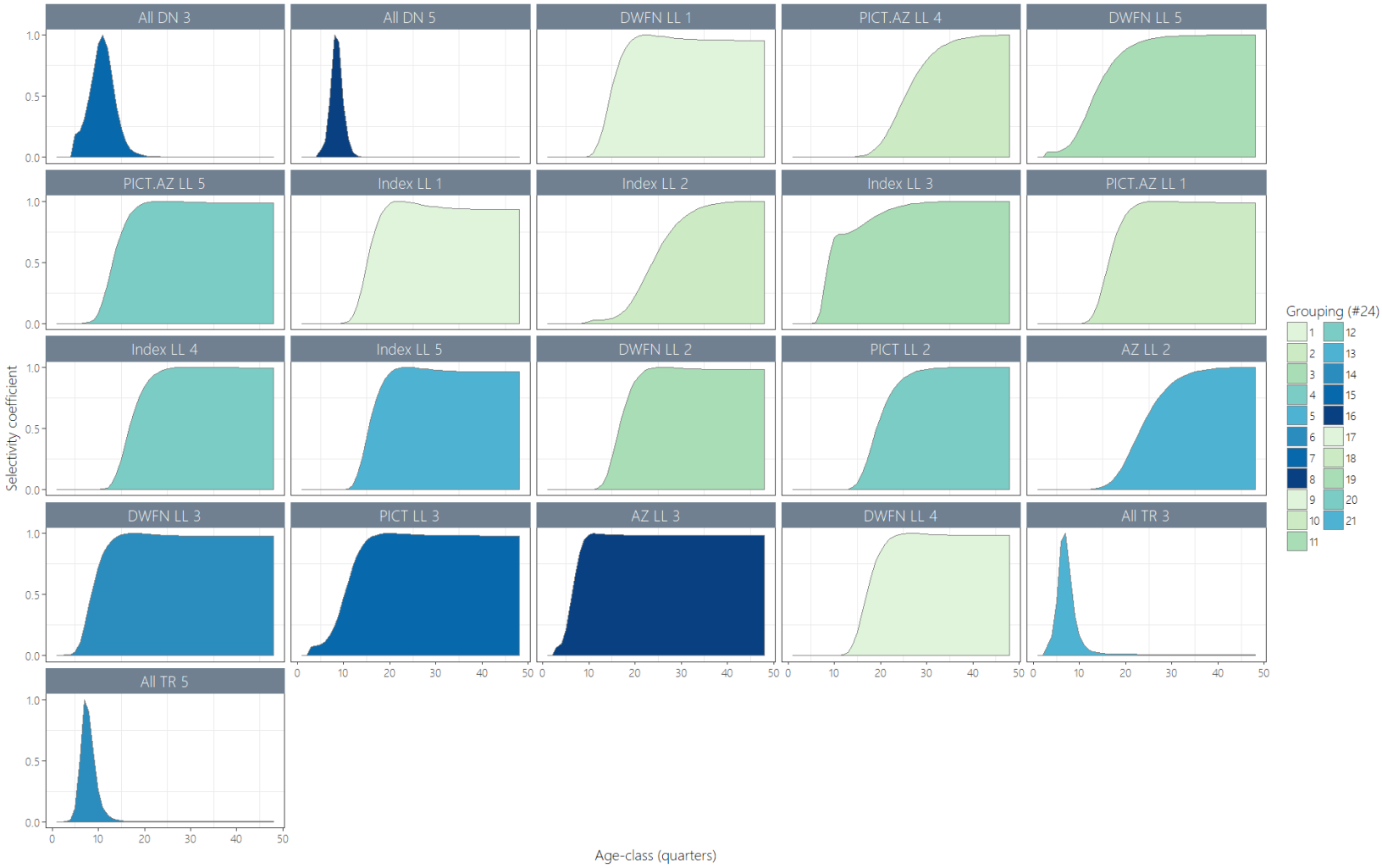

Figure 29: Estimated age-specific selectivity coefficients by fishery for the diagnostic case model. The colours indicate the groupings of the fisheries with respect to selectivity, such that fisheries sharing the same colour in the plot also share selectivity functions in the model.

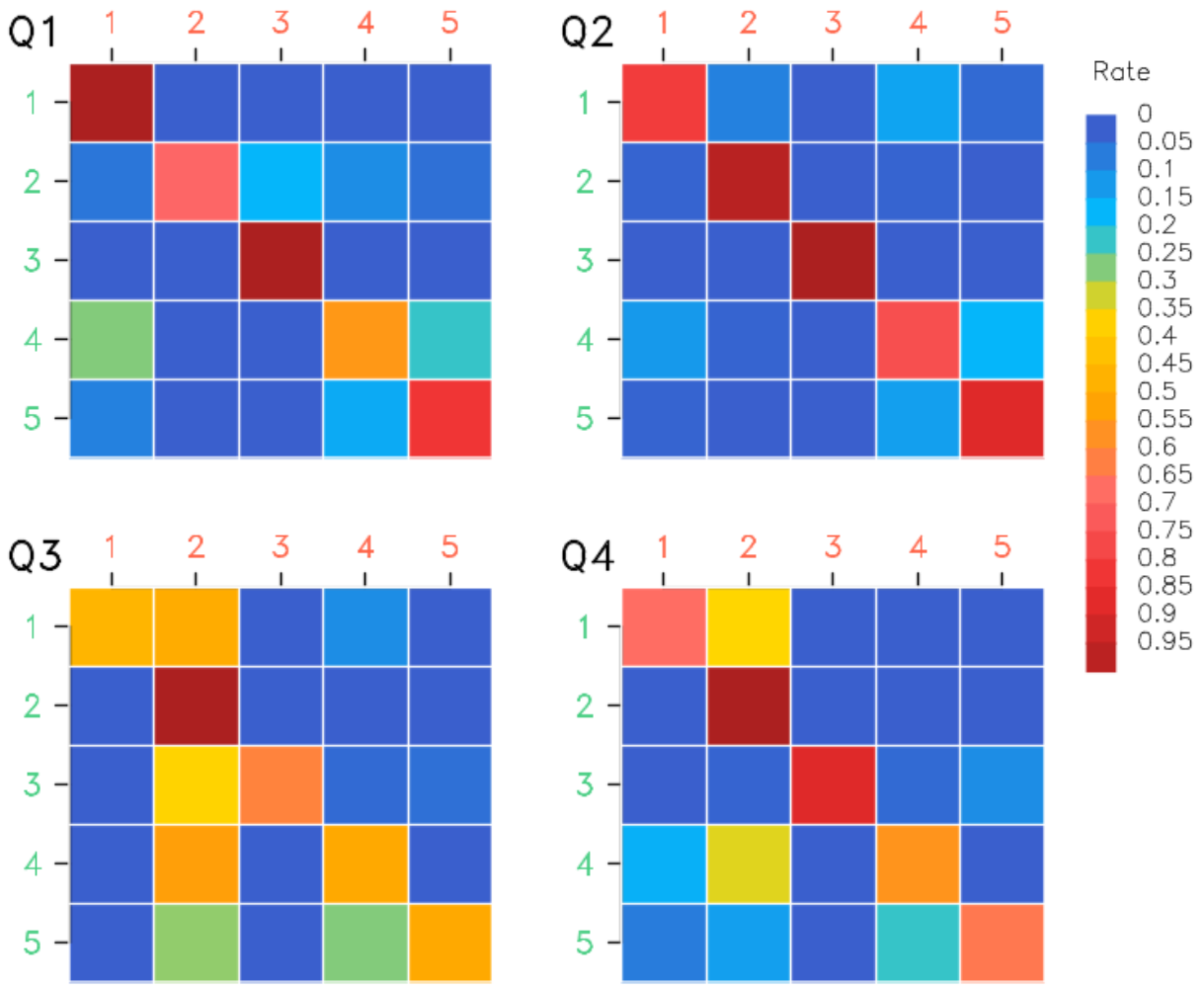

Figure 30: Estimated movement coefficients by quarter for the diagnostic case model. The green numbers (vertical axis) indicate the source model region, the red numbers (horizontal axis) indicate the receiving regions. The colour of the tile shows the magnitude of the movement rate (proportion of individuals from region x moving to region y in that quarter), with each row adding up to 1.

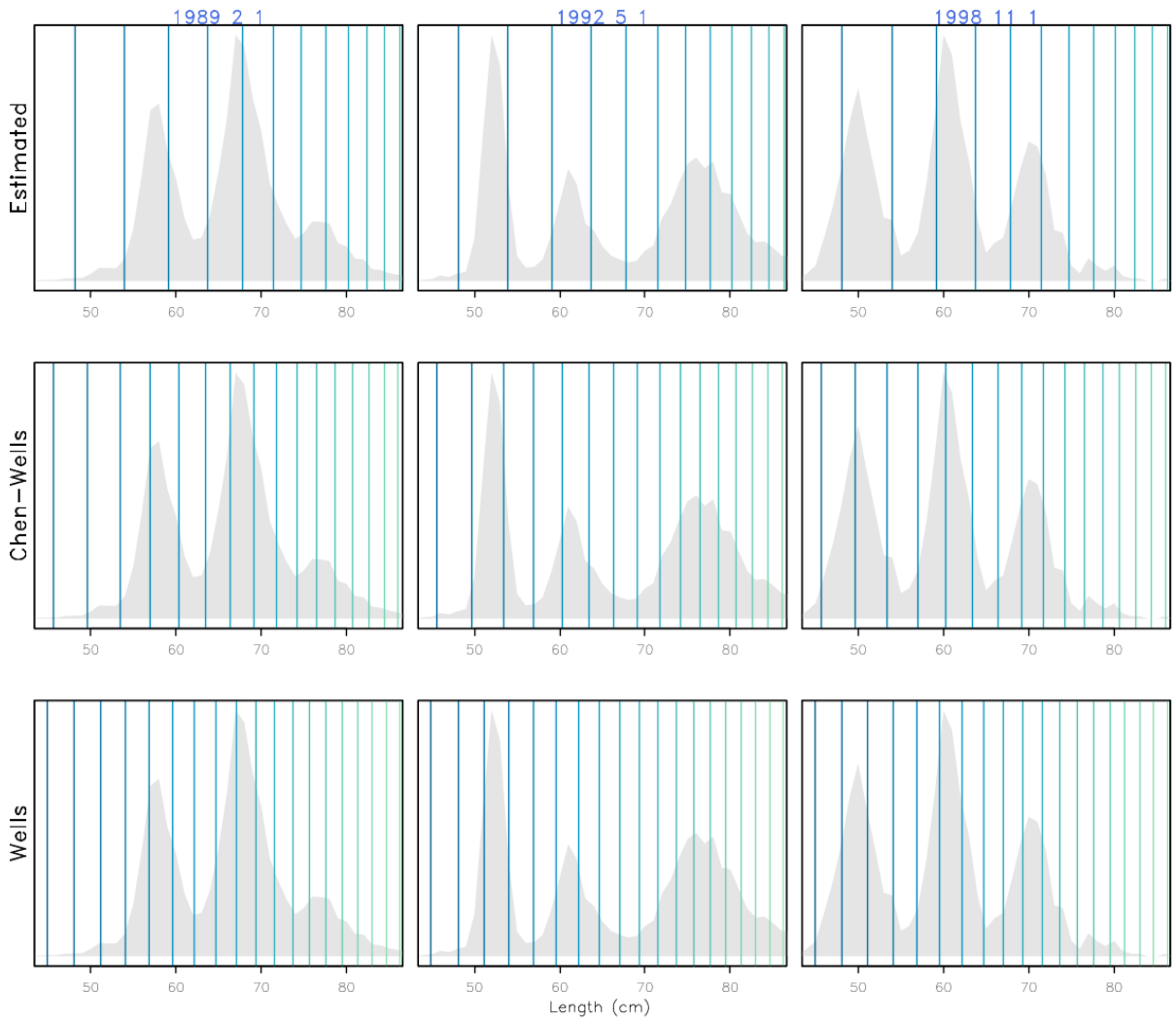

Figure 31: Fits to annual modes in the troll length frequency (grey distributions) from three sample years with clear modes (1989, February; 1992, May; 1998, Nov), and corresponding quarterly size estimates (vertical lines) under three alternative growth models examined during model development: estimated growth (diagnostic case; top row), Chen-Wells fixed growth (grid axis, middle row), Wells fixed growth from (Wells et al., 2013) (used in exploratory phase, bottom row). Under the assumption that these length modes are annual, there should be four vertical quarterly lines between each length mode.

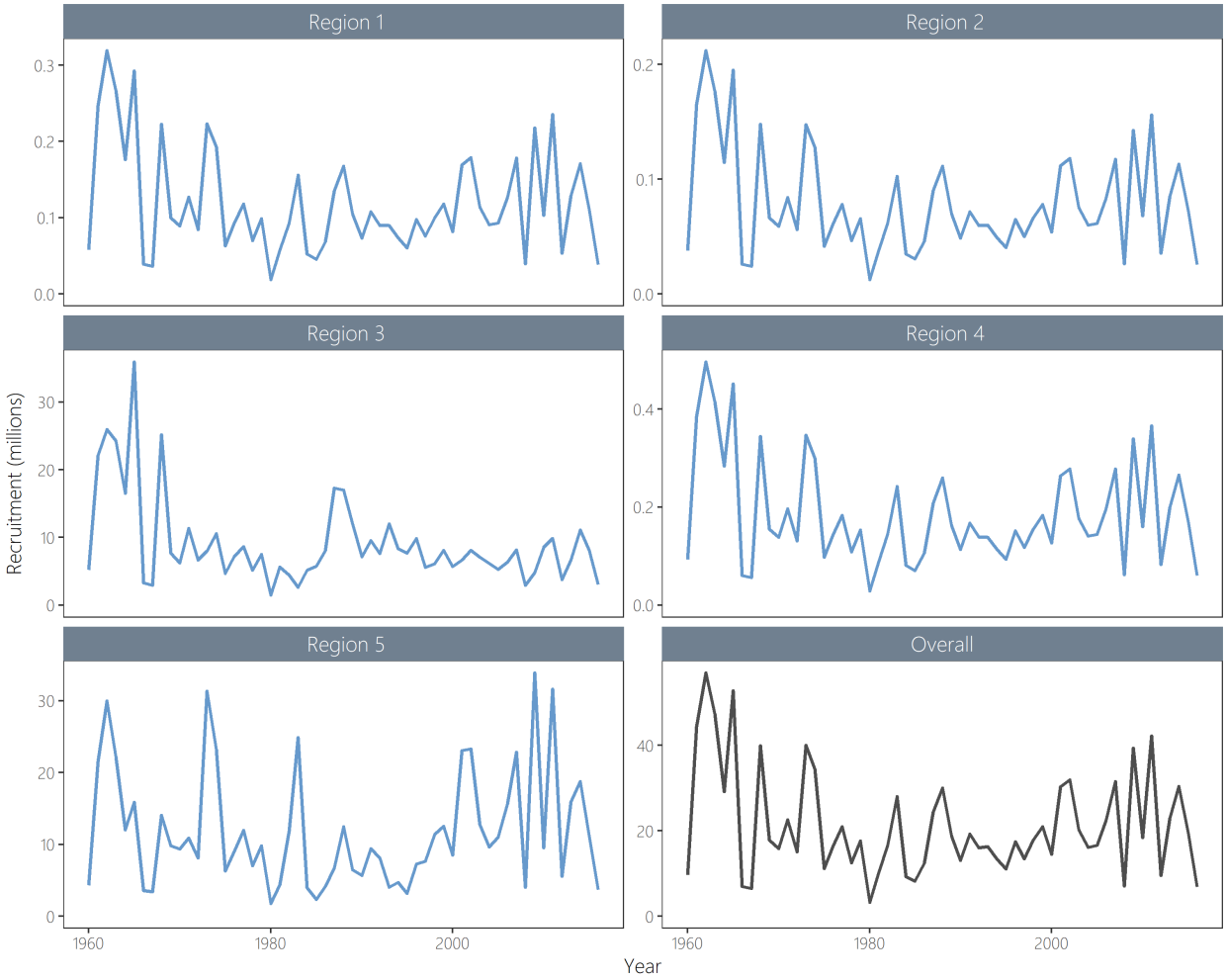

Figure 32: Estimated annual, temporal recruitment by model region for the diagnostic case model. Note that the scale of the y-axis is not constant across regions.

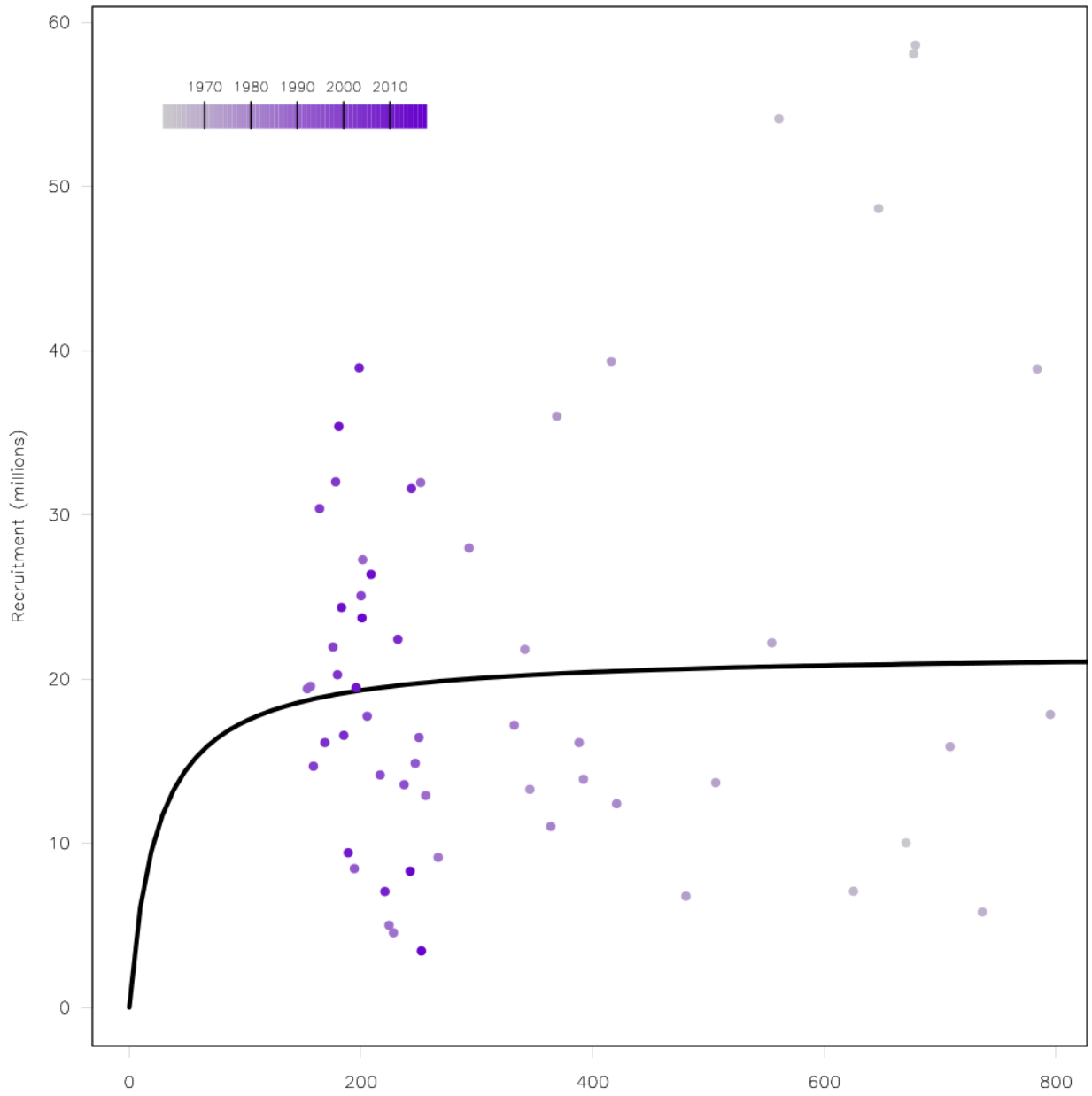

Figure 33: Estimated relationship between recruitment and spawning potential based on annual values for the diagnostic case model. The darkness of the circles changes from light to dark through time.

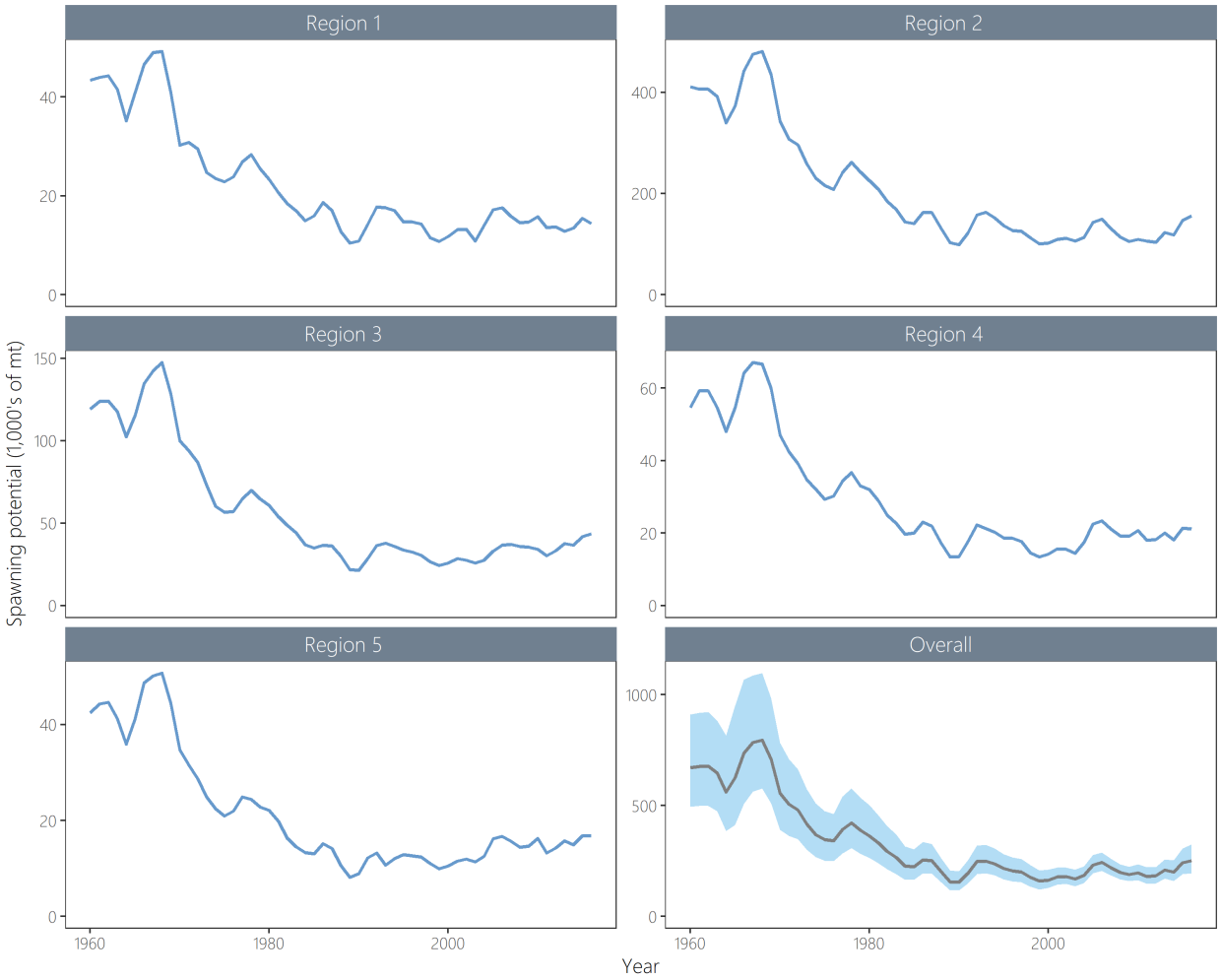

Figure 34: Estimated temporal spawning potential by model region for the diagnostic case model. Note that the scale of the y-axis is not constant across regions.

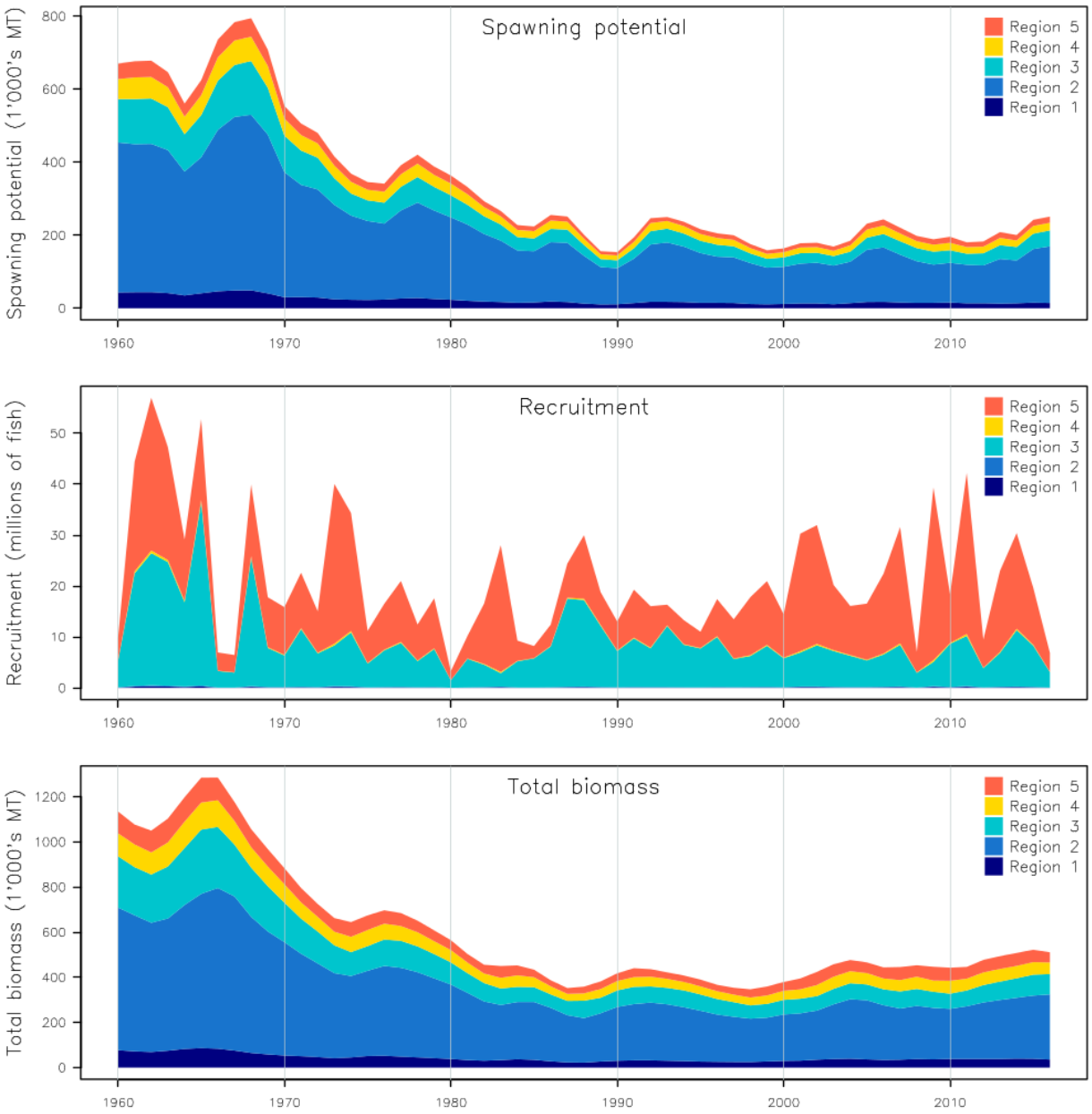

Figure 35: Estimated annual average recruitment, spawning potential and total biomass by model region for the diagnostic case model, showing the relative sizes among regions.

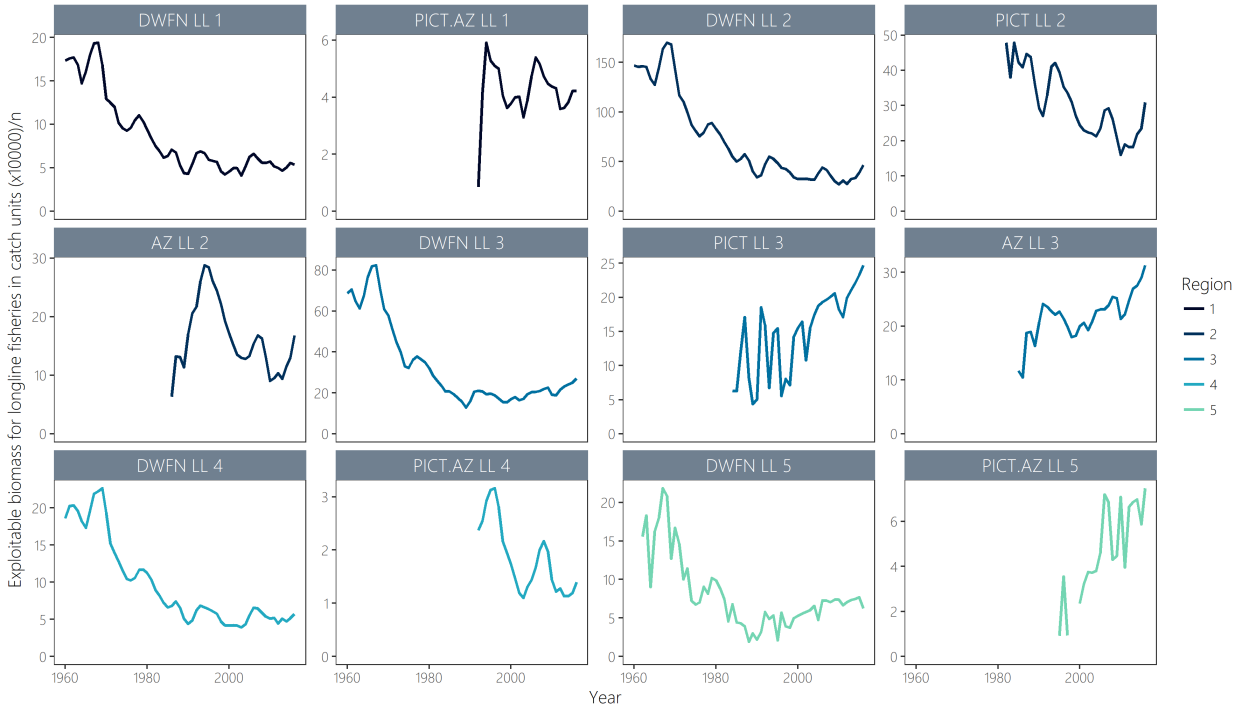

Figure 36: Vulnerable (exploitable) biomass by longline fleet by region, where vulnerable biomass is the product of catch in numbers by weight-at-age and selectivity for a given fleet in region.

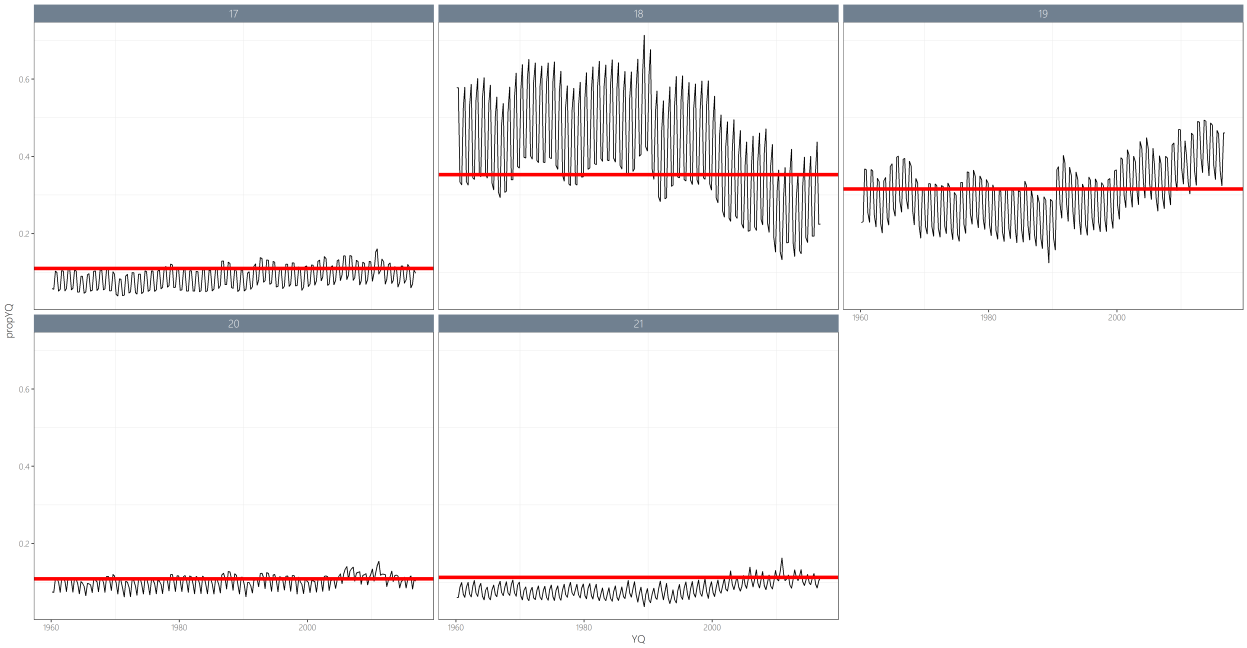

Figure 37: Vulnerable (exploitable) biomass by region for the index fisheries compared to regional weights (red line) as specified in the CPUE.

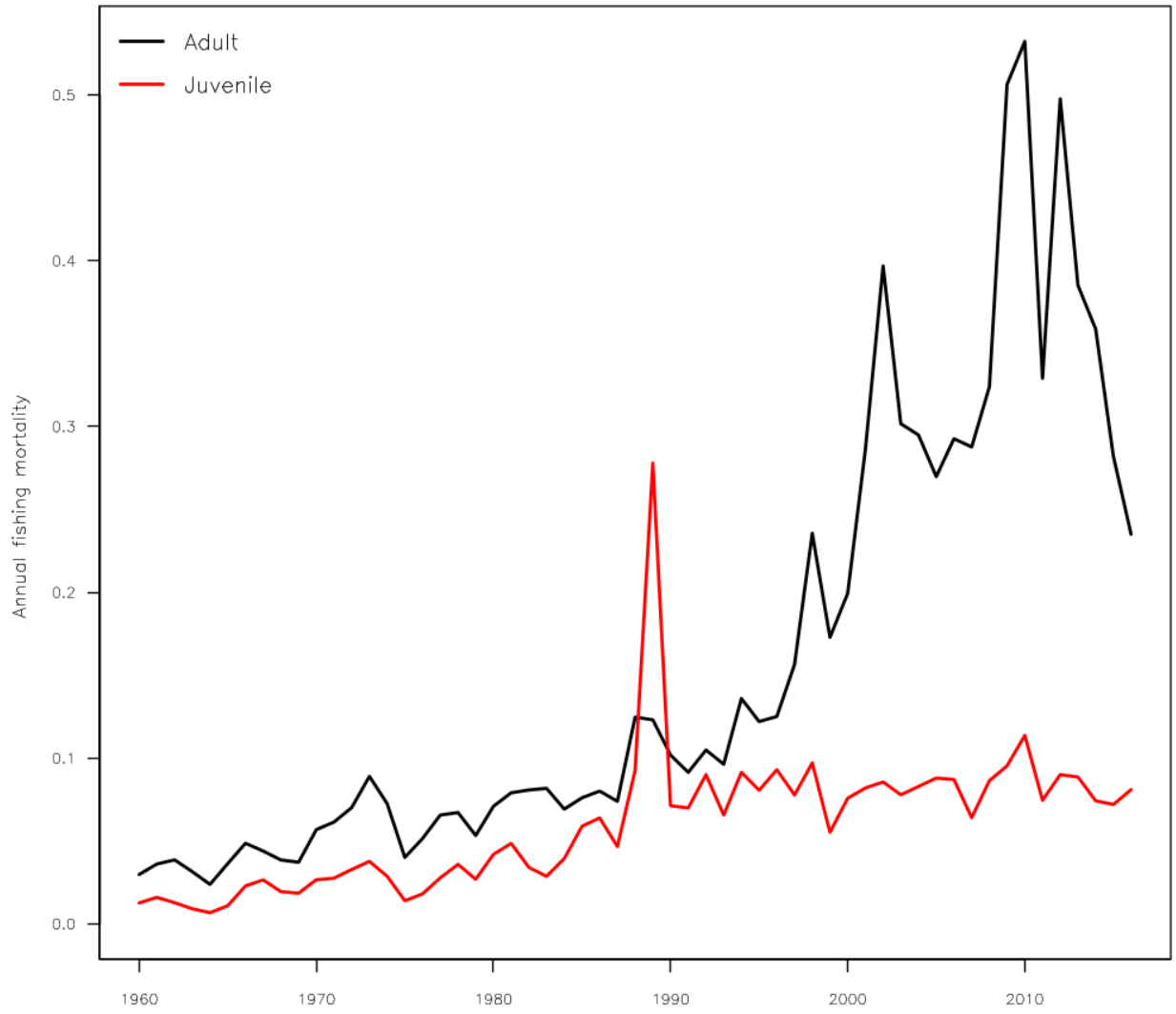

Figure 38: Estimated annual average juvenile and adult fishing mortality for the diagnostic case model.

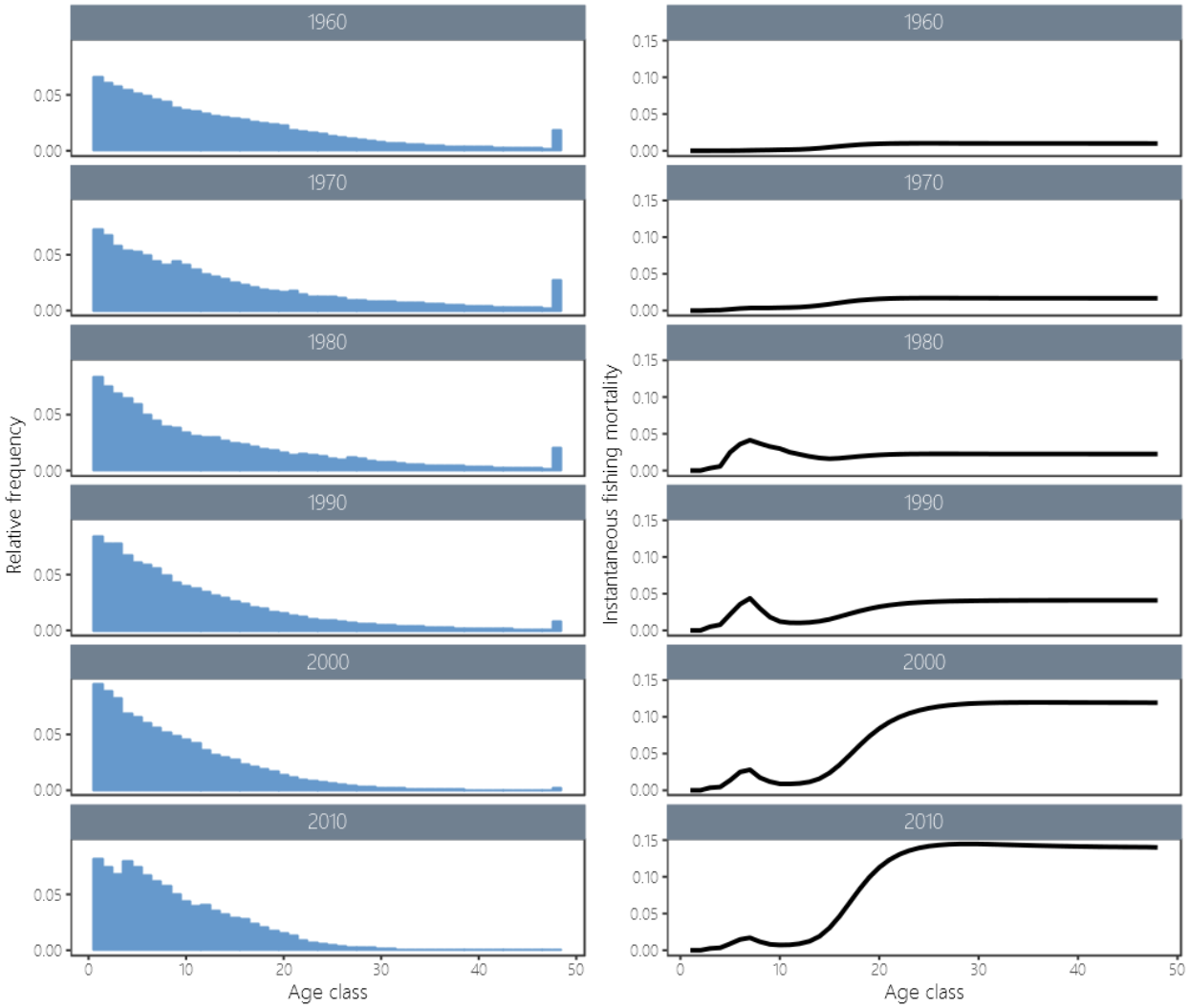

Figure 39: Estimated proportion of the population at-age (quarters; left panels) and fishing mortality-at-age (right panels), at decadal intervals, for the diagnostic case model.

Figure 40: Estimated age-specific fishing mortality for the diagnostic case model, by region and overall.

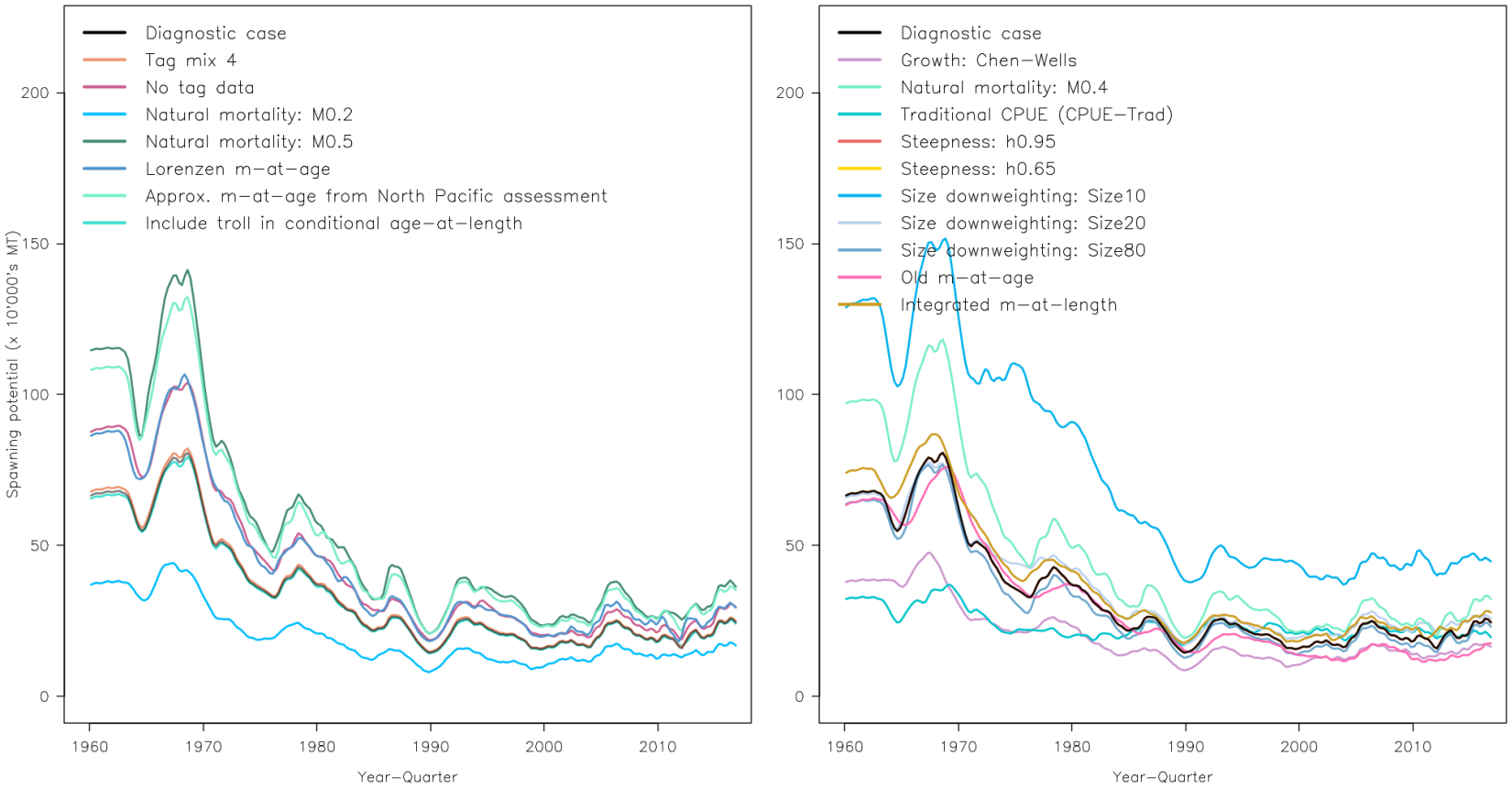

Figure 41: Estimated spawning potential for each of the one-off sensitivity models investigated in the assessment. The models are separated into two groups, (a) and (b), to prevent obstruction of lines. Details of the models can be found in Section 6.2.

Figure 42: Estimated spawning potential for each of the one-off sensitivity models investigated in the assessment. The models are separated into two groups, (a) and (b), to prevent obstruction of lines. Details of the models can be found in Section 6.2.

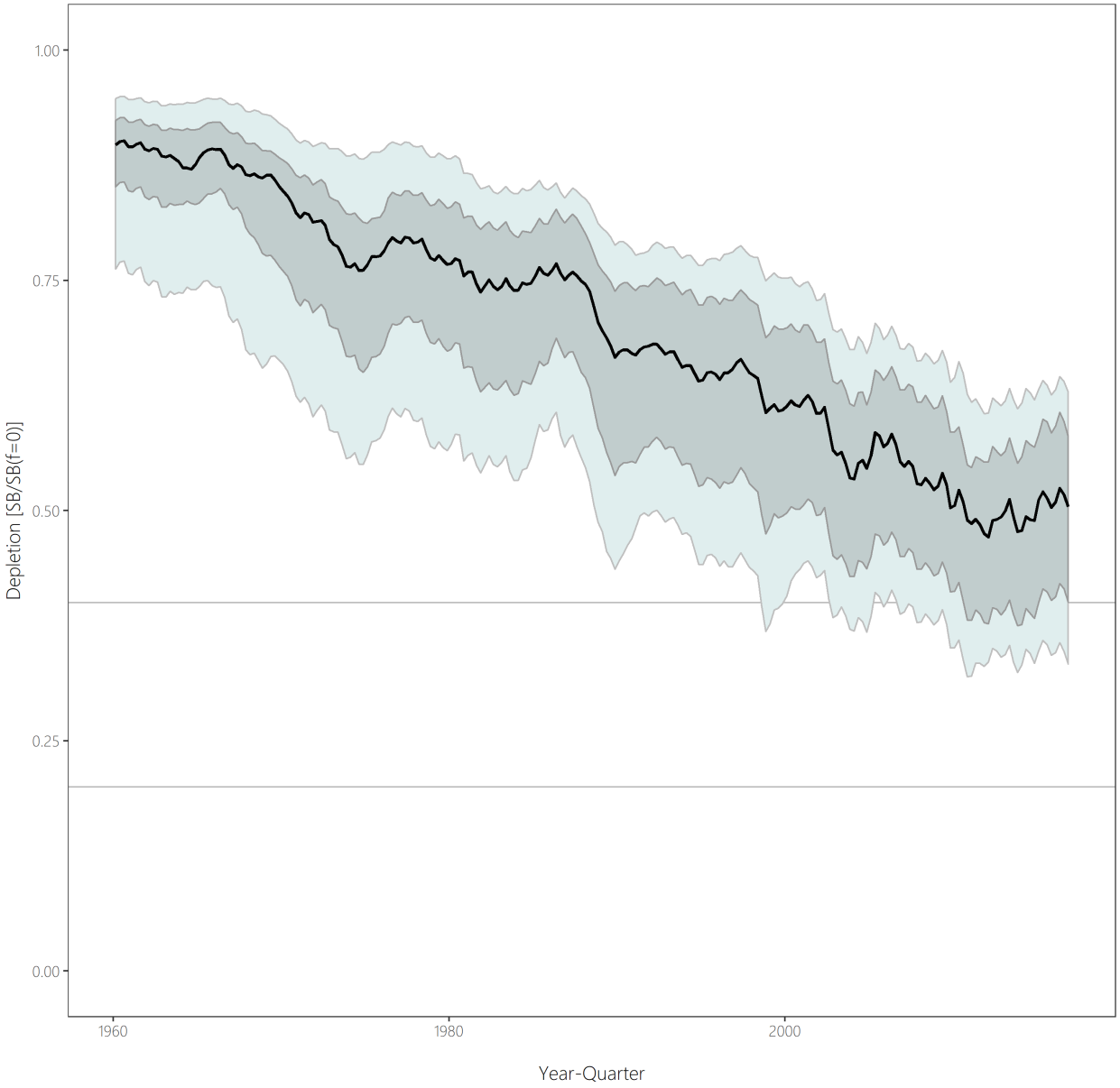

Figure 43: Distribution of time series depletion estimates across the structural uncertainty grid. Black line represents the grid median trajectory, dark grey region represents the 50%ile range, light grey the 90%ile range.

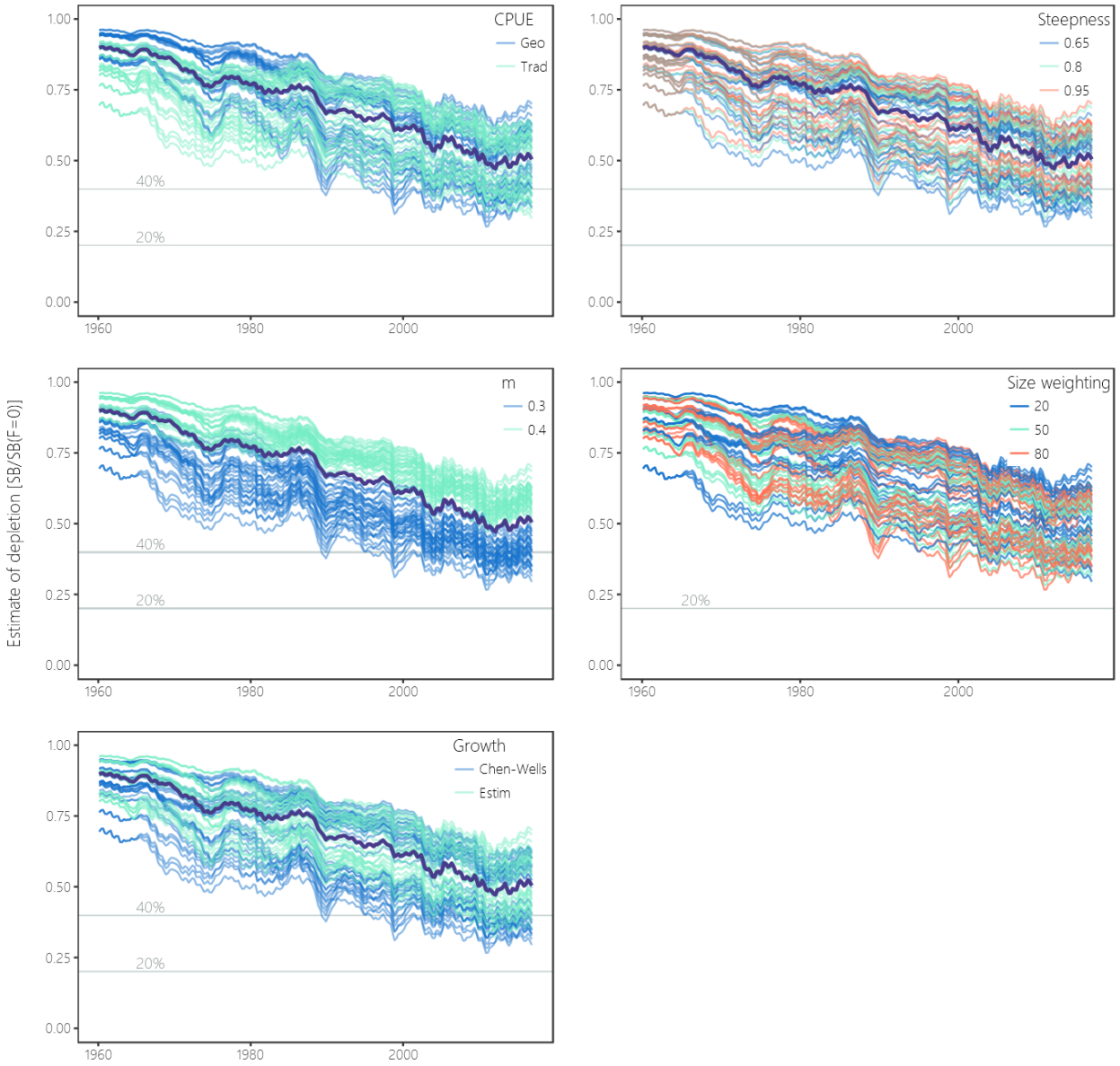

Figure 44: Plots showing the trajectories of fishing depletion (of spawning potential) for the model runs included in the structural uncertainty grid (see Section 6.2 for details of the structure of the grid models). The five panels show the models separated on the basis of the five axes used in the grid, with the colour denoting the level within the axes for each model.

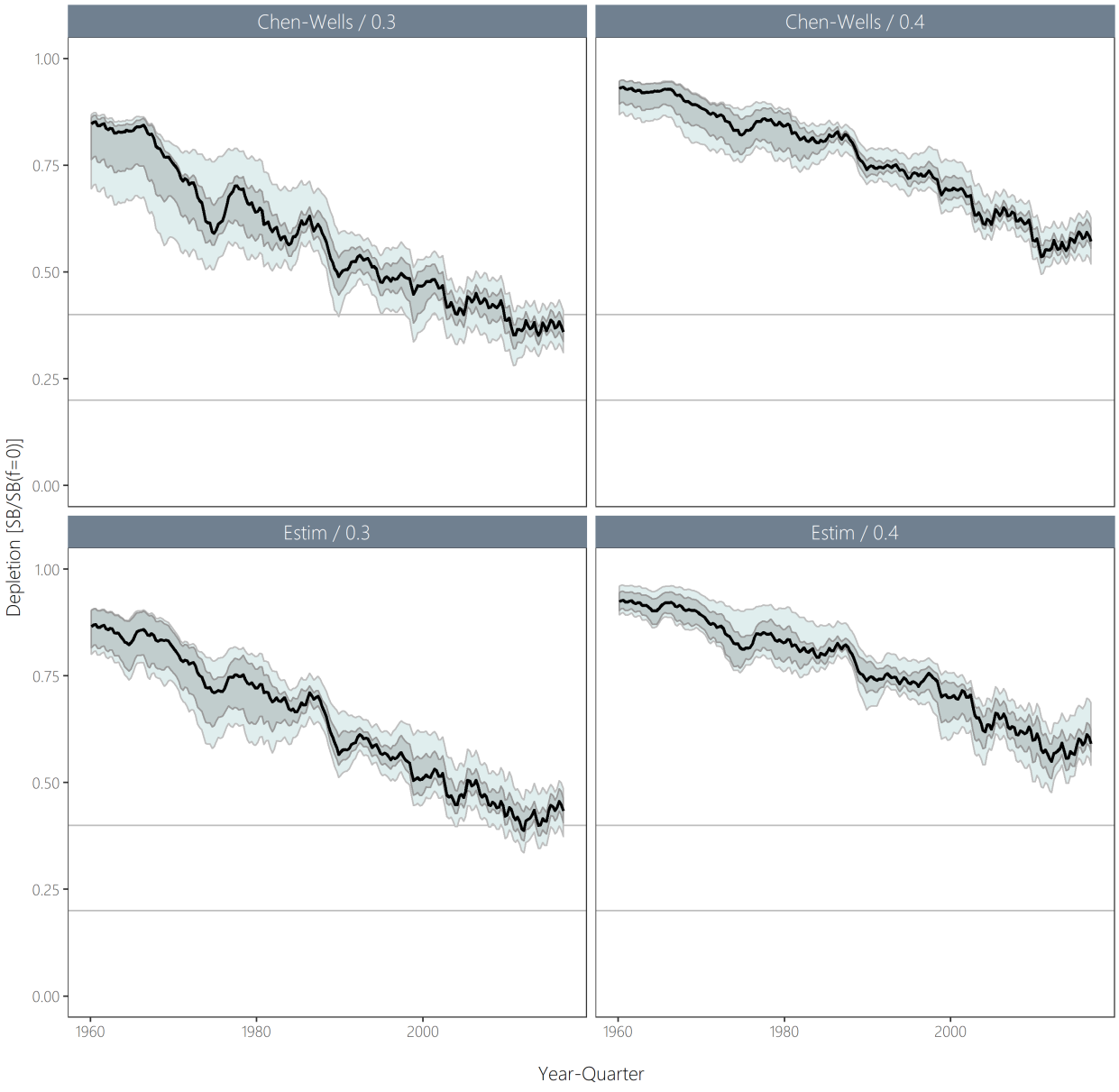

Figure 45: Distribution of time series depletion estimates across the structural uncertainty grid split by key grid subsets. Black line represents the grid median trajectory, dark grey region represents the 50%ile range, light grey the 90%ile range.

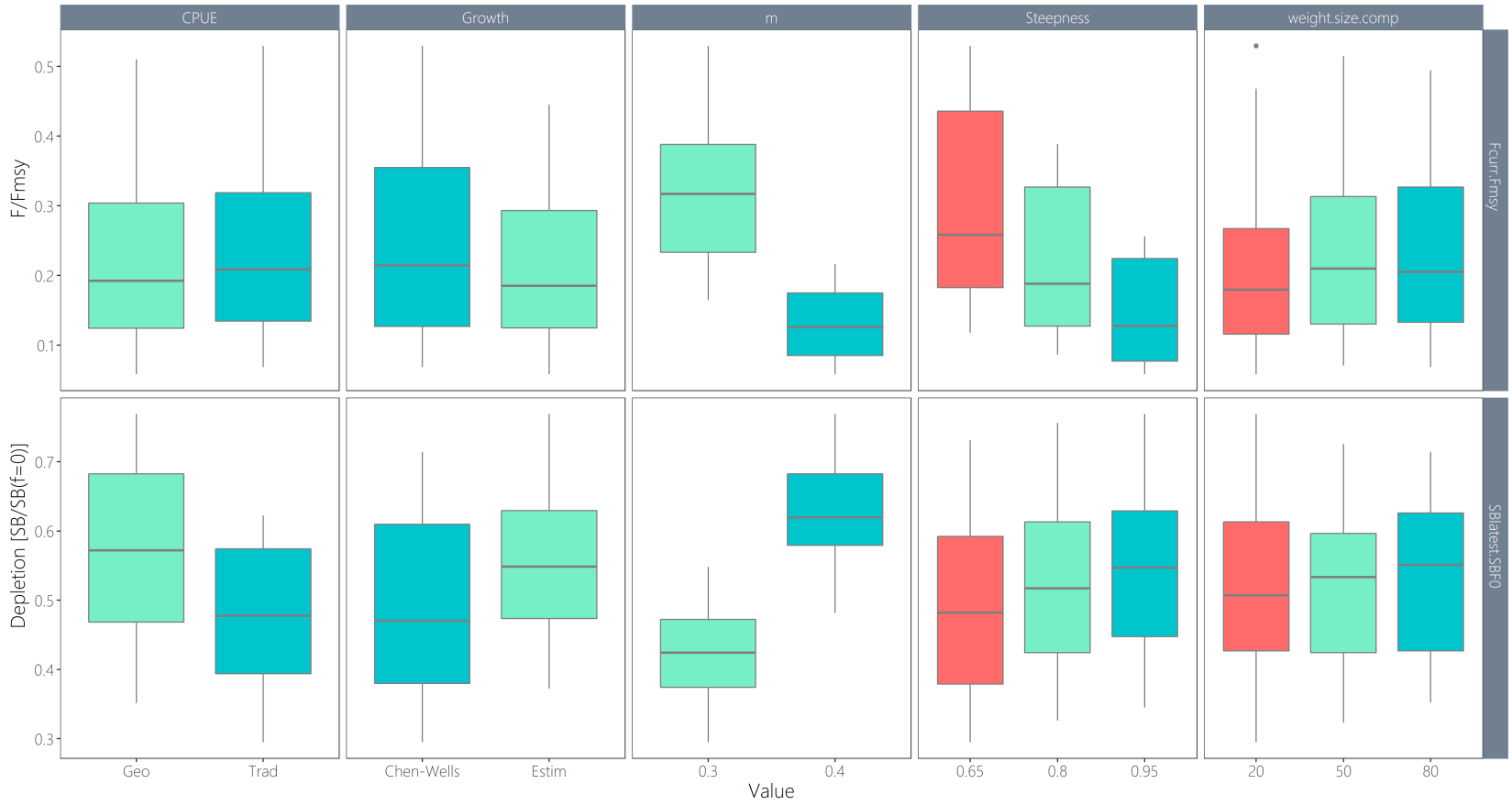

Figure 46: Boxplots summarising the results of the structural uncertainty grid with respect to the spawning potential reference point (left panels), and the fishing mortality reference point $F_{recent}/F_{\mathrm{MSY}}$ (right panels). The colours indicate the level of the model with respect to each uncertainty axis.

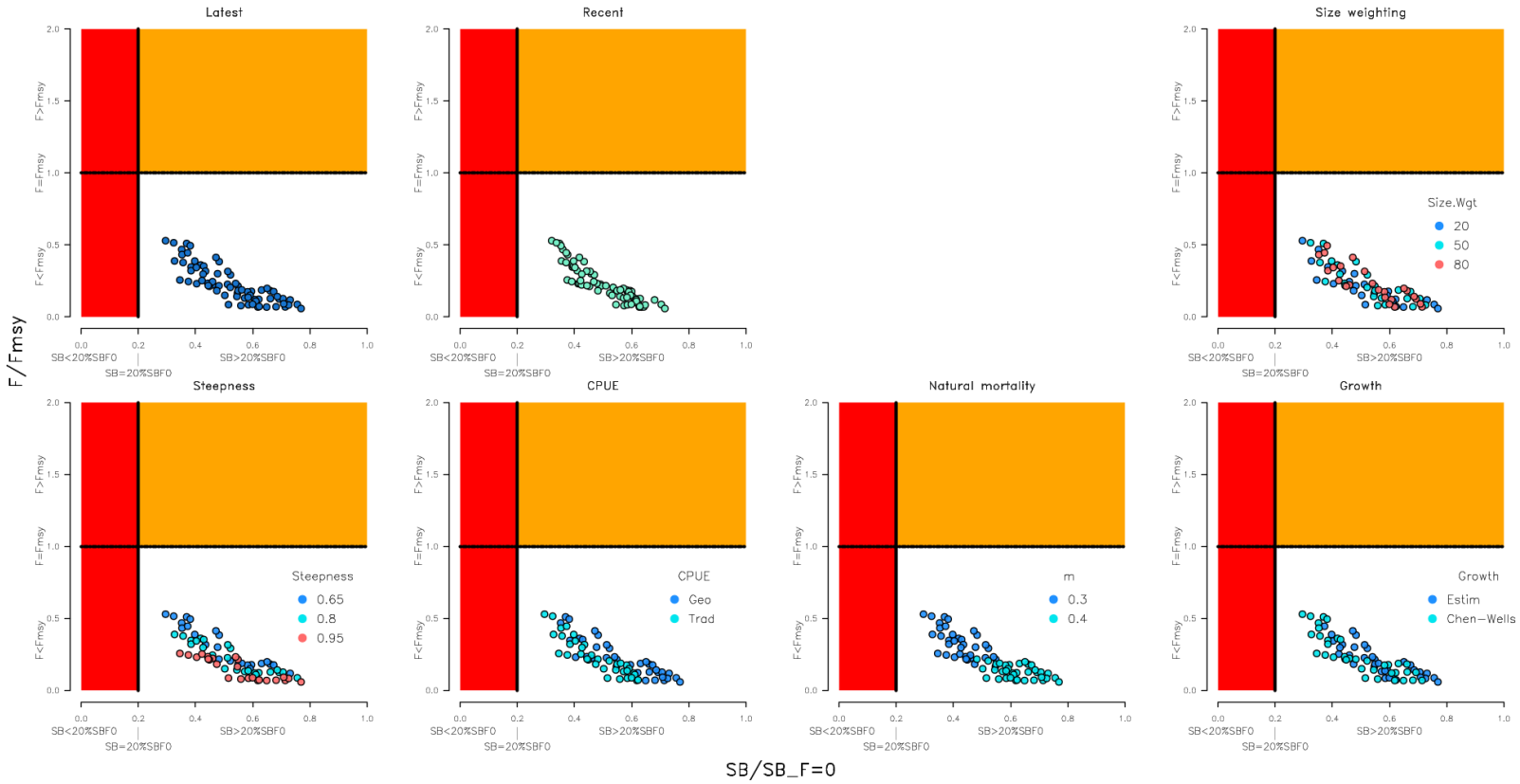

Figure 47: Majuro plots summarising the results for each of the models in the structural uncertainty grid. The plots represent estimates of stock status in terms of spawning potential depletion and fishing mortality. The red zone represents spawning potential levels lower than the agreed limit reference point which is marked with the solid black line. The orange region is for fishing mortality greater than F_{MSY} (F_{MSY} is marked with the black dashed line). The points represent $SB_{latest}/SB_{F=0}$ for each model run except in panel (b) where $SB_{recent}/SB_{F=0}$ is displayed. The remaining panels show the estimates for the different levels for the five axes of the grid.

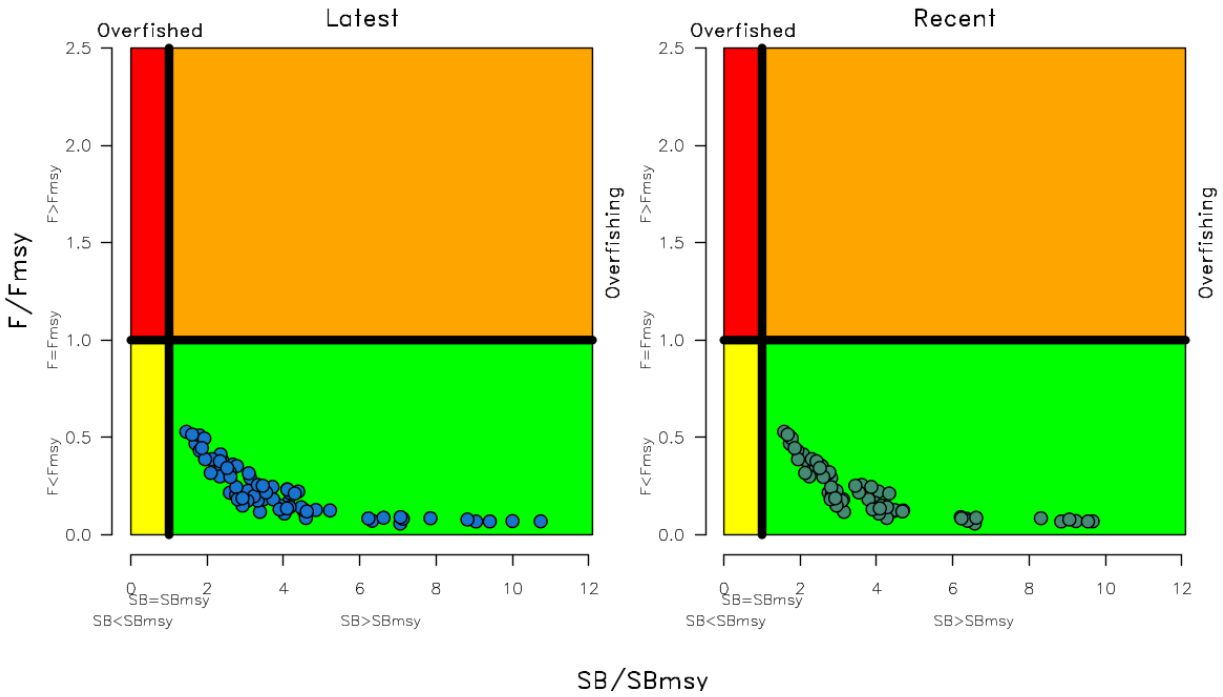

Figure 48: Kobe plots summarising the results for each of the models in the structural uncertainty grid under the $SB_{latest}/SB_{F=0}$ and the $SB_{recent}/SB_{F=0}$ reference points.

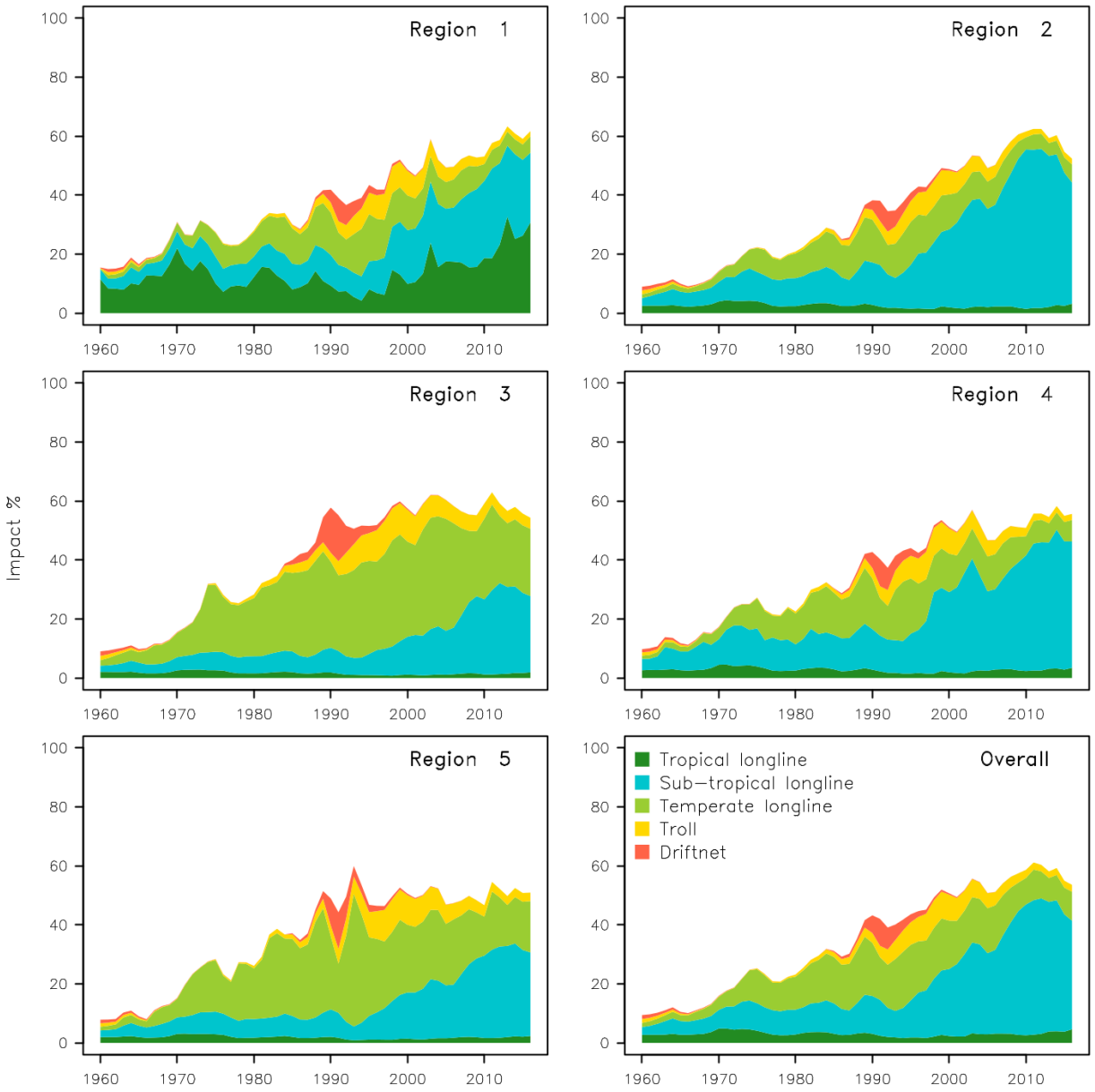

Figure 49: Estimates of reduction in spawning potential due to fishing (fishery impact = $1-SB_{latest}/SB_{F=0}$) by region, and over all regions (lower right panel), attributed to various fishery groups for the diagnostic case model.

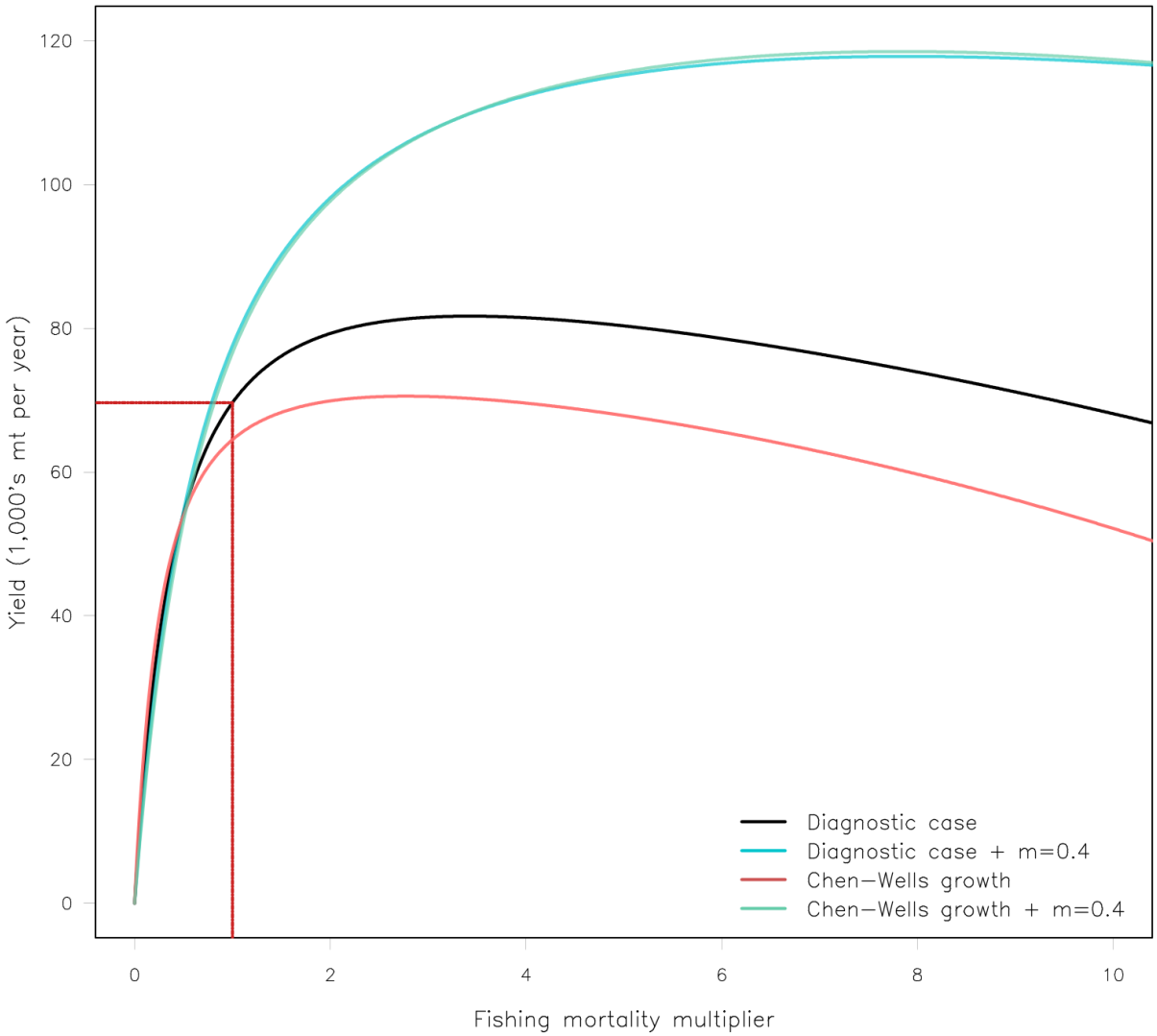

Figure 50: Estimated yield as a function of fishing mortality multiplier for four example models. The black line is the estimated yield curve for the diagnostic case model (estimated growth with natural mortality of 0.3) and the red line indicates the equilibrium yield at current fishing mortality. The other models displayed are the alternative M model with M=0.4 (turquoise), and the alternative growth model *Chen-Wells*, with $M = 0.3$ (red line) and $M = 0.4$ (green line).

Figure 51: History of the annual estimates of MSY (red line) for the diagnostic case model compared with annual catch by the main gear types. Note that this is a "dynamic" MSY which is explained further in Section 5.7.4.

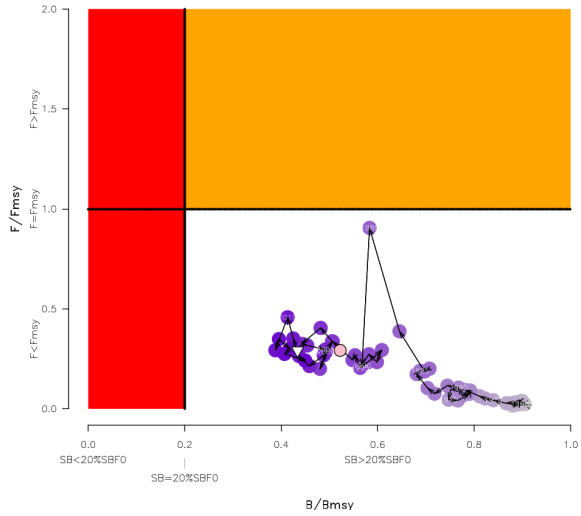

(a) Example: estimated growth/M=0.3 (Diagnostic case)

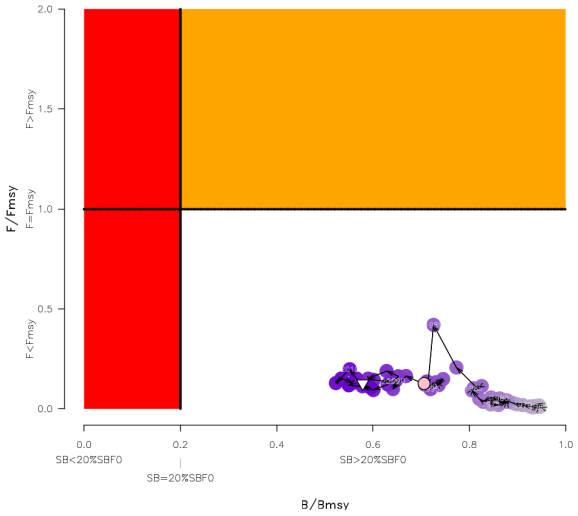

(b) Example: estimated growth/M=0.4

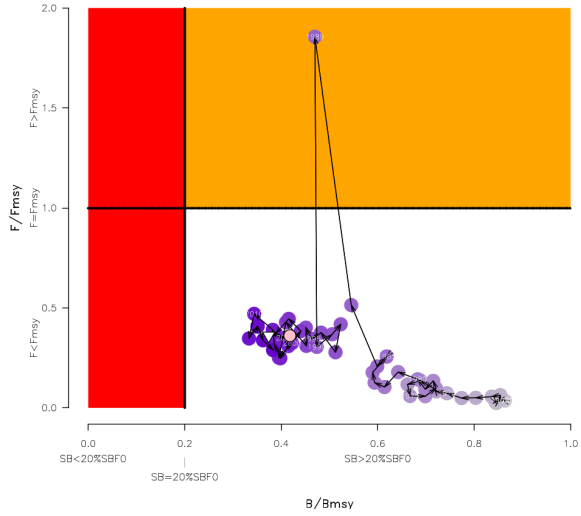

(c) Example: Chen-Wells growth/M=0.3

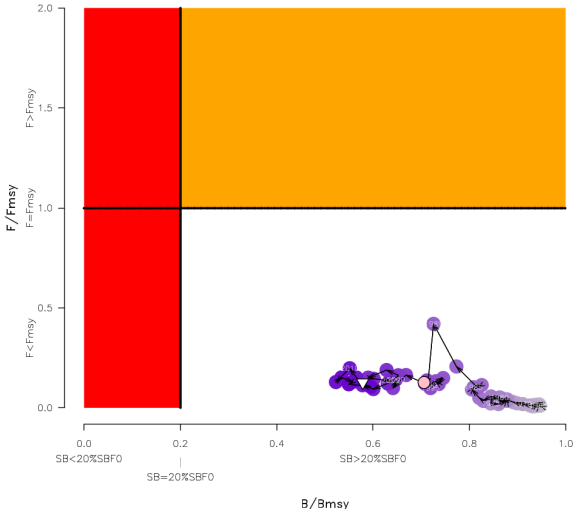

(d) Example: Chen-Wells growth/M=0.4

Figure 52: Estimated time-series (or "dynamic") Majuro plots for four example models from the assessment (one from each of the combinations of growth types, and natural mortality M set to 0.3 or 0.4). These plots are interpreted in the same manner as the description in Figure 47 except that they show the temporal change in stock status with respect to the reference points $F_{recent}/F_{\text{MSY}}$ and $SB_{latest}/SB_{F=0}$, rather than the terminal estimates presented in previous figures. Note that the process of estimating a "dynamic" Majuro plot is explained further in Section 5.7.4.

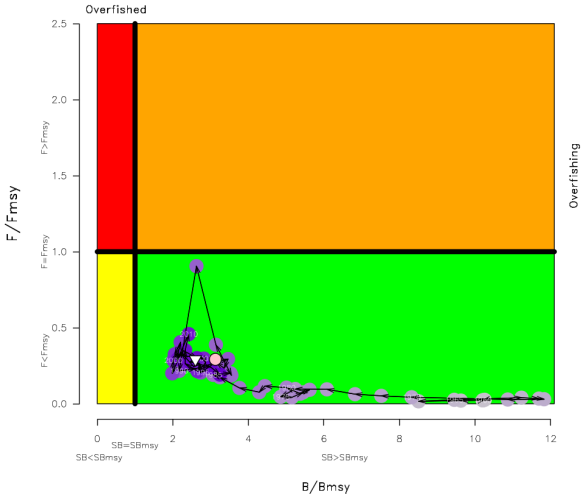

(a) Example: estimated growth/M=0.3 (Diagnostic case)

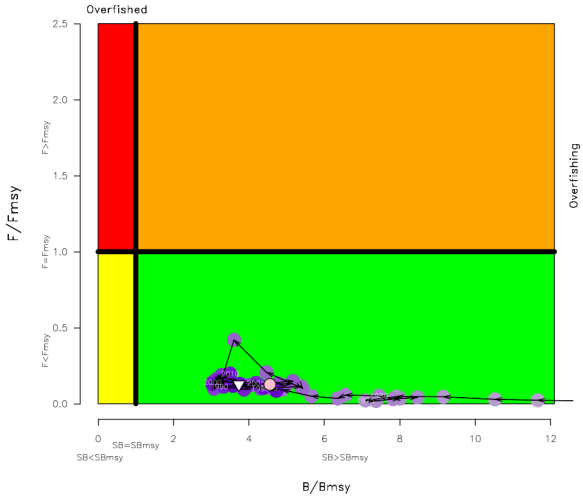

(b) Example: estimated growth/M=0.4

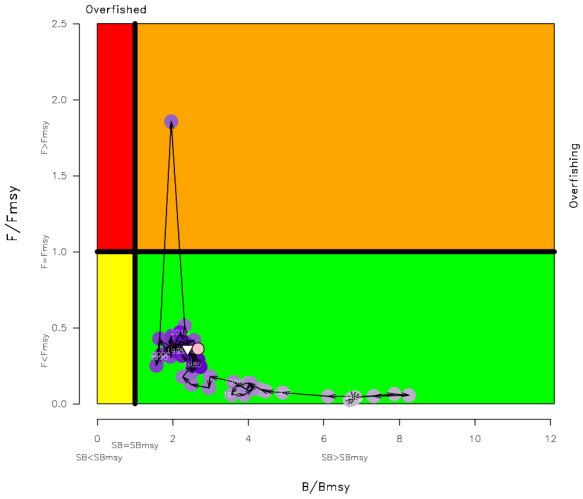

(c) Example: Chen-Wells growth/M=0.3

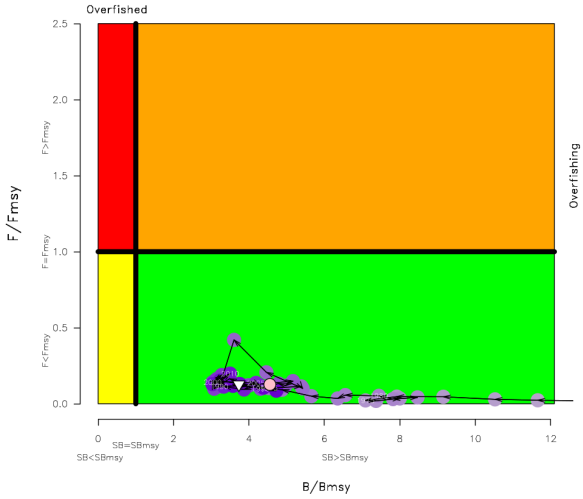

(d) Example: Chen-Wells growth/M=0.4

Figure 53: Estimated time-series (or "dynamic") Kobe plots for four example models from the assessment (one from each of the combinations of growth types, and natural mortality M set to 0.3 or 0.4). Note that the process of estimating a "dynamic" Kobe plot is explained further in Section 5.7.4.

References

Berger, A. M., McKechnie, S., Abascal, F., Kumasi, B., Usu, T., and Nicol, S. J. (2014). Analysis of tagging data for the 2014 tropical tuna assessments: data quality rules, tagger effects, and reporting rates. WCPFC-SC10-2014/SA-IP-06, Majuro, Republic of the Marshall Islands, 6–14 August 2014.

Brouwer, S., Pilling, G., Williams, P., and the WCPFC Secretariat (2018). Trends in the south Pacific albacore longline and Troll fisheries. Technical Report WCPFC-SC14-2018/SA-WP-08.

Cadigan, N. G. and Farrell, P. J. (2005). Local influence diagnostics for the retrospective problem in sequential population analysis. *ICES Journal of Marine Science: Journal du Conseil*, 62(2):256–265.

Cadrin, S. and Vaughan, D. (1997). Retrospective analysis of virtual population estimates for Atlantic menhaden stock assessment. *Fishery Bulletin*, 95(3):256–265.

Chen, K.-S., Shimose, T., Tanabe, T., Chen, C.-Y., and Hsu, C.-C. (2012). Age and growth of albacore *thunnus alalunga* in the north pacific ocean. *Journal of Fish Biology*, 80(6):2328–2344.

Davies, N., Fournier, D. A., Takeuchi, Y., Bouye, F., and Hampton, J. (2018). Recent developments and future plans for MULTIFAN-CL. WCPFC-SC14-2018/SA-IP-02, Busan, Korea, August 8–16 2018.

Farley, J. H., Hoyle, S. D., Eveson, J. P., Williams, A. J., Davies, C. R., and Nicol, S. J. (2014). Maturity ogives for south pacific albacore tuna (*Thunnus alalunga*) that account for spatial and seasonal variation in the distributions of mature and immature fish. *PLoS ONE*, 9(1).

Farley, J. H., Williams, A. J., Clear, N. P., Davies, C. R., and Nicol, S. J. (2013). Age estimation and validation for South Pacific albacore *Thunnus alalunga*. *Journal of Fish Biology*, 82(5):1523–1544.

Fournier, D., Hampton, J., and Sibert, J. (1998). MULTIFAN-CL: a length-based, age-structured model for fisheries stock assessment, with application to South Pacific albacore, *Thunnus alalunga*. *Canadian Journal of Fisheries and Aquatic Sciences*, 55:2105–2116.

Fournier, D. A. and Archibald, C. P. (1982). A general theory for analyzing catch at age data. *Canadian Journal of Fisheries and Aquatic Science*, 39.

Fournier, D. A., Skaug, H. J., Ancheta, J., Ianelli, J., Magnusson, A., Maunder, M. N., Nielson, A., and Sibert, J. (2012). AD Model Builder: using automatic differentiation for statistical inference of highly parameterized complex nonlinear models. *Optimization Methods and Software*, 27(2):233–249.

Francis, R. I. C. C. (1992). Use of risk analysis to assess fishery management strategies: A case study using orange roughy (*Hoplostethus atlanticus*) on the Chatham Rise, New Zealand. *Canadian Journal of Fisheries and Aquatic Science*, 49:922–930.

Francis, R. I. C. C. (1999). The impact of correlations in standardised CPUE indices. NZ Fisheries Assessment Research Document 99/42, National Institute of Water and Atmospheric Research. (Unpublished report held in NIWA library, Wellington.).

Hampton, J. and Fournier, D. (2001). A spatially-disaggregated, length-based, age-structured population model of yellowfin tuna (*Thunnus albacares*) in the western and central Pacific Ocean. *Marine and Freshwater Research*, 52:937–963.

Harley, S. J. (2011). A preliminary investigation of steepness in tunas based on stock assessment results. WCPFC-SC7-2011/SA-IP-08, Pohnpei, Federated States of Micronesia, 9–17 August 2011.

Harley, S. J., Davies, N., Tremblay-Boyer, L., Hampton, J., and McKechnie, S. (2015). Stock assessment of south Pacific albacore tuna. WCPFC-SC11-2015/SA-WP-06, Pohnpei, Federated States of Micronesia, 5–13 August 2015.

Hoyle, S., Hampton, J., and Davies, N. (2012). Stock assessment of albacore tuna in the South Pacific Ocean. WCPFC-SC8-2012/SA-WP-04, Busan, Republic of Korea, 7–15 August 2012.

Hoyle, S., Langley, A. D., and Hampton, J. (2008a). General structural sensitivity analysis for the bigeye tuna stock assessment. WCPFC-SC4-2008/SA-WP-03, Port Moresby, Papua New Guinea, 11–22 August 2008.

Hoyle, S. D. (2011). Stock assessment of albacore tuna in the south Pacific Ocean. WCPFC-SC7-2011/SA-WP-06, Pohnpei, Federated States of Micronesia, 9–17 August 2011.

Hoyle, S. D. and Davies, N. (2009). Stock assessment of albacore tuna in the south Pacific Ocean. WCPFC-SC5-2009/SA-WP-06, Port Vila, Vanuatu, 10–21 August 2009.

Hoyle, S. D., Langley, A. D., and Hampton, J. (2008b). Stock assessment of albacore tuna in the south Pacific Ocean. WCPFC-SC4-2008/SA-WP-08, Port Moresby, Papua New Guinea, 11–22 August 2008.

Ianelli, J., Maunder, M. N., and Punt, A. E. (2012). Independent review of the 2011 WCPO bigeye tuna assessment. WCPFC-SC8-2012/SA-WP-01, Busan, Republic of Korea, 7–15 August 2012.

ISC Albacore Working Group (2017). Stock Assessment of Albacore Tuna in the North Pacific Ocean in 2017. Technical Report Report to the Albacore Working Group, International Scientific Committee for Tuna and Tuna-like Species in the North Pacific Ocean, Vancouver, Canada, 12-17 July 2017.

ISSF (2011). Report of the 2011 ISSF stock assessment workshop. Technical Report ISSF 2011-02, Rome, Italy, March 14–17.

Kinney, M. J. and Teo, S. L. H. (2016). Meta-analysis of North Pacific albacore tuna natural mortality. ISC16/ALBWG-02/07, Nanaimo, Canada, 8-14 November 2016.

Kleiber, P., Fournier, D. A., Hampton, J., Davies, N., Bouye, F., and Hoyle, S. D. (2017). *MULTIFAN-CL User's Guide*. http://www.multifan-cl.org/.

Kolody, D. S., Eveson, J. P., and Hillary, R. M. (2016). Modelling growth in tuna RFMO stock assessments : Current approaches and challenges. *Fisheries Research*, 180:177–193.

Kristensen, K., Nielsen, A., Berg, C. W., Skaug, H., and Bell, B. M. (2016). TMB: Automatic differentiation and Laplace approximation. *Journal of Statistical Software*, 70(5):1–21.

Langley, A. (2004). An examination of the influence of recent oceanographic conditions on the catch rate of albacore in the main domestic longline fisheries. Technical Report Working Paper SA-4., 17th Standing Committee on Tuna and Billfish. 9–18 August 2004. Majuro, Republic of Marshall Islands.

Lehodey, P., Senina, I., Nicol, S., and Hampton, J. (2015). Modelling the impact of climate change on south pacific albacore tuna. *Deep Sea Research Part II: Topical Studies in Oceanography*, 113:246–259.

Leroy, B. and Lehody, P. (2004). Note on the growth of the south Pacific albacore. INFO-BIO-2, 17th Standing Committee on Tuna and Billfish, Majuro, Republic of Marshall Islands, 9–18 August 2004.

Lorenzen, K. (1996). The relationship between body weight and natural mortality in juvenile and adult fish: a comparison of natural ecosystem and aquaculture. *Journal of Fish Biology*, 42:627–647.

Maunder, M. N. and Piner, K. R. (2017). Dealing with data conflicts in statistical inference of population assessment models that integrate information from multiple diverse data sets. *Fisheries Research*, 192:16–27.

McKechnie, S. (2014). Analysis of longline size frequency data for bigeye and yellowfin tunas in the WCPO. WCPFC-SC10-2014/SA-IP-04, Majuro, Republic of the Marshall Islands, 6–14 August 2014.

McKechnie, S., Hampton, J., Pilling, G. M., and Davies, N. (2016a). Stock assessment of skipjack tuna in the western and central Pacific Ocean. WCPFC-SC12-2016/SA-WP-04, Bali, Indonesia, 3–11 August 2016.

McKechnie, S., Ochi, D., Kiyofuji, H., Peatman, T., and Caillot, S. (2016b). Construction of tagging data input files for the 2016 skipjack tuna stock assessment in the western and central Pacific Ocean. WCPFC-SC12-2016/SA-IP-05, Bali, Indonesia, 3–11 August 2016.

McKechnie, S., Pilling, G., and Hampton, J. (2017a). Stock assessment of bigeye tuna in the western and central Pacific Ocean. WCPFC-SC13-2017/SA-WP-05, Rarotonga, Cook Islands, 9–17 August 2017.

McKechnie, S., Tremblay-Boyer, L., and Harley, S. J. (2015). Analysis of Pacific-wide operational longline CPUE data for bigeye tuna. WCPFC-SC11-2015/SA-WP-03, Pohnpei, Federated States of Micronesia, 5–13 August 2015.

McKechnie, S., Tremblay-Boyer, L., and Pilling, G. (2017b). Background analyses for the 2017 stock assessments of bigeye and yellowfin tuna in the western and central Pacific Ocean. WCPFC-SC13-2017/SA-IP-06, Rarotonga, Cook Islands, 9–17 August 2017.

Muhling, B. A., Lamkin, J. T., Alemany, F., García, A., Farley, J., Ingram, G. W., Berastegui, D. A., Reglero, P., and Carrion, R. L. (2017). Reproduction and larval biology in tunas, and the importance of restricted area spawning grounds. *Reviews in Fish Biology and Fisheries*, 27(4):697–732.

Murua, H., Rodriguez-Marin, E., Neilson, J. D., Farley, J. H., and Juan-Jordá, M. J. (2017). Fast versus slow growing tuna species: age, growth, and implications for population dynamics and fisheries management. *Reviews in Fish Biology and Fisheries*, 27(4):733–773.

Nikolic, N., Morandeau, G., Hoarau, L., West, W., Arrizabalaga, H., Hoyle, S., Nicol, S. J., Bourjea, J., Puech, A., Farley, J. H., et al. (2017). Review of albacore tuna, thunnus alalunga, biology, fisheries and management. *Reviews in fish biology and fisheries*, 27(4):775–810.

Pilling, G. and Brouwer, S. (2018). Report from the SPC pre-assessment workshop, Noumea, April 2018. Technical Report WCPFC-SC14-2018/SA-IP-01, Busan, Korea, 8–16 August 2018.

Scott, R. D. and McKechnie, S. (2015). Analysis of longline length frequency compositions for South Pacific albacore tuna. WCPFC-SC11-2015/SA-IP-07, Pohnpei, Federated States of Micronesia, 5–13 August 2015.

Tremblay-Boyer, L. and McKechnie, S. (2018). Background analyses for the 2018 stock assessment of South Pacific albacore tuna. Technical Report WCPFC-SC14-2018/SA-IP-07.

Tremblay-Boyer, L., McKechnie, S., and Harley, S. J. (2015a). Spatial and fisheries structure and regional weights for the 2015 south Pacific albacore tuna (*Thunnus alalunga*) assessment. WCPFC-SC11-2015/SA-IP-07, Pohnpei, Federated States of Micronesia, 5–13 August 2015.

Tremblay-Boyer, L., McKechnie, S., and Harley, S. J. (2015b). Standardized CPUE for south Pacific albacore tuna (*Thunnus alalunga*) from operational longline data. WCPFC-SC11-2015/SA-IP-03, Pohnpei, Federated States of Micronesia, 5–13 August 2015.

Tremblay-Boyer, L., McKechnie, S., Pilling, G., and Hampton, J. (2017). Stock assessment of yellowfin tuna in the Western and Central Pacific Ocean. WCPFC-SC13-2017/SA-WP-06, Rarotonga, Cook Islands, 9–17 August 2017.

Wang, S.-P. and Maunder, M. N. (2017). Is down-weighting composition data adequate for dealing with model misspecification, or do we need to fix the model? *Fisheries Research*, 192:41–51.

Wells, R. D., Kohin, S., Teo, S. L., Snodgrass, O. E., and Uosaki, K. (2013). Age and growth of North Pacific albacore (*Thunnus alalunga*): implications for stock assessment. *Fisheries Research*, 147:55–62.

Williams, A., Nicol, S., Hampton, J., Harley, S., and Hoyle, S. (2009). South Pacific Albacore Tagging Project: 2009 Summary Report. WCPFC-SC5-2009/GN-IP-16, Port Vila, Vanuatu, 10–21 August 2009.

Williams, A. J., Farley, J. H., Hoyle, S. D., Davies, C. R., and Nicol, S. J. (2012). Spatial and sex-specific variation in growth of albacore tuna (*Thunnus alalunga*) across the South Pacific Ocean. *PLoS ONE*, 7(6):e39318. doi:10.1371/journal.pone.0039318.

Williams, P. and Reid, C. (2018). Overview of tuna fisheries in the Western and Central Pacific Ocean, including economic conditions–2017. WCPFC-SC14-2018/GN-WP-01, Busan, Korea, 8–16 August 2018.

Xu, Y., Sippel, T., Teo, S. L. H., Piner, K., Chen, K.-S., and Wells, R. J. (2014). Meta-analysis of north pacific albacore tuna natural mortality. ISC14/ALBWG/04, La Jolla, USA, 14-28 April 2014.

11 Appendix

11.1 Retrospective analyses

Retrospective analyses involve rerunning the selected model by consecutively removing successive years of data to estimate model bias (Cadrin and Vaughan, 1997; Cadigan and Farrell, 2005). A series of five additional models were fitted starting with the full data-set (through 2016), followed by models with the retrospective removal of all input data for the years 2016–2011 sequentially. The models are named below by the final year of data included (e.g., 2011–2016). A comparison of the spawning potential, recruitment and depletion trajectories are shown in Figure 54.

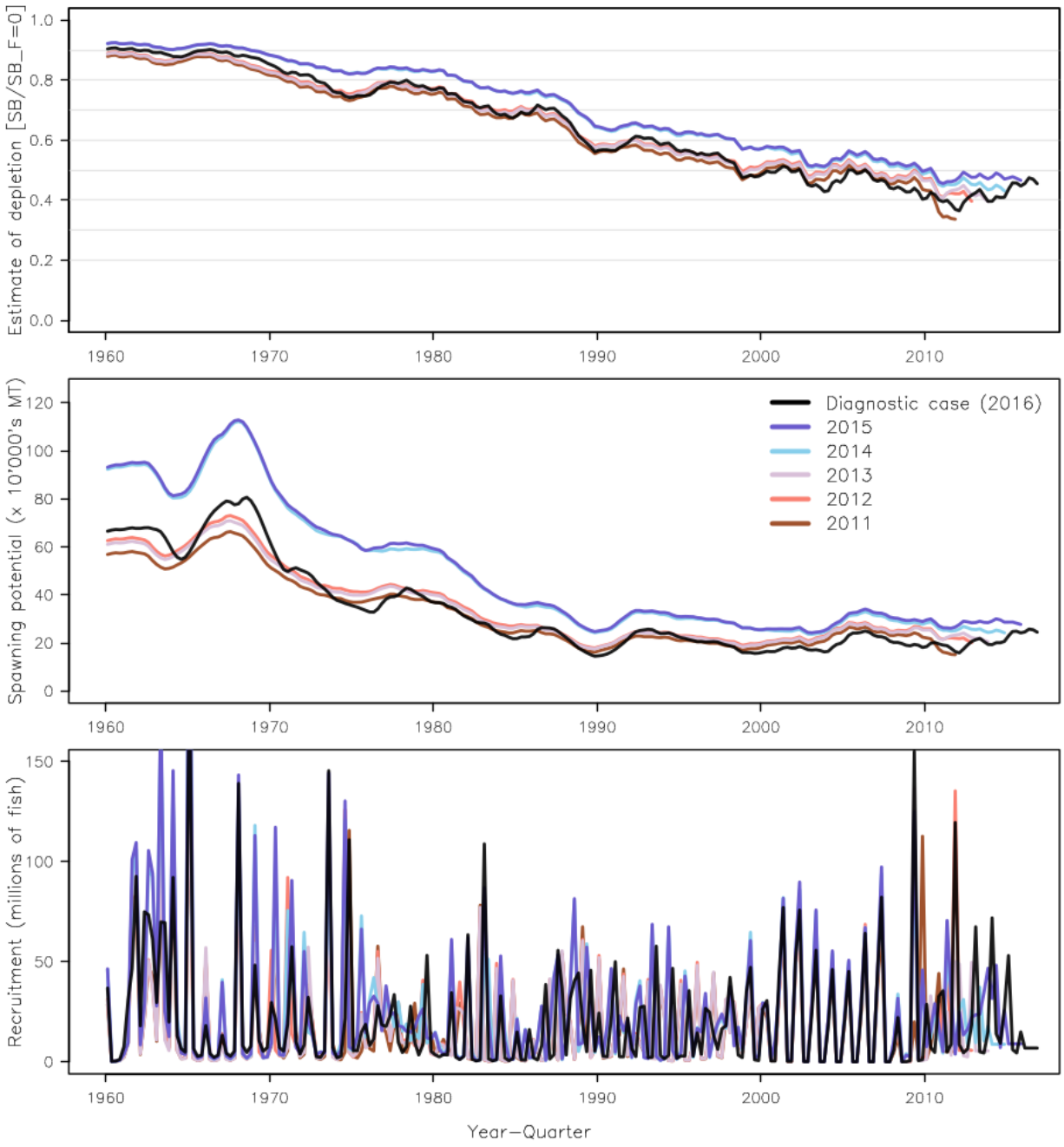

Figure 54: Estimated spawning potential, recruitment and fishery depletion ($SB/SB_{F=0}$) for each of the retrospective models.

11.2 Sensitivity analyses reference points and likelihood values

In the current assessment, inferences about stock status and recommendations for management advice are based on the structural uncertainty grid, rather than the diagnostic case model and the one-off sensitivity model runs, which have received more focus in recent assessments. To this end, the estimates of reference points for the one-off sensitivity model runs are presented here in the Appendix for relative comparisons against the diagnostic case model, and among these models, rather than focusing on the absolute estimates that they provide. The set of focal reference points for these models are presented below in two sets, along with those of the diagnostic case model for context:

Table 11: Reference points for the diagnostic case model and the first set of one-off sensitivity models

Quantity	Diagno	TagMix4	NoTag	m0.2	m0.4	m0.5	Lorenzen	MAA.NorthPac	ALtroll
C_{latest}	62220	62317	61990	61962	61594	61257	61257	61534	62114
MSY	81680	82520	90160	65640	117800	160360	160360	137480	81560
$YF_{current}$	69640	69960	73320	64840	77600	81040	81040	79360	69560
fmult	3.42	3.52	4.03	1.40	7.89	15	15	11	3.44
F_{MSY}	0.07	0.07	0.07	0.07	0.08	0.08	0.08	0.08	0.07
$F_{recent}/F_{\text{MSY}}$	0.29	0.28	0.25	0.71	0.13	0.07	0.07	0.09	0.29
SB_{MSY}	80390	81210	89520	99270	71940	61540	61540	67660	79690
SB_0	442800	447300	495000	508300	472000	488200	488200	485200	441100
SB_{MSY}/SB_0	0.18	0.18	0.18	0.20	0.15	0.13	0.13	0.14	0.18
$SB_{F=0}$	481327	484413	512319	590031	464142	459091	459091	467502	479645
$SB_{\text{MSY}}/SB_{F=0}$	0.17	0.17	0.17	0.17	0.15	0.13	0.13	0.14	0.17
SB_{latest}/SB_0	0.57	0.57	0.61	0.34	0.69	0.77	0.77	0.74	0.56
$SB_{latest}/SB_{F=0}$	0.52	0.53	0.59	0.29	0.71	0.82	0.82	0.77	0.52
$SB_{latest}/SB_{\text{MSY}}$	3.13	3.14	3.35	1.75	4.55	6.08	6.08	5.29	3.11
$SB_{recent}/SB_{F=0}$	0.47	0.47	0.52	0.27	0.63	0.72	0.72	0.68	0.46
$SB_{recent}/SB_{\text{MSY}}$	2.81	2.82	2.96	1.60	4.06	5.40	5.40	4.73	2.80

Table 12: Reference points for the diagnostic case model and the second set of one-off sensitivity models

Quantity	Diagno	Chen-Wells	TradCPUE	Steepness0.95	Steepness0.65	SizeWgt10	SizeWgt20	SizeWgt80	2015MAL	IntgrMAL
C_{latest}	62220	61783	63704	62206	62210	61190	61593	62318	60877	62210
MSY	81680	70560	135280	80600	85360	132160	88480	79560	85760	82200
$YF_{current}$	69640	64480	71680	66080	75880	78360	70400	69240	74880	69600
fmult	3.42	2.77	7.70	4.66	2.60	7.32	4.42	3.16	2.56	3.69
F_{MSY}	0.07	0.06	0.07	0.08	0.07	0.08	0.07	0.07	0.07	0.08
$F_{recent}/F_{\mathrm{MSY}}$	0.29	0.36	0.13	0.21	0.38	0.14	0.23	0.32	0.39	0.27
SB_{MSY}	80390	63830	129400	60190	105300	127800	85890	77200	57590	94320
SB_0	442800	353800	754100	413600	493500	739700	482700	428100	419500	494200
SB_{MSY}/SB_0	0.18	0.18	0.17	0.15	0.21	0.17	0.18	0.18	0.14	0.19
$SB_{F=0}$	481327	407711	801558	458317	520919	714232	515646	465035	422700	535754
$SB_{\mathrm{MSY}}/SB_{F=0}$	0.17	0.16	0.16	0.13	0.20	0.18	0.17	0.17	0.14	0.18
SB_{latest}/SB_0	0.57	0.48	0.64	0.61	0.51	0.61	0.55	0.56	0.41	0.56
$SB_{latest}/SB_{F=0}$	0.52	0.42	0.61	0.55	0.48	0.64	0.51	0.51	0.41	0.52
$SB_{latest}/SB_{\mathrm{MSY}}$	3.13	2.67	3.75	4.17	2.39	3.55	3.07	3.09	2.98	2.96
$SB_{recent}/SB_{F=0}$	0.47	0.39	0.63	0.49	0.43	0.63	0.49	0.45	0.35	0.47
$SB_{recent}/SB_{\mathrm{MSY}}$	2.81	2.51	3.93	3.75	2.15	3.55	2.95	2.74	2.56	2.68

Table 13: Likelihood components for the diagnostic case model and the first set of one-off sensitivity models

Component	Diagno	TagMix4	NoTag	m0.2	m0.5	Lorenzen	MAA.NorthPac	ALtroll
Beverton Holt	1.6	1.3	1.4	1.3	0.8	0.8	1.3	1.2
Effort devs	2845.5	2865.5	2852.4	2994.2	2702.0	2702.0	2715.3	2870.4
Catch devs	106.6	109.1	104.9	119.0	104.5	104.5	104.6	108.7
Length comps	-297303.8	-297300.6	-297310.6	-297193.4	-297390.4	-297390.4	-297365.6	-297296.5
Tagging	661.7	708.5	–	730.0	594.2	594.2	603.1	670.0
Age-Length	3219.3	3196.7	3218.2	3196.0	3198.9	3198.9	3206.1	4295.3
Total	290352.2	290299.4	291025.6	290042.1	290684.8	290684.8	290629.1	289231.0

Table 14: Likelihood components for the diagnostic case model and the second set of one-off sensitivity models

Component	Diagno	Chen.Wells	m0.4	TradCPUE	Steepness0.95	Steepness0.65	SizeWgt10	SizeWgt20	SizeWgt80	X2015MAL	IntgrMAL
Beverton Holt	1.6	0.8	1.4	0.7	1.3	1.4	0.8	1.1	1.5	1.1	1.3
Effort devs	2845.5	2924.5	2754.9	2030.1	2863.5	2863.6	3287.9	3054.9	2807.5	2892.2	2863.4
Catch devs	106.6	113.5	105.4	98.2	108.3	108.4	107.2	110.2	107.3	106.7	108.3
Length comps	-297303.8	-297213.0	-297350.0	-297325.5	-297297.1	-297297.1	-438378.3	-378466.9	-255186.2	-297348.2	-297297.0
Tagging	661.7	690.9	617.7	665.3	671.1	671.2	671.8	683.8	663.8	649.2	671.2
Age-Length	3219.3	0.0	3205.2	3225.5	3195.5	3195.5	3349.8	3234.9	3181.6	3202.2	3195.5
Total	290352.2	293389.2	290557.4	291171.0	290338.0	290337.9	430816.3	371242.2	248315.6	290381.1	290337.9